Abstract

The Influence of Energy Expenditure on Mitochondrial Functions, Oxidative Stress and Insulin Resistance under Metabolic Oversupply Conditions

by Chien-Te Lin

July, 2011

Director: P. Darrell Neufer, Ph.D.

DEPARTMENT OF KINESIOLOGY

Mitochondrial respiratory capacity and oxidative stress have been implicated in the development of insulin resistance (IR) and type II diabetes. A causative role of mitochondrial oxidative stress in the etiology of diet-induced IR has been suggested. Metabolic oversupply causes mitochondrial oxidative stress and leads to IR; however, how the other side of the metabolic balance equation, energy expenditure, may compensate for oversupply is less appreciated. Based on the principles of bioenergetics, in the condition of substrate oversupply without sufficient energy expenditure, the mitochondrial membrane potential ($\Delta\Psi_m$) is high and an exponential increase in superoxide generation occurs within a small range of $\Delta\Psi_m$ exceeding about -160mV. The inverse occurs when the mitochondrial energy expenditure rises. In this context, it

was hypothesized that a mild increase in energy expenditure can sufficiently attenuate the over-nutrition caused H_2O_2 emission and IR.

To examine this hypothesis acutely, Sprague-Dawley (S-D) rats received a lipid oral gavage with or without 1h of subsequent low intensity exercise. Mitochondria of permeabilized skeletal muscle fibers were studied. The results show that, without a change in respiratory capacity, a single lipid loading quickly elevated $\Delta\Psi_m$, mitochondrial H_2O_2 emitting potential ($_mE_{H2O2}$) and reduced calcium retention capacity (an index of the resistance of mitochondrial permeability transition) in state IV and/or under "clamped" physiological state III respiration conditions. These effects can be quickly and sufficiently attenuated by a single bout of postprandial low intensity exercise. These findings provide evidence that mitochondrial H_2O_2 production/emission and related effects, but not respiratory capacity, are acutely and dynamically regulated by the metabolic status of skeletal muscle.

Further, to examine this hypothesis chronically, S-D rats were high fat diet (HFD, 60%) fed for 7 weeks with or without either low intensity exercise or β-guanidinopropionic acid (β-GPA), which chronically elevates mitochondrial energy turnover. The results show that HFD decreased insulin action and increased $_mE_{H2O2}$, whereas both were preserved by either exercise or β-GPA. The treatment effects of HFD, exercise or β-GPA were mitochondrial respiratory function and fatty acid oxidation rate independent. However, 5'-AMP-activated protein kinase (AMPK) activity, an energy sensing kinase that increases glucose uptake, was also increased by β-GPA treatment. To determine whether AMPK mediated the β-GPA-induced improvements in insulin action, skeletal and cardiac muscle-specific AMPK α2 catalytic subunit dominant negative mutated (non-functional) mice and their wild-type littermates were fed a HFD

with or without β-GPA for 10 weeks. β-GPA treatment again prevented the increase in $_{m}E_{H2O2}$ and IR in both wild-type and AMPKα2 dominant negative mice fed a HFD. These findings indicate that AMPKα2 does not mediate the effects of β-GPA on insulin action, supporting the hypothesis that the reduction in mitochondrial H_2O_2 emission is a primary mechanism by which exercise and β-GPA attenuate HFD-induced IR.

In the context of both acute and chronic manipulation of positive (oversupply) and negative (expenditure) cellular energy balance, together these findings support the concept that the governance of mitochondrial oxidant production is a primary factor regulating insulin sensitivity in skeletal muscle. Following the principles of bioenergetics, these data demonstrate that a mild increase in energy expenditure can sufficiently attenuate the HFD-induced H_2O_2 emission and IR. On the mitochondrial level, the balance of substrate supply and energy expenditure on a daily basis is critical for maintaining a proper cellular redox environment, function and whole body metabolic status.

The Influence of Energy Expenditure on Mitochondrial Functions, Oxidative Stress and Insulin Resistance under Metabolic Oversupply Conditions

A DISSERTATION

Presented To

The Faculty of the Department of Kinesiology

East Carolina University

In Partial Fulfillment

of the Requirements for the Degree

Doctor of Philosophy in Bioenergetics and Exercise Science

by

Chien-Te Lin

July, 2011

The Influence of Energy Expenditure on Mitochondrial Functions, Oxidative Stress and Insulin Resistance under Metabolic Oversupply Conditions

The Influence of Energy Expenditure on Mitochondrial Functions, Oxidative Stress and Insulin Resistance under Metabolic Oversupply Conditions

By

Chien-Te Lin

APPROVED BY:

DIRECTOR OF DISSERTATION:_____
P. Darrell Neufer, Ph.D.

COMMITTEE MEMBER:_____
Joseph A. Houmard, Ph.D.

COMMITTEE MEMBER:_____
Ronald N. Cortright, Ph.D.

COMMITTEE MEMBER:_____
David A. Brown, Ph.D.

CHAIR OF THE DEPARTMENT OF KINESIOLOGY:

_____
Stacey R. Altman, J.D.

DEAN OF THE COLLEGE OF HEALTH AND HUMAN PERFORMANCE:

_____
Glen G. Gilbert, Ph.D.

DEAN OF THE GRADUATE SCHOOL:

_____
Paul J. Gemperline, Ph.D.

DEDICATION

I dedicate this dissertation to my wonderful families,

父: 林聰憬 Cong-Jing Lin, 母: 鄭蓉笑 Han-Xiao Zheng,

妻: 洪睿聲 Jui-Sheng (Ann) Hung, & 子: 林宏恩 Owen Lin.

– 林建得 Chien-Te (Peter) Lin.

ACKNOWLEDGEMENTS

The completion of this dissertation was made possible through the support of many individuals. I am tremendously grateful for the enthusiastic encouragement and guidance of my mentor, Dr. Darrell Neufer. I also want to thank my committee members, Drs. Joseph Houmard, Ronald Cortright, and David Brown, for their direction and assistance in completing this project. I gratefully acknowledge the essential role of all my colleagues from Dr. Neufer's lab, and from the collaborative labs in assisting with the experiments, helping me learn my way around the lab, and developing confidence in my research skills. Lastly, I tenderly express my love and gratitude to my family members, who have provided me with unconditional love, motivation and support.

I also gratefully acknowledge 臺灣 TAIWAN Ministry of Education [09411221US015] for the majority of my personal financial support and U.S. National Institute of Health grants R01 [073488] (PDN) for the financial support of these studies.

TABLE OF CONTENTS

LIST OF FIGURES

LIST OF SYMBOLS AND ABBREVIATIONS

ACR	Adenylate control ratio, uncoupled respiration/ state III respiration
$^{1}O_2$	Singlet oxygen
2-DOG	2-deoxyglucose
^{3}H-2-DOG	^{3}H-2-deoxyglucose
^{31}P MRS	^{31}P -Magnetic resonance spectroscopy, can be used as a non-invasive tool for measuring the relative intracellular concentrations of several phosphorus metabolites in different organs
4-HNE	4-Hydroxynonenal, an α,β-unsaturated hydroxyalkenal which is produced by lipid peroxidation in cells
acyl-CoAs	A coenzyme involved in the metabolism of fatty acids
ADP	Adenosine diphosphate
AICAR	5-aminoimidazole-4-carboxamide-ribonucleoside
AIF	Apoptosis inducing factor
Akt	Protein kinase B
AMPK	5'-adenosine monophosphate-activated protein kinase
AMPKα1	AMPK alpha 1 catalytic subunit dominant
AMPKα2	AMPK alpha 2 catalytic subunit dominant
AMPKα2-DN	Mice express a dominant negative mutant (non-functional) form of the AMPK alpha2 catalytic subunit specifically in both skeletal and cardiac muscle
Amplex Red	N-acetyl-3,7-dihydroxyphenoxazine, a redox-sensitive fluorescent dye
Amplex Ultra-Red	Improved amplex reagent, offering brighter fluorescence and enhanced sensitivity on a per-mole basis in peroxidase or peroxidase-coupled enzyme assays
ANOVA	Analysis of variance

ANT	Adenine nucleotide translocase
Antimycin A	Inhibitor of the cytochrome c reductase portion of complex III
AS160	Akt substrate of 160 kda
ATP	Adenosine triphosphate
AU	Arbitrary units
AUC	Area under curve
BCA	Bicinchoninic acid, used to determine total level of protein in solution
Bleb	Blebbistatin, an inhibitor of myosin II
BMI	Body mass index, $kg/(m)^2$
BSA	Bovine serum albumin
BTS	N-Benzyl-p-toluene sulphonamide, an inhibitor of myosin II
C/EBPα	Transcription factor CCAAT enhancer binding protein α
Ca5N	Fluorescence probe calcium green 5N salt
CK-M	Muscle creatine kinase
CoA	Coenzyme A
Complex I	NADH:ubiquinone oxidoreductase
Complex II	Succinate dehydrogenase
Complex III	Coenzyme Q : cytochrome c — oxidoreductase
Complex IV	Cytochrome c oxidase
Complex V	Mitochondrial ATP synthase
COX-IV	Cytochrome C oxidase, isoform IV
CuZn-SOD	CuZn-superoxide dismutase
Cys	Cysteine

Cyto C	Cytochrome C, a small heme protein loosely bound to the outer surface of the inner mitochondrial membrane which transfers electrons from complex III to IV
DAG	Diacylglycerol, also called diglyceride
ddH_2O	Double distilled water
DMSO	Dimethyl sulfoxide
DNA	Deoxyribonucleic acid
DN-HF	Ampkα2-DN mice fed with HFD
DN-HF-GPA	Ampkα2-DN mice fed with HFD plus β-GPA oral gavage
DTT	Dithiothreitol, a strong chemical reductant
ECL	Enhanced chemiluminescence
EDL	Extensor digitorum longus muscle, mostly fast-twitch fibers
EDTA	Ethylenediaminetetraacetic acid, a polyamino carboxylic acid used as a chelating agent
EGTA	Ethylene-bis(oxyethylenenitrilo)tetraacetic acid
ELISA	Enzyme-linked immunosorbant assay
ETC	Electron transport chain
ETF	Electron transfer flavoprotein, involved in transferring electrons from β-oxidation of fatty acids to the mitochondrial electron transfer flavoprotein dehydrogenase
ETS	Mitochondrial electron transport system (a.k.a. Electron transport chain, ETC)
EX group	Fast + water oral gavage + exercise
$FADH_2$	Flavin adenine dinucleotide, a redox cofactor
FALDH	Fatty aldehyde dehydrogenase
FAO	Fatty acid oxidation

FCCP	Carbonylcyanide-p-trifluoromethoxyphenylhydrazone, a lipophilic iononophore used to experimentally uncouple oxidative phosphorylation in mitochondria
FFA	Free fatty acid
FMN	Flavin mononucleotide, a prosthetic group in the mitochondrial complex I
G	Glutamate
G3P	Glycerol-3-phosphate
GapDH	Glyeraldehyde-3-phosphate dehydrogenase
GK rat	Diabetic Goto-Kakizaki rat
GLUT4	Glucose transporter protein 4
Grx	Glutaredoxin
GSH	Reduced glutathione
GSSG	Oxidized glutathione
H_2O_2	Hydrogen peroxide
HEPES	4-(2-hydroxyethyl)-1-piperazineethanesulfonic acid, an organic chemical buffering agent
HF	High fat diet fed animals group
HFD	High fat diet
HF-EX	The animals given a high fat diet were also administered with low intensity exercise
HF-GPA	The animals given a high fat diet were also administered with β-GPA
HK	Hexokinase
HO•	Hydroxyl radical, the neutral form of the hydroxide ion
HOCl	Hypochlorous acid

HR	Heart rate
HRP	Enzyme horseradish peroxidase
Hsp33	Heat shock protein 33
IKK	IκB kinase
IKKβ	Iκb kinase β
in situ	Is a Latin phrase which translated literally as “In position” or “on-site”
iNOS	Inducible nitric oxide synthase
IP	Immunoprecipitation
IPGTT	Intraperitoneal glucose tolerance test
IR	Insulin resistance
IRS	Insulin receptor substrate protein
IRS1	Insulin receptor substrate protein 1
ISE	Ion selective electrode
IκB	Inhibitor of κb
JH_2O_2	Mitochondrial H_2O_2 emission rate
JO_2	Mitochondrial oxygen respiration rate
kDa,	Kilodalton
KHB	Krebs-Henseleit buffer
KO	Specific gene knock out model
LCACoA	Long chain acyl coenzyme A
Lipid group	Fast + lipid oral gavage
Lipid+Ex	Fast + lipid oral gavage + exercise
LKB1	A kinase capable of phosphorylating 5'-adenine monophosphate-activated protein kinase (AMPK)

LOOH	Lipid hydroperoxide
M	Malate
$_{m}Ca^{2+}_{RC}$	Mitochondrial calcium retention capacity
MDA	Malondialdehyde, an often-measured end product of lipid peroxidation
$_{m}E_{H2O2}$	Mitochondrial H_2O_2 emission potential. The H_2O_2 produced by the mitochondria minus that which is scavenged by the mitochondria
$_{m}$FRL%	Mitochondrial free radical leak percentage
MnSOD	Manganese-containing superoxide dismutase, a mitochondrial enzyme catalyzing the dismutation of superoxide ($O2^{-}$•) to H_2O_2
$MnSOD^{+/-}$	Manganese superoxide dismutase heterozygous knockout
mPTP	Mitochondrial permeability transition pore
mRNA	Messenger ribonucleic acid
mtDNA	Mitochondrial deoxyribonucleic acid
NADH	Reduced nicotinamide adenine dinucleotide
NEFA	Non-esterified fatty acid
NF1	Neurofibromatosis type 1
NFκB	Nuclear factor kappa-light-chain-enhancer of activated B cells
NRF-1	Nuclear respiratory factor 1
$O2^{-}$•	Superoxide anion, the product of one-electron reduction of dioxygen
O2K	Oroboros oxygraph-2 k
OAA	Oxaloacetate
OGTT	Oral glucose tolerance test
OH•	Hydroxyl radical
Oligo	Oligomycin , inhibitor of mitochondrial ATP synthase (complex V)

$ONOO^-$	Peroxynitrite
OXPHOS	Oxidative phosphorylation
OxyR	a peroxide sensor and transcription regulator, which can sense the presence of reactive oxygen species and induce antioxidant system
P13K	Phosphatidylinositol 3-kinase
PC	Palmitoyl-L-carnitine
PCR	Polymerase chain reaction
PDH	Pyruvate dehydrogenase
PDK	Phosphoinositi-dedependent kinase
PGC-1α	Peroxisome proliferator-activated receptor gamma coactivator 1 alpha
PGC-1β	Peroxisome proliferator-activated receptor gamma coactivator 1 beta
PI3K	Phosphoinositide 3-kinase, an enzyme involved in the insulin signaling pathway
PIP3	Phosphatidylinositol 3,4,5-trisphosphate
pKa	The acid dissociation constant at logarithmic scale
PKA	Camp-dependent protein kinase
PKC	Protein kinase C
PmFB	Saponin-permeabilized skeletal muscle fiber
PPAR	Peroxisome proliferator-activated receptor
PTEN	Phosphatase and tensin homolog, a protein tyrosine phosphatase
PTP1B	Protein tyrosine phosphatase 1B
PVDF	Polyvinylidene fluoride, a highly non-reactive and pure thermoplastic fluoropolymer
Pyr	Pyruvate

QNMR	The Quantitative Neuroscience with Magnetic Resonance
RCR	Respiratory control ratio, quotient of state III to state IV respiration
RER	Respiratory exchange ratio (VCO_2/ VO_2)
RG	Red gastrocnemius
RNA	Ribonucleic acid
RNS	Reactive nitrogen species, reactive molecules primarily derived from nitric oxide
ROS	Reactive oxygen species, reactive molecules derived from dioxygen
RS-	Thiolate anions
S	Succinate
-S-	Thioether
S.D.	Standard deviation
S.E.M.	Standard error mean
S-D	Sprague-Dawley rat
SDS	Sodium dodecyl sulfate
SDS-PAGE	Sodium dodecyl sulfate polyacrylamide gel electrophoresis
S.E.	Standard error
Ser	Serine, an amino acid
-SH	Thiol, protonated thiol
Sir2	Silent information regulator 2
-SNO	Nitrosothiols
$-SO^-$	Sulfenate
$-SO_2^-$	Sulfinate
$-SO_2H$	Sulfinic acid

$-SO_3^-$	Sulfonate
$-SO_3H$	Sulfonic acid
SOD	Superoxide dismutase
-SOH	Sulfenic acid
SR	Sarcoplasmic reticulum
-SS-	Disulfide
State I	Respiration supported by mitochondria alone
State II	Respiration supported by ADP alone
State III	Respiration supported by substrates and ADP, actively phosphorylating respiration
State IV	Non-phosphorylating respiration
T2D	Type II diabetes
TAG	Triacylglycerol, also called triglyceride (TG)
TBARS	Thiobarbituric acid reactive substances
TCA cycle	Tricarboxylic acid cycle, also known as the Krebs cycle or the citric acid cycle
Thr	Threonine, an amino acid
TNF-α	Tumor necrosis factor-alpha
TPP^+	Tetraphenylphosphonium cation
Triton X-100	A nonionic surfactant
TZD	Thiazolidinedione
UCP3	Uncoupling protein isoform 3
UCR	Uncoupling control ratio, the quotient of FCCP-uncoupled respiration to oligomycin-inhibited state IV respiration

VDAC	Voltage dependent anion channel, maybe a component of the mitochondrial permeability transition pore
Vmax	The maximum reaction velocity of an enzyme or enzymes
VO_2max	The maximal velocity of oxygen uptake
WG	White gastrocnemius
WT	Wild-type littermates
WT-Chow	WT mice were fed standard chow
WT-HF	WT mice were fed with HFD
WT-HF-GPA	WT mice were fed with HFD plus β-GPA oral gavage
β-GPA	Beta-Guanidinopropionic acid
$\Delta\mu_{H+}$	Mitochondrial proton electrochemical gradient
$\Delta\Psi_m$	Mitochondrial membrane potential

The Influence of Energy Expenditure on Mitochondrial Functions, Oxidative Stress and Insulin Resistance under Metabolic Oversupply Conditions

CHAPTER 1: Review of Literature

Lipid Metabolism and IR in Skeletal Muscle

A progressive reduction of insulin sensitivity, particularly in skeletal muscle (the major insulin-mediated glucose disposal organ[1]), is an initial and principle feature in the etiology of type II diabetes (T2D)[2]. The development of insulin insensitivity is associated with elevated intramyocellular lipid content and circulating free fatty acid concentration. It was suggested that the accumulation of fatty acid metabolites such as fatty acyl-CoAs and diacylglycerols (DAG) and/or ceramides directly or indirectly alters insulin signaling[3-5]. One of the main hypotheses is that DAG activates protein kinase C-θ (PKC-θ) (or other PKC families) which in turn activates a serine kinase cascade such as IKK and cJNK-1 and further phosphorates IRS-1 on one or more serine/threonine residues and therefore blocks IRS-1 tyrosine phosphorylation by insulin receptor[6-12]. In turn, insulin-stimulated glucose transport signaling pathway is suppressed and ultimately leads to insulin resistance (IR). Chronically, elevated intracellular fatty acyl-CoAs may affect the expression and/or activity of PPAR family, PGC-1α and/or the NRF-1, in turn altering the expression of some key metabolic related signaling proteins[13-16].

Mitochondrial Dysfunction Recently Implicated in the Pathogenesis of T2D

The precise cause of IR and T2D is still unknown and should be multi-factorial. However, a strong association between IR, lipid accumulation and mitochondrial dysfunctions has been frequently reported. Insulin resistant populations have elevated intramyocellular lipid content[17,18]. Reduced mitochondrial functions have been shown to associate with IR or T2D[19-22]. These include reduced mitochondrial content[23], size[23], enzyme activity[24-26], electron transport system (ETS) complexes and oxidative phosphorylation (OXPHOS) activity or respiration[16,17,27,28], TCA cycle flux rates[29], ATP production[25,26], decreased expression of OXPHOS related genes[15,30,31]. Furthermore, mitochondrial dysfunction was associated with IR at the early development stage of T2D[31,32]. Thus, it is speculated that mitochondrial dysfunction and associated mal-regulation of fatty acid metabolism, particularly in skeletal muscle, is a causal factor linked to the development of IR[6,33,34].

No Clear Cause–Effect Relationship between Mitochondrial Dysfunction and IR

Mounting evidence suggests that mitochondrial dysfunction is not the only one, at least, primary etiological factor in the development of IR or T2D, but rather represents a secondary event. Asian Indians displayed higher mtDNA content, OXPHOS genes expression and enzyme activity and ATP production rates in muscle, despite being more insulin resistant than age-, sex- and BMI-matched North Americans[35]. Moreover, Asian-Indian individuals with T2D and higher muscle lipid levels have similar mitochondrial oxidative capacity compared with Asian Indians without T2D[35]. Post-exercise mitochondrial capacity of phospho-creatinine and ADP recovery kinetics measured by in vivo ^{31}P MRS found no differences between sedentary normal controls and obese patients in either early or advanced stages of T2D[36]. A longitudinal Zucker

diabetic fatty rat study showed that the development of diabetes is associated with increased intramyocellular lipid content, whereas skeletal muscle complex II activity, citrate synthase activity remain comparable to the lean heterozygote littermates and mitochondrial fatty acid oxidation (FAO) activity was increased compared with lean littermates[37]. Other reports from animal and human studies have also shown high-fat diet may not affect[38-40], or may even promote[41-45] skeletal muscle mitochondrial function.

It has been reported that skeletal muscle-specific knockout mouse model with progressive reduction in each ETS complex I~IV activities does not result in either T2D or IR but instead display an increased peripheral glucose uptake[46]. Mice with either muscle-specific PGC-1α KO or with a loss-of-function mutation of PGC-1β also show reduction in OXPHOS genes' expression and defects in muscle mitochondrial function; however, in these animals, muscle insulin sensitivity is slightly improved compared to control mice[47,48]. On the other hand, muscle-specific PGC-1α transgenic overexpression mice exhibit no alteration in glucose tolerance or insulin sensitivity under standard chow diet feeding condition despite improved exercise capacity and increased mitochondrial gene expression, mtDNA and mitochondrial enzyme activity compared with wild-type littermates[49]. Other animal models of mitochondrial dysfunction including skeletal muscle specific PGC-1α KO mice[50] do not show IR. Overall, altering mitochondrial function using various gene-manipulation models has failed to demonstrate a consistent association between mitochondrial dysfunction and insulin action.

In fact, a decrease in mitochondrial function observed in insulin-resistant humans may not limit muscle fatty acids oxidation nor lead to lipid accumulation[22]. Recent studies in which reduced rates of FAO or total mitochondrial oxidation capacity observed in muscle from elderly individuals, family offspring of diabetics, or

obese/diabetic have been interpreted as indicative of a diminished FAO capacity[17,18,23]. However, the muscle mitochondrial FAO capacity, such as during maximal exercise, is far in excess of the rate measured under resting conditions when energy demand, and thus the rate of FAO, is low. In other words, it is questionable whether mitochondrial deficiencies would have a considerable limitation on the rate of FAO under normal resting conditions when energy demand is low[22]. Moreover, although short-term or early stage of HFD feeding could promote mitochondrial density and FAO activity due to a prompt adaptive response[19,44,51], oversupply of fuel can over-ride mitochondrial compensation[19]. In this context, the imbalance of substrate supply and consumption capacity (i.e., energy demand) of healthy mitochondria, but not dysfunctional mitochondria, may be a primary factor leading to lipid accumulation and IR [19,42,45]. ***Most importantly, and perhaps most germane, it is imperative to recognize that the rate of mitochondrial respiration (i.e., oxidative metabolism) in cells is governed mainly by energy demand (basal + ADP-driven)***[52,53]. In tissues that mainly rely on FAO such as cardiac muscle, it has been shown that the key regulator of FAO is energy demand, not substrate supply[53]. In other words, based on principles of mitochondrial bioenergetics, the underlying problem thought to be responsible for the development of IR (i.e., intramyocellular lipid accumulation) is created whenever the supply of lipids exceeds the energy needs of the cell, independent of mitochondrial content. A reduction in mitochondrial density, if it does occur, will reduce overall basal non-ADP driven state IV respiration (i.e., basal energy demand) since mitochondria account for approximately 25% of basal metabolic rate[54,55], but the underlying problem if lipid accumulates is still supply outpacing demand.

The Cause–Effect Relationship between Mitochondrial Oxidative Stress and IR

It was recently reported that global (80%) as well as tissue specific (muscle- and liver-specific) knockout of apoptosis inducing factor (AIF) ablation caused a pattern of progressive OXPHOS deficiency (decreased OXPHOS gene expression and complex activity but no increased reactive oxygen species (ROS) accumulation due to increased respiratory chain coupling) that closely mimicked that of human IR but resulted in increased glucose tolerance, a reduced fat mass and increased insulin sensitivity after HFD[56]. In addition, there is much evidence indicating that short-term starvation (up to 36 h) increases FFA utilization and causes IR, mitochondrial dysfunction[57], lower ATP/ADP ratio and oxidative stress in tissues[58,59] while it is attenuated by small amounts of carbohydrate loading[57]. Recently, it was identified that reduced mitochondrial OXPHOS is a consequence rather than a cause of lipid-induced IR in the condition of prolonged fasting (60 h)[22]. These reports lead to the speculation that FAO triggered ROS production[60,61] maybe a key factor linked to IR.

Elevated ROS production was found in dexamethasone and TNF-α induced insulin-resistant cells while IR in cell and animal models was attenuated when ROS production was suppressed by diverse treatments[62]. A recent study in mice also found that skeletal muscle mitochondrial dysfunction (i.e., reduced structure and function) does not occur until after several months on a high fat diet, well after the appearance of IR[63]. In this study, C_2C_{12} myotubes cultured with high [lipid] or high [glucose] also increased ROS production but was prevented by antioxidant treatment. Addition of H_2O_2 in cell culture caused decreased mtDNA levels and citrate synthase activity in C_2C_{12} myotube while co-culture of H_2O_2 with N-acetylcysteine, a general antioxidant, counteracted these H_2O_2 effects[63]. These data suggest that mitochondrial dysfunction

does not precede the onset of IR but results from increased mitochondrial ROS production[63]. Furthermore, our previous work has shown in both rodents and humans that high dietary fat intake increases skeletal muscle mitochondrial H_2O_2 emitting potential ($_mE_{H2O2}$) and shifts the cellular redox environment to a more oxidized state (i.e., reduced GSH/GSSG ratio) in the absence of any change in mitochondrial respiratory function[64]. Moreover, attenuated $_mE_{H2O2}$, either by treating rats with a mitochondrial-targeted antioxidant or by genetically engineering the overexpression of catalase in muscle mitochondria of mice, completely preserves insulin sensitivity in animal model despite a high-fat diet[64]. In line with this, acute induction of mitochondrial $O2^{-}$• production by complex III antagonist antimycin A caused a decreased insulin action independent of canonical PI3K/Akt pathway in a cell model. HFD induced IR was partially prevented in MnSOD transgenic mice model while $MnSOD^{+/-}$ mice were glucose intolerant even on a standard chow diet[65].

Additional evidence supporting a potential role for mitochondrial ROS production comes from recent studies with metformin. Metformin is one of the most widely prescribed insulin-sensitizing drugs for the treatment of IR and T2D although the mechanism is still under debate. Several previous reports have suggested that the antidiabetic actions of metformin are mediated, at least in part, by directly reducing energy charge[66] due to the inhibition of ETS complex I[67,68]. However, the key information that was missed is ROS production. A partial inhibition of complex I may alter ROS production by at least two mechanisms: 1) by decreasing the efficiency of coupling between respiration and ATP synthesis, resulting a lower $\Delta\Psi_m$ and an increase in electron flux downstream of complex I, or 2) by reducing reverse electron flux back into complex I. Indeed, we recently found that metformin inhibits reverse electron

flux-mediated $_{m}E_{H2O2}$ at ETS complex I in skeletal muscle under therapeutic doses approximately 2 orders of magnitude lower than that required to inhibit electron flux in the forward direction (respiratory O_2 flux)[69]. Collectively, these findings suggest that reducing oxidative stress is crucial for treating T2D and can be accomplished by metformin or reduced energy charge.

The evidence above places the etiology of IR in the context of mitochondrial bioenergetics by demonstrating that mitochondrial oxidative stress serves as both a gauge of energy balance and a regulator of cellular redox environment, linking intracellular metabolic balance to the control of insulin sensitivity.

Mitochondrial Electron Transport System (ETS)

Mitochondria electron transport system (ETS) (or more frequently termed as mitochondria electron transport chain (ETC)) consists of several multi-polypeptide protein complexes (I~V) embedded in the inner mitochondrial membrane (Fig. 1-1) that receive electrons from soluble matrix dehydrogenases. These electrons from reducing equivalent, NADH and $FADH_2$, with high redox potential (tendency to give up electrons) are then transferred through a series of electron carriers in the respiratory system in the order of high to low redox potential progressively. Eventually theese electrons are transferred to O_2 (low redox potential, high tendency to accept electrons), ultimately reducing $^{1/2}O_2$ to H_2O. In three of these complexes (I, III and IV), the energy from the fall in redox potential across the oxidation-reduction reactions is sufficient to drive the translocation of protons from the matrix to the inter-membrane space of the mitochondria. This creates a proton gradient across the inner membrane that is composed of both the electrical potential ($\Delta\tilde{u}_{H^+}$) and the chemical concentration

difference (ΔpH) . Conventionally, $\Delta\tilde{u}_H^+$ is converted to units of electrical potential, i.e., mV, and commonly referred to as the mitochondrial membrane potential ($\Delta\Psi_m$). Although ΔpH and $\Delta\Psi_m$ together comprise the total proton motive force (Δp), $\Delta\Psi_m$ is by far the dominant component and often used synonymously with Δp. The essence of the chemiosmotic theory is that the electrical-chemical potential created by the accumulation of $\Delta\Psi_m$ is sufficient to drive the synthesis of ATP as protons flow back through the ATP synthase (complex V) into the matrix. Proton leak constitutes another means of re-entry for protons which is more important during basal respiration. In non-phosphorylating or very low phosphorylating mitochondria, the rate of proton leak is directly proportional to the respiratory rate.

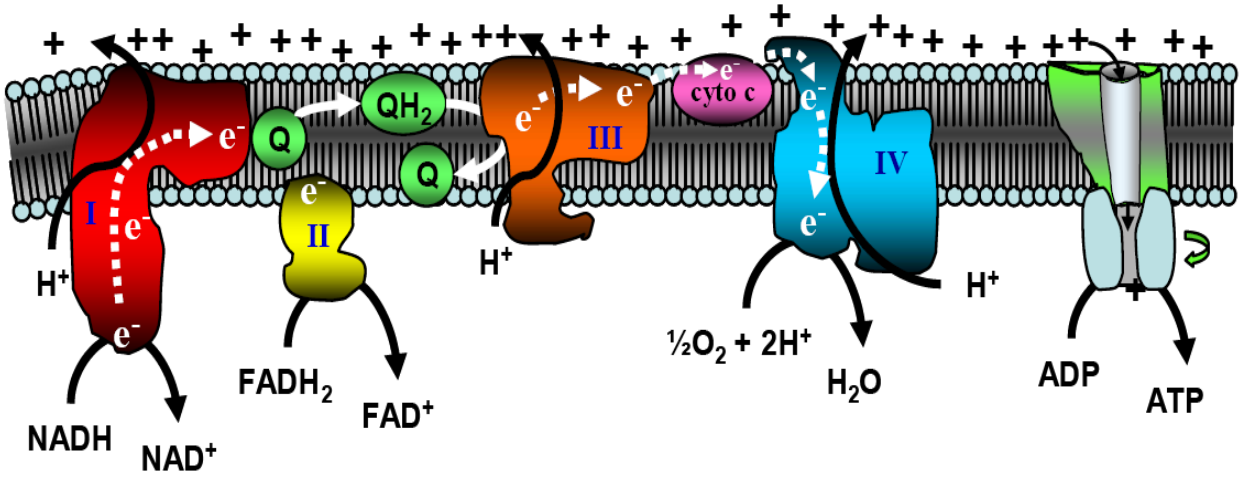

Figure 1-1. The ETS showing electron flow, proton export, and proton reentry driving ATP synthesis. Courtesy of P. Darrell Neufer, Ph.D..

Mitochondrial Respiration States

As depicted in figure 1-2, the background rate of mitochondria respiratory oxygen flux (JO_2) is termed state I respiration when oxygen content is sufficient but no any

substrate presented. The basal JO_2 is termed state II respiration and is defined as the JO_2 generated in the presence of respiratory substrates (i.e., glutamate, malate, succinate, glycerol-3-phosphate, palmitoyl-L-carnitine) but not ADP. If ADP is then added into the system, respiration significantly increases to match the drop in $\Delta\Psi_m$ that occurs as a consequence of rapid proton re-entry via ATP synthesis (complex V). The high JO_2 that is achieved upon addition of ADP is termed state III respiration. Once all of the ADP is converted to ATP, a new basal JO_2 will be achieved and is termed as state IV respiration. States II and IV respiration are often used synonymously to refer to basal (non-phosphorylating) respiration condition. When the oxygen in the system is exhausted (anoxia condition), the respiration is stopped and termed as state V respiration.

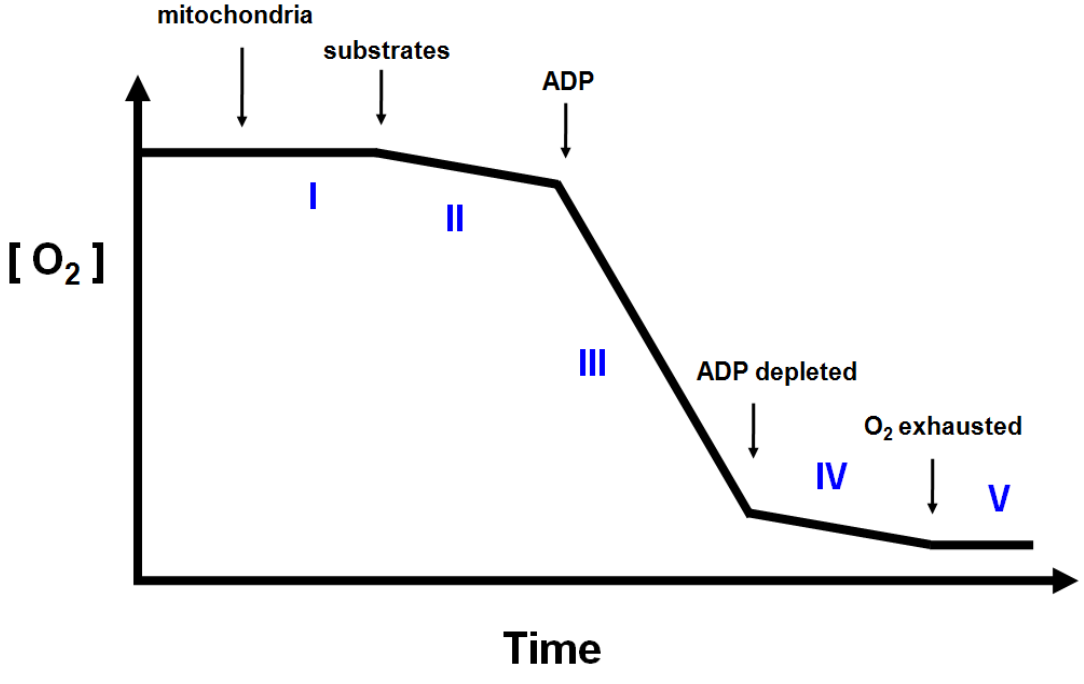

Figure 1-2. Typical experimental trace of mitochondrial respiration in vitro and defined mitochondrial respiration states. See text for detail.

The Fundamental Bioenergetic Control of ROS Production

ROS are successive one unpaired electron reduction products of molecular oxygen en route to the production of water[70-73]. Mitochondrial respiration is the major source of ROS and ETS was believed to leak about 0.15%[74] or even 1~2%[73,75] of its electrons as superoxide (O_2^{-}•) by the addition of one electron to the outer orbital of diatomic oxygen. Although the mechanism is still unclear, the majority of mitochondrial O_2^{-}• production occurred in the matrix face of complex I, particularly triggered by reverse electron flux, and the minority of mitochondrial O_2^{-}• production occurred in the inter-membrane space face of complex III. O_2^{-}•, one of the most destructive ROS, is very short-lived and rapidly undergoes dismutation either spontaneously or through reactions catalyzed by O_2^{-}• dismutase (SOD) to form H_2O_2. H_2O_2 may in turn undergo further reduction to water by glutathione peroxidase. Other ROS include hydroxyl radical (OH•), peroxynitrite ($ONOO^{-}$), hypochlorous acid (HOCl) and singlet oxygen ($^1O_2$)[76]. In order for O_2 to become reduced by one electron, the reducing potential of the molecule donating the electron non-enzymatically needs to be close to or exceed about -160mV (the ΔE for conversion of O_2 to O_2^{-}•) in physiological condition in vivo[77]. Not only do a number of redox couple components within the ETS meet this thermodynamic requirement, many steps involve single electron reactions.

As depicted in figure 1-4 (proved in figure 2-7) that under state IV and low state III respiration condition, the rate of mitochondrial ROS production is highly dependent on $\Delta\Psi_m$ and inversely related to the availability of ADP used to drive ATP synthesis[78-80]. In low state III condition, decreasing of ADP levels (i.e., ↑ ATP and ↓ energy demand) induces an increase in the $\Delta\Psi_m$, which, in turn, decreases the respiratory rate and

further leads to stimulation of O_2^{-}• generation due to the relatively higher reduced state of the ETS components. In state IV condition, without ADP supply, the $\Delta\Psi_m$ is very high and an exponential increase in O_2^{-}• generation occurs within a small range of $\Delta\Psi_m$ values exceeding about -160mV[79,81-84]. The inverse occurs when the mitochondrial ADP levels rise (↑ energy expenditure) which lead to the reduction of the $\Delta\Psi_m$ through F_1F_0 ATP synthase complex activity[85,86].

From the preceding discussion, it is clear that a chronic increase in metabolic substrate oversupply without a corresponding increase in energy demand results in elevated ROS production and IR[19,63,87]. It follows from the principles of bioenergetics that, when close to state IV respiration condition, a small increase in energy expenditure can reduce $\Delta\Psi_m$ and may be sufficient to lower ROS production and prevent IR under metabolic substrate oversupply condition. This is the central question of this proposal.

Redox-Sensitive Protein Modification – Potential Mechanism linking ROS to IR

As detailed above, compelling evidence is accumulating suggesting a cause and effect relationship between mitochondrial ROS production and IR under HFD and T2D conditions in cell, animal, and human models[62-65]. However, the detailed molecular pathway as to how ROS leads to IR is still not clear. Other than causing oxidative damage (e.g., lipids, proteins or DNA), ROS have been implicated in several serine kinases that target and disrupt IRS-1 signaling[88]. ROS activates a number of stress-sensitive signaling pathways such as the NFκB/IKB/IKKβ signaling pathway which can lead to the phosphorylation and inactivation of IRS-1. Pharmacologically or genetically blocking this pathway has been shown to protect against HFD-induced IR[89]. To go one step further, what is the mechanism that makes signaling pathways

redox-sensitive and insulin sensitivity potentially redox-regulated? Both mitochondrial proteins and insulin signaling proteins appear to be regulated by redox-sensitive protein modification which alters protein function and insulin sensitivity.

The thioether (-S-) of methionine (Met) and the better studied thiol (-SH) of cysteines (Cys) are the two common functional groups that undergo reversible oxidation-reduction reactions mediated by ROS, reactive nitrogen species (RNS), lipid hydroperoxides, aldehydes, quinones, disulfides (e.g. GSSG) and others[90]. What makes Cys residues particularly redox-sensitive and proteins potentially redox-regulated? The reactivity of regulatory Cys thiol modification is mainly determined by the Cys's structural environment and its pKa value[91]. Most cytoplasmic protein thiols have pKa values of greater than 8.0, which render the thiol groups predominantly protonated and largely nonreactive at intracellular pH[91,92]. On the other hand, thiol groups of redox-sensitive cysteines have much lower pKa values, ranging from as low as ~3.5 in thiol transferase to ~5.1 to 5.6 in protein tyrosine phosphatases[91]. These thiols are therefore present as deprotonated, highly reactive thiolate anions (RS-), under physiological cellular pH conditions[91,93,94]. The low pKa values of redox-sensitive cysteines are primarily due to the charge-charge interactions between the thiolate anion and neighboring positively charged or aromatic side chains[91,95,96]. In contrast to their protonated counterparts, thiolate anions can easily undergo a diverse spectrum of oxidative modifications upon oxidation by ROS or RNS[91,97]. These thiolate anions include disulfide (-SS-), sulfenate ($-SO^-$)/ sulfenic acid (-SOH), sulfinate ($-SO_2^-$)/ sulfinic acid ($-SO_2H$), and sulfonate ($-SO_3^-$)/ sulfonic acid ($-SO_3H$), or nitrosothiols (-SNO) and others[90,98-100]. Fortunately, most common forms in cells are the more reduced protonated thiol (-SH) and disulfide (-SS-) species[90] while cysteine sulfenic acids and

their deprotonated cysteine-sulfenates are remarkably reactive and versatile oxidation products, which are frequently formed[91]. As detailed by Jones[90], the regulation of biological functions by redox-sensitive thiols occurs in three general ways: 1) chemically alter active site Cys residues ("on-off" switch), 2) alter macromolecular interactions, and 3) regulate protein activity through modification of allosteric Cys. Furthermore, individual proteins often contain multiple Cys residues. Different redox-sensitive elements within a single protein allow its function to be simultaneously regulated by multiple independent redox signals/ mechanisms[90]. When in response to ROS or RNS, the thiol-based redox switches are used as molecular tools in many proteins to regulate their activity including either their activation (e.g., OxyR, Hsp33)[101,102] or inactivation (e.g., PTEN, GapDH)[103,104]. Reversible oxidative thiol modifications have been found to modulate the biological function of proteins involved in many different pathways including receptor activation, signal transduction, transcription factor activation, gene expression, epigenetic control, cell proliferation, differentiation, senescence and apoptosis, metabolism, angiogenesis, protein trafficking, protein synthesis and degradation, immune response, cytoskeletal structure and other processes[90,91,105-120].

Redox-Sensitive Protein Modification in Insulin Signaling Pathway

Based on the evidence described below, oxidation of redox-sensitive proteins might lead to suppression of insulin signaling via Ras, PKC PI3 kinase, and Akt. Conversely, oxidation of a number of redox modified proteins (PTP1B, PTEN, PKA and PP2A) could promote improved insulin signaling.

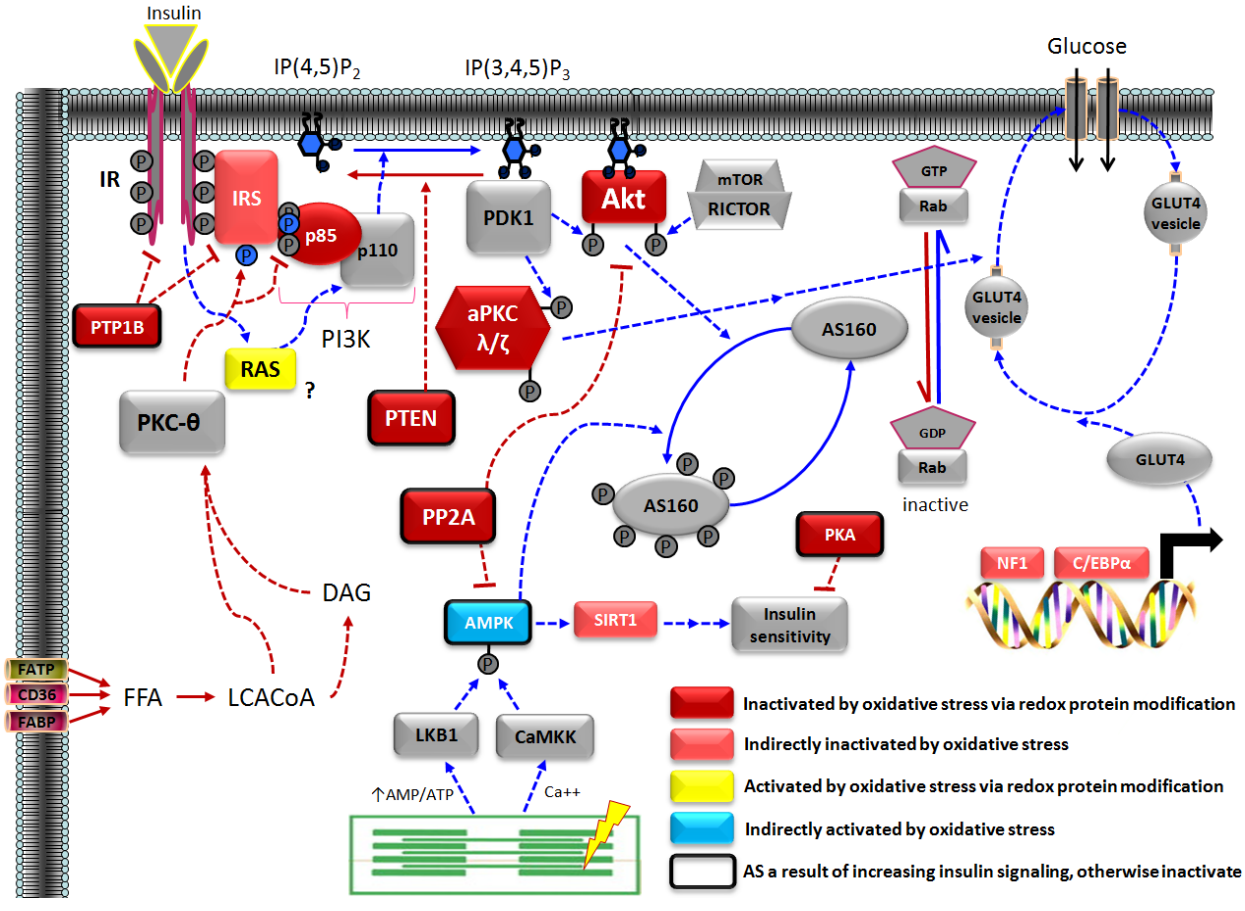

Figure 1-3. Summary of potential redox regulation in insulin signaling pathway. See text for detail.

IRS

Both increased degradation and impaired insulin-induced tyrosine phosphorylation (activation) of Insulin-Receptor-Substrate protein (IRS) have been implicated in oxidant-mediated decrease in insulin action[121]. In 3T3-L1 adipocytes, H_2O_2 incubation induced increased IRS-1 degradation and Ser307 phosphorylation (inactivation)[122]. Incubation with lipid peroxidation product 4-HNE at nontoxic concentrations exhibited enhanced IRS-1 and IRS-2 degradation and increased serine

phosphorylation of IRS-1 which is alleviated by HNE detoxify enzyme, fatty aldehyde dehydrogenase (FALDH)[123]. In vascular smooth muscle cells, angiotensin II decreased IRS-1 protein levels via ROS-mediated IRS-1 Ser307 phosphorylation and subsequent proteasome-dependent degradation[124].

Ras

Even though Ras activates P13K (phosphatidylinositol 3-kinase), which should increase insulin action, peroxynitrite mediated glutathionylation on Cys118 and consequent activation of Ras resulted in endothelial IR while insulin signaling was restored with Glutaredoxin (Grx) overexpression[125].

PKC

Many PKC isoforms appear to be sensitive to redox inhibition by S-glutathionylation or unknown protein modification[114,126-128]. Among them, atypical PKC λ/ζ (aPKC λ/ζ) are the isoforms that link to insulin-stimulated GLUT4 translocation and glucose uptake. Purified human recombinant aPKC- ζ is subject to oxidative inactivation by S-glutathiolation induced by the concentration-dependent thiol-specific oxidant diamide, which induces disulfide bridge formation[129].

PI3K

High glucose- or peroxynitrite-treated cells showed significant increases in tyrosine nitration on the p85 subunit of PI3 kinase and cause its dissociation from the catalytic p110 subunit which further blocked PI 3-kinase and Akt-1 kinase activity[130]. Inhibiting peroxynitrite formation or blocking tyrosine nitration of p85 restored the activity of PI3 kinase and Akt-1 kinase[130].

Akt (PKB)

H_2O_2 exposure resulted in impaired Akt activation in both 3T3-L1 adipocytes and L6 muscle cells[131,132], while lipoic acid, by its capacity to maintain intracellular redox state, protects against oxidative stress induced impairment in Akt activity[133]. A link between Akt activity and glutathione reductase 1 status was indirectly suggested[134], although the Akt glutathionylation has not been directly demonstrated. Furthermore, Akt is reversibly inactivated by S-nitrosylation[135] specifically in Cys224[136] or Cys296[137]. Treating with exogenous NO resulted in S-nitrosation of insulin receptor β subunit (IR-β), Akt and IRS-1 which led to either decreased enzyme activity or expression. These effects were reversed by reduced iNOS expression[138] or acute exercise[139] yielded an improvement in insulin action.

GLUT4

Studies suggest that oxidants appear to reduce GLUT4 gene expression by either oxidation of transcription factor NF1 or suppression of transcription factor C/EBPα expression[6,121,140-142].

PTP1B

PTP1B (Protein tyrosine phosphatase 1B) negatively regulates both insulin signaling pathway and leptin sensitivity[91,143-147]. The catalytic site Cys215 is reduced in active PTP1B[148-151]. Upon mild oxidative stress (100μM H_2O_2), a reversible cyclic sulfenyl-amide is formed in the Cys215 and leads to PTP1B inhibition by changing the conformation of the active site, while the conformational and phosphatase activity change can be restored by reducing agents such as GSH or DTT[152,153]. Similar oxidative inhibition of PTP1B has also shown in other studies[154-158].

PTEN

The active site Cys residues of PTEN (tumor suppressor phosphatase with sequence homology to tensin), which regulates the activity of the PI3 kinase signaling[91,159], is reversibly oxidized and inactivated by either ROS or RNS. Oxidative inactivation of PTEN leads to increased phosphatidylinositol (3,4,5)-trisphosphate (PIP3) level and increased Akt–phosphorylation[159], which will potentially increase insulin action. Further study shown ROS inactivate PTEN by thiol-glutathionylation (*S*-Glutathionylation) and lead to Akt pathway activation[160]. Inhibition of PTEN by peroxynitrite activated the PI3K/Akt pathway[161].

PKA

PKA (cAMP-dependent protein kinase) acts counter to insulin effect by inhibiting lipogenesis and promoting net gluconeogenesis and other effects. PKA is inhibited by oxidative glutathionylation[162-164] and can be reactivated by thioredoxin[165].

PP2A

B56 regulatory subunit of the PP2A inactivates insulin signaling through the dephosphorylation of Akt[166] and AMPK[167-170]. PP2A is inhibited by H_2O_2 in a process that involves reversible glutathionylation[171].

AMPK

Although not necessarily due to direct redox-sensitive protein modification, recent evidence has suggested that ROS may activate skeletal muscle AMPK activity[172,173]. However, this effect may not directly relate to glucose uptake and other signaling proteins may be involved[174]. In rat skeletal muscle incubated with H_2O_2, the AMPKα1 activity was dose-dependently increased, and it was prevented by treatment with the antioxidant, Nacetyl-L-cysteine[173]. Further, contraction-induced increases in mouse skeletal muscle AMPK activity were inhibited (~50%) by N-acetyl-L-cysteine

treatment[172]. However, although skeletal muscle incubated with H_2O_2 increased AMPK α1, α2[174] and Akt activities[174,175], the glucose uptake did not differ between wild type and either whole body AMPK α1 knock out or muscle specific AMPK α2 kinase-dead mice[174]. These results suggest that H_2O_2 stimulated skeletal muscle glucose uptake does not require AMPK catalytic activity, activation of other signal proteins may be involved.

Others

In addition to the above redox sensitive proteins, other key enzymes or transcription factors involved in metabolism or insulin action such as Sirtuin 1[176], Silent information regulator 2 (Sir2)[177], NF-kappaB and AP-1[178] were also reported to be redox-sensitive although no direct evidence has shown specific redox-sensitive active site cysteine residues yet. Other metabolic enzymes inculding, muscle creatine kinase-M (CK-M)[179], glyeraldehyde-3-phosphate dehydrogenase (GapDH)[180] and carbonic anhydrase 3[181] also contain redox-sensitive Cys in their active sites.

Conclusion of Literature Review

Mitochondrial FAO/OXPHOS capacity and oxidative stress have been implicated in the development of IR and T2D. Based on the literature, the reduced mitochondrial FAO/OXPHOS capacity may be secondary to the development of IR. Conversely, mounting evidence favors a causative role of mitochondrial oxidative stress in the etiology of diet induced IR. Metabolic oversupply causes mitochondrial oxidative stress and leads to IR; however, how the other side of the metabolic balance equation, energy expenditure, may compensate and/or protect against energy oversupply is less appreciated. Furthermore, the molecular mechanism of how oxidative stress causes IR

is still largely unknown. Redox-sensitive protein modifications may be a crucial mechanism for determining how oxidative stress regulates the insulin signaling cascade.

Central Hypothesis

Whole body metabolic imbalance is the underlying cause of metabolic diseases. At the cellular level, metabolic balance is a function of how well substrate supply matches metabolic demand, and vice versa. Recent research has provided evidence that the oversupply of fuel to cells induced by high dietary fat intake elevates mitochondrial oxidative stress which, in turn, causally leads to the loss of insulin sensitivity[62-65]. Mitochondrial $O_2^{-}\bullet$ production is directly related to the $\Delta\Psi_m$ which, at any given time, reflects the balance between 1) the local intracellular rate of ATP utilization (metabolic demand) and 2) the rate at which reducing equivalents (NADH and $FADH_2$) are presented to the mitochondria; (e.g., $\Delta\Psi_m$ is high, $O_2^{-}\bullet$ or H_2O_2 emission is favored when ATP demand is low and intracellular metabolic supply is high). As such, $_mE_{H2O2}$ has been proposed to serve as both a gauge of energy balance (i.e., reducing potential of the electron transport system) and regulator of redox state within cells, ultimately linking cellular metabolic balance to the control of insulin sensitivity[64]. Our previous work[64] however tested the impact of nutritional oversupply only under very low demand (state IV) respiratory conditions. The interplay between metabolic supply and $_mE_{H2O2}$ under conditions of ATP turnover (state III) more typical of the conditions present in vivo, and the extent to which metabolic expenditure can compensate for over nutrition in terms of $_mE_{H2O2}$, cellular redox state and insulin sensitivity is unknown. The objective of this study was to examine both chronic and acute influence of energy expenditure as

well as the interplay of factors governing mitochondrial function under metabolic oversupply conditions on the control of $_mE_{H2O2}$ and IR. It was hypothesized that both chronic and acute increases in energy expenditure normalize energy oversupply-induced elevated $_mE_{H2O2}$ and IR.

Specific Aim 1

To determine if a mild increase in energy expenditure (low intensity exercise) is sufficient to attenuate the increase in mitochondrial membrane potential, oxidant emitting potential, and the reduction in calcium retention capacity in skeletal muscle of rats induced by a single lipid loading.

Previous findings from our lab provide evidence that state IV $_mE_{H2O2}$ in muscle is acutely increased by a single glucose or lipid meal. To further examine the potential acute impact of lipid oversupply and low intensity exercise on the interplay between energetic expenditure and cellular metabolic supply on the control of $\Delta\Psi_m$, $_mE_{H2O2}$, and mitochondrial calcium retention capacity ($_mCa^{2+}_{RC}$) particularly under state III condition, the following were addressed:

a) How does substrate supply relative to metabolic demand (i.e., state III respiration rate) impact $_mE_{H2O2}$ in permeabilized red gastrocnemius of rats?
b) How is the governance of mitochondrial OXPHOS capacity and state III $\Delta\Psi_m$, $_mE_{H2O2}$, $_mCa^{2+}_{RC}$ affected by single lipid loading?
c) Does a single bout of low intensity exercise sufficient to normalize the governance of mitochondrial OXPHOS capacity and state III $\Delta\Psi_m$, $_mE_{H2O2}$, $_mCa^{2+}_{RC}$ affected by single lipid loading?

Specific Aim 2

To determine if a chronically modest increase in energy expenditure is sufficient to prevent the increase in mitochondrial oxidant emitting potential and decrease in insulin sensitivity induced by a high fat diet.

Increasing physical activity (energy expenditure) represents one of the most effective means for reversing IR in skeletal muscle of overweight/obese patients at high risk for developing T2D. Beta-Guanidinopropionic acid (β-GPA), an antidiabetic/antihyperglycemic agent[182-184], is a non-metabolized creatine analog that reduces cellular creatine phosphate and ATP content and compensatorily increases energy expenditure and mitochondrial biogenesis in rodent skeletal muscle[185]. It is hypothesized that only a small increase in cellular ATP turnover is sufficient to relieve the "reducing pressure" (i.e., potential of the respiratory system to leak electrons) and thus normalize $_{m}E_{H2O2}$ and IR in a HFD setting. To test this hypothesis, the following were addressed:

a) Is low intensity daily treadmill exercise sufficient to normalize $_{m}E_{H2O2}$ and preserve insulin sensitivity in rats consuming a HFD?

b) Is daily treatment with β-GPA sufficient to normalize $_{m}E_{H2O2}$ and preserve insulin sensitivity in rats consuming a HFD?

Both exercise[186-188] and β-GPA[185,189-191] have also been shown to activate AMPK, and AMPK-mediated signaling is known to stimulate glucose uptake independent of insulin[192]. This suggests that any metabolic effects induced by β-GPA, if occurring, may be mediated by AMPK and/or $_{m}E_{H2O2}$. To distinguish between these two possibilities, the following was addressed:

c) Does β-GPA treatment normalize $_{m}E_{H2O2}$ and IR in AMPKα2 dominant negative mice consuming a HFD?

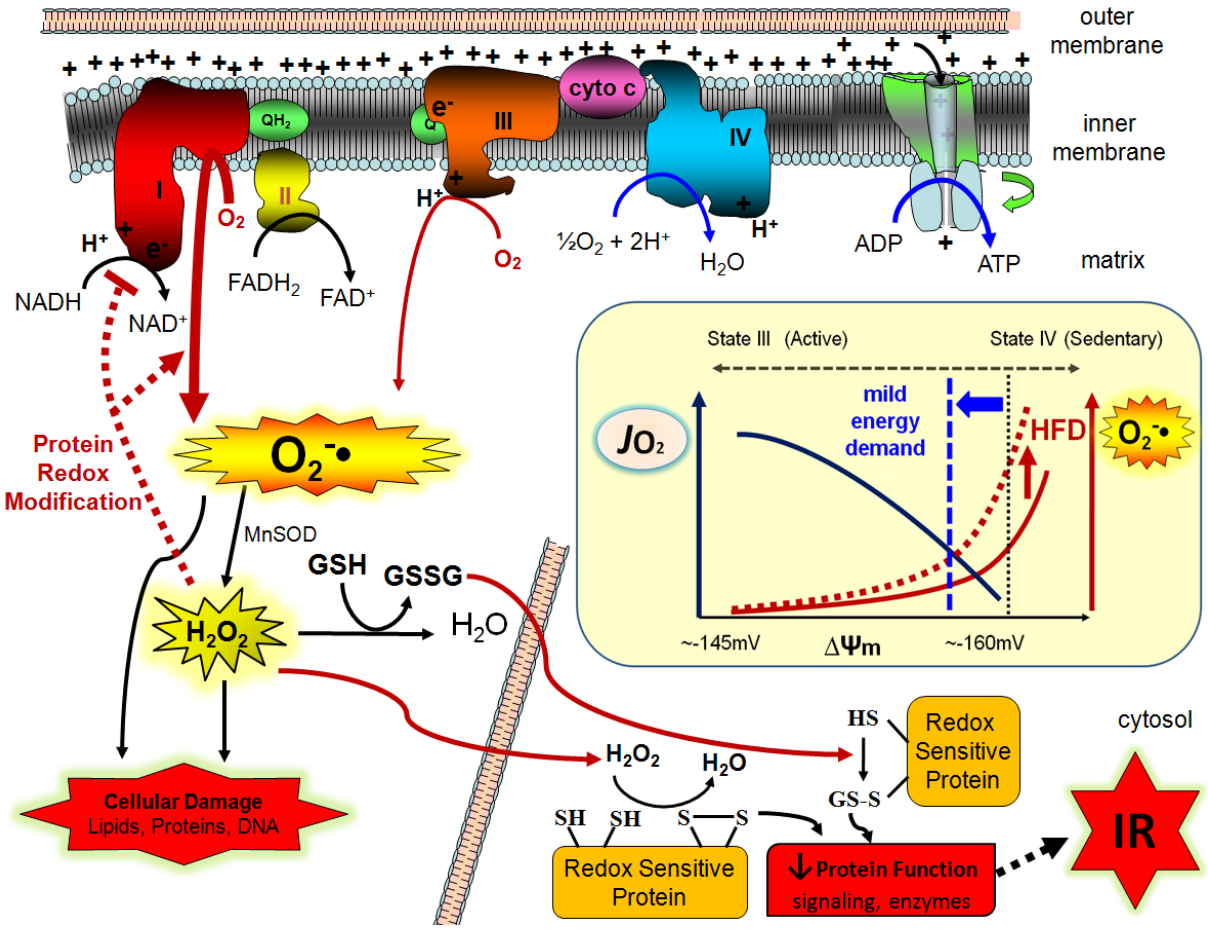

Figure 1-4. Central hypothesis. Mitochondria respiration status in the regulation of ROS production rate and redox-sensitive protein modification. HFD causes increases in membrane potential and ROS production, which leads to redox-sensitive protein modifications within mitochondria and insulin signaling proteins and ultimately leads to IR. Increased energy expenditure, however, decreases the membrane potential and ROS production, further preserving insulin sensitivity.

Significance

The interplay between substrate supply and metabolic demand is at the heart of cellular metabolic balance and the consequences of metabolic imbalance. These

studies provide mechanistic insights on the impact of cellular substrate supply relative to energy demand on the control of $_{m}E_{H2O2}$ and insulin sensitivity.

CHAPTER 2: Low Intensity Exercise is Sufficient to Attenuate Acute Lipid Loading-Induced Elevations in Mitochondrial Membrane Potential, H_2O_2 Emitting Potential, and Reduction in Mitochondrial Calcium Retention Capacity in Rat Skeletal Muscle

Abstract

Postprandial lipidemia causes acute oxidative stress. Whether it also acutely affects other related mitochondrial parameters is unknown. Based on the principles of bioenergetics, mildly increasing mitochondrial respiration (energy expenditure) from very low state III respiration condition reduces mitochondrial membrane potential ($\Delta\Psi_m$) and exponentially reduces $O_2^{-}\bullet$ generation, and vice versa when substrate supply is high. The objective of this study was to determine if a mild increase in energy expenditure, by low intensity exercise, is sufficient to attenuate the increases in $\Delta\Psi_m$, mitochondrial H_2O_2 emitting potential ($_mE_{H2O2}$), the potential reduction in mitochondrial calcium retention capacity ($_mCa^{2+}_{RC}$, an index of the resistance of the permeability transition) and oxidative phosphorylation capacity (OXPHOS) in the skeletal muscle of rats after a single lipid loading. Sprague-Dawley rats received a lipid oral gavage (20% intralipid at 45 Kcal/kg lean body mass, ~12% of the daily total caloric intake) followed by either 2h of rest or 1h of exercise (treadmill, 15m/min, 0 grade) after 1h of rest. Red gastrocnemius permeabilized myofibers were prepared for measures of mitochondrial function. The results show that, without a change in OXPHOS, a single lipid load quickly elevates $\Delta\Psi_m$, $_mE_{H2O2}$ and reduces $_mCa^{2+}_{RC}$ in state IV and/or "clamped" physiological state III respiration condition. These effects can be sufficiently attenuated by a single

bout of postprandial low intensity exercise. These findings provide evidence that several aspects of mitochondrial function, including oxidant production, are very sensitive to and dynamically regulated by metabolic status. It further suggests $\Delta\Psi_m$ and oxidative stress are the preceding factors acutely caused by lipid loading, and may be responsible for the loss in mitochondrial density observed in long-term substrate oversupply conditions, ultimately leading to mitochondrial dysfunction (reduced OXPHOS) and metabolic diseases (e.g. diabetes). The balance of substrate supply and energy demand on a daily basis is critical for maintaining a proper cellular redox environment and therefore cellular function.

Introduction

Postprandial lipidemia (hypertriglyceridemia particularly)[193-195] and hyperglycemia[196,197] have been proposed to have acute deleterious effects on metabolic regulation and cardiovascular function. In addition to hypertriglyceridemia, circulating markers of oxidative stress are elevated following a single high-fat meal[193,198-200]. Other studies also show oxidative stress levels positively correlate with postprandial circulating triacylglycerol (TAG) levels[193,201]. Furthermore, previous findings from our group provide direct evidence showing that skeletal muscle mitochondrial H_2O_2 emitting potential ($_mE_{H2O2}$), under state IV respiration, is acutely increased by a single lipid meal, and the intracellular redox environment (GSH/GSSG) is shifted to a more oxidized state by an acute glucose injection or long-term high-fat feeding[64]. However, whether a single lipid load acutely increases skeletal muscle mitochondria membrane potential ($\Delta\Psi_m$) and $_mE_{H2O2}$ particularly under state III respiration, which is a more physiological condition, is still unknown. Moreover, it is still under debate whether mitochondrial

dysfunction (i.e., oxidative phosphorylation (OXPHOS) capacity), content reduction or oxidative stress elevation is the preceding/primary cause of diet-induced insulin resistance and type II diabetes. While it has been long observed that a single high-fat meal[193,198-200,202] acutely induces postprandial oxidative stress, there is limited evidence on the effect of postprandial OXPHOS capacity. By examining the effect of an acute lipid load on OXPHOS capacity, oxidative stress, and other metabolic parameters, the initiating factor leading to diet-induced insulin resistance (mitochondrial dysfunction or oxidative stress) may be revealed.

It may seem unlikely that a single high calorie meal will have detectable deleterious effects on metabolic control and that a single bout of mild exercise will benefit the overall metabolic condition. However, both may have acute effects at the cellular and/or molecular level. It is our hypothesis that chronic diseases associated with chronic metabolic imbalance are rooted in the cellular conditions that exist during and between meals. Based on the rationale that oxidative stress levels positively correlate with postprandial circulating TAG levels[193,201] and a single bout (>30 minutes) of aerobic exercise can promote fatty acid utilization and activate antioxidant defense pathways hours after exercise, many investigators have focused on the effects of prior exercise on postprandial lipidemia and oxidative stress. A growing body of evidence indicates that a single session of low-moderate intensity aerobic exercise of sufficient energy expenditure performed hours before a fat meal reduces postprandial lipidemia[193,203-207]. The energy expenditure level of prior exercise appears to be the major factor influencing postprandial lipidemia[208]. Although a single session of low-moderate intensity exercise (walking exercise performed at 50% $\dot{V}O_2$max for 90 minutes) decreases postprandial hypertriglyceridemia irrespective of the timing of the exercise relative to a high-fat meal

(i.e., premeal versus postmeal)[205], a single session of prior aerobic exercise seems to have limited effect on attenuating postprandial oxidative stress measured by circulating oxidative stress biomarkers (trolox equivalent antioxidant capacity, xanthine oxidase activity, hydrogen peroxide, and malondialdehyde (MDA))[209,210]. Contrarily, a single session of moderate exercise (1 h of 60% max HR exercise) performed 2 hours following a high fat meal (69% kcal% fat) can ameliorate the elevation of postprandial oxidative stress markers. Circulating serum lipid hydroperoxides (LOOH) $O2^{-}\bullet$ dismutase (SOD) were decreased immediately after exercise, with LOOH levels remaining depressed up to 1 hour post exercise session[193]. Collectively, it appears that significant activation of antioxidant defense pathways may not be required under a balanced energetic state (i.e., balanced cellular redox status in the pre-meal exercised condition). On the other hand, in the metabolically challenged state (i.e., substrate oversupply, post-meal exercise condition), aerobic exercise of sufficient energy expenditure theoretically can prevent ROS production due to the increase in mitochondrial respiration (i.e., ↑ energy expenditure causing state IV → state III respiration shift which markedly lowers the "reducing pressure") and/or the rapid activation of antioxidant defense pathways. However, evidence that a mild increase in energy expenditure (mild exercise) can attenuate acute lipid loading induced high oxidative stress (postprandial lipidemia status) is still indirect and limited[193].

Based on the principles of bioenergetics, the rate of mitochondrial ROS production, in close to state IV respiration condition, is highly dependent on $\Delta\Psi_m$ and inversely related to the availability of ADP used to drive the ATP synthesis[78-80]. In low state III condition, decreasing ADP levels (i.e., ↑ ATP and ↓ energy demand) induces an increase in the $\Delta\Psi_m$, which, in turn, decreases the respiratory rate and increases

superoxide (O_2^{-}•) generation due to the relatively more reduced state of the ETS components. In state IV or very low state III condition, without sufficient ADP supply or energy expenditure, the $\Delta\Psi_m$ is very high and an exponential increase in O_2^{-}• generation occurs within a small range of $\Delta\Psi_m$ values exceeding about -160mV (method dependent)[79,81-84]. The inverse occurs when the mitochondrial ADP levels rise (↑ energy expenditure) which lead to the reduction of the $\Delta\Psi_m$ through F_1F_0 ATP synthase complex activity[85,86]. It follows the principles of bioenergetics that a small increase in mitochondrial energy expenditure from idling should reduce $\Delta\Psi_m$ and thereby exponentially decrease ROS production under metabolic substrate overload. Based on this premise, we hypothesized that mild energy expenditure (low intensity exercise) can reduce $\Delta\Psi_m$ and $_mE_{H2O2}$ under acute metabolic substrate overload (single lipid loading).

To address this hypothesis, we determined the rate of $_mE_{H2O2}$ as well as $\Delta\Psi_m$ and mitochondrial calcium retention capacity ($_mCa^{2+}{}_{RC}$) under both state IV and "clamped" physiological state III respiration conditions in saponin-permeabilized rat skeletal muscle fibers (PmFBs, *in situ*) harvested after acute lipid ingestion with or without a single session of mild exercise. The $_mCa^{2+}{}_{RC}$ is an index of the resistance of the permeability transition pore (mPTP) opening following matrix Ca^{2+} accumulation[211]. The purpose of this study was to determine if mild exercise is sufficient to attenuate the potential increase in $\Delta\Psi_m$ and $_mE_{H2O2}$, and the potential reduction in $_mCa^{2+}{}_{RC}$ in skeletal muscle of rats after receiving a single lipid load. The results show that, without a change in OXPHOS, a single lipid load quickly elevates $\Delta\Psi_m$, $_mE_{H2O2}$ and reduces $_mCa^{2+}{}_{RC}$. These effects can be prevented or attenuated by a single bout of low intensity exercise.

Methods

Animals

Animal studies were approved by the East Carolina University Institutional Animal Care and Use Committee. Young male Sprague-Dawley rats (n=8-10/group; 300~325g; Charles River Laboratories, Inc.) were randomly assigned to each group. Rats were maintained on a standard 12h/12h light/dark cycle (7:00 am light) and fed with standard chow diet *ad libitum*.

Design

All rats were acclimated to the treatment condition for 3 days. Rats from all groups received one single water gavage orally and exercised on a treadmill (20 min of 15m/min) 2-3 days before receiving the treatment. The day before treatment all rats received one single water gavage orally and were not exercised. The day of treatment, rats received the following treatment at the times indicated in figure 2-1: 1) Control group: fast + water oral gavage; 2) Lipid group: fast + lipid oral gavage; 3) Ex group: fast + water oral gavage + exercise; 4) Lipid+Ex group: fast + lipid oral gavage + exercise. The exercise protocol was 60 minutes of moderate walking on the treadmill (15m/min and 0 grade). The lipid gavage consisted of a 20% intralipid emulsion (8.37 MJ/L, Sigma I141) which is an aqueous emulsion of 20% soybean oil (containing 50% linoleic acid, 26% oleic acid, 10% palmitic acid, 8% linolenic acid and 3.5% stearic acid), 2.25% glycerin, and 1.25% egg yolk phospholipids in water. The oral gavage volume was 25ml/kg lean body mass for either water or intralipid gavage which yields 45 Kcal/kg lean body mass. The Charles River Laboratories volume guideline for gastric gavage in rats is 20ml/kg whole body mass. Body composition analysis (Echo Magnetic Resonance Imaging (EchoMRI-900™), Echo Medical System, Houston, TX) of rats

revealed a lean body mass of 79.25±1.087% (M±SD, n=24). After considering the energy content and lean to whole body mass ratio, the maximal lipid the animals received by a single oral gavage was 45 Kcal/kg lean body mass. This was equivalent to only 11.9% of average total daily energy intake in rats fed a regular pellet form of 60%HFD (Research Diets D12492) as determined by an indirect calorimetry module (CaloSys V2.1, TSE Systems) for 48h after a 3-4 day of acclimation period (data not shown).

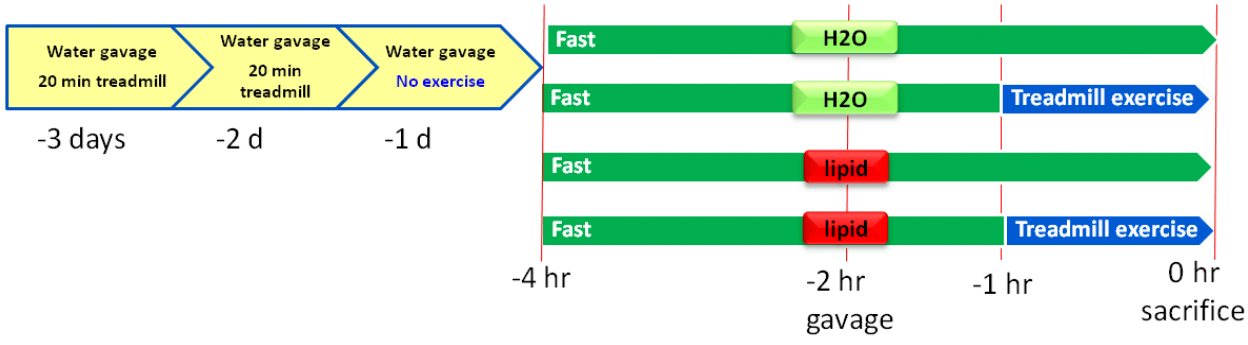

Figure 2-1. Experiment design.

Tissue Sampling and Permeabilized Myofibers (PmFBs) Preparation

Tissue sampling. Immediately after the treatment, the rats were anaesthetized (~5 minutes) by IP injection of ketamine & xylazine mixture. Gastrocnemius muscle was dissected out within 10 minutes after the treatment was completed. The same portion of fresh red gastrocnemius from each rat was immediately trimmed, saponin-permeabilized, and maintained (4°C) in buffer to determine $\Delta\Psi_m$, $_mE_{H2O2}$, JO_2 and $_mCa^{2+}_{RC}$.

Myofiber separation. Briefly, after dissection, connective tissue was removed and fresh fiber bundles were separated to maximize the exposure surface using fine forceps

under a binocular dissecting microscope in ice-cold buffer X containing (in mM) 60 K-Mes, 35 KCl, 7.23 K_2EGTA, 2.77 CaK_2EGTA, 20 imidazole, 20 taurine, 5.7 ATP, 15 phosphocreatine 6.56 $MgCl_2 \cdot 6H_2O$ (pH adjusted to 7.10) plus 0.5 glutamate (G) and 0.2 malate (M).

Myofiber permeabilization and washing. After separation, cytosolic membrane of myofiber bundles were permeabilized in buffer X plus 0.5mM G, 0.2mM M and 40 μg/ml saponin gently shaken on a rocker at 4°C for 30 min. To washout the extra-mitochondrial components, the PmFBs were further washed (3 x 5~8 min) in buffer Z containing (in mM) 105 K-Mes, 30 KCl, 10 K_2HPO_4, 5 $MgCl_2 \cdot 6H_2O$ and 0.5mg/ml bovine serumalbumin (pH adjusted to 7.40) plus freshly added 1 EGTA, and gently shaken on a rocker at 4°C. 25μM blebbstatin (myosin II inhibitors, inhibition of contraction[212-215]) was added into the buffer of 3rd washing.

Measuring Mitochondrial Respiration Rate (JO_2) or JO_2 Simultaneously with Mitochondrial Membrane Potential ($\Delta\Psi_m$) in PmFBs

Washed PmFBs (~0.5mg after freeze-dried) $\Delta\Psi_m$ and/or JO_2 was measured by high-resolution respirometry (Oroboros Oxygraph-2 K (O2K), Innsbruck, Austria) at 25°C in assay buffer containing buffer Z plus 1mM EGTA, 25μM blebbistatin and 20mM creatine under the following protocols. JO_2 protocol: 2mM M + 25μM palmitoyl-L-carnitine (PC) + 2mM ADP + 5mM G + 10mM succinate (S) + 10μM cytochrome C (Cyto C) (as a quality control of the PmFB preparation) + 10μg/ml Oligomycin (Oligo, inhibitor of mitochondrial ATP synthase) + 2μM FCCP (carbonylcyanide-p-trifluoromethoxy-phenylhydrazone, a potent protonophoric uncoupler of OXPHOS). In another protocol, JO_2 & $\Delta\Psi_m$ were simultaneously measured from the same PmFBs. The newly developed Oroboros tetraphenylphosphonium (TPP^+)

-selective electrode is an ion selective electrode (ISE) that integrates into the O2K chamber for simultaneous recording of oxygen and TPP^+. TPP^+ accumulates in the mitochondrial matrix as a function of the $\Delta\Psi_m$. 2U/ml hexokinase (HK)/ 5mM 2-deoxyglucose (2-DOG)/ 10mM G/ 15mM pyruvate (Pyr)/ 2mM M/ 10mM Glycerol-3-Phosphate (G3P)/ 10mM S were added into the chamber in the beginning. After the $pTPP^+$ signal reaches a steady status, the TPP^+-selective electrode was calibrated by a 5 point titration range from 1.1 to 1.5μM TPP^+. The sensitivity was calculated from the actual TPP^+ working range. PmFB was added into the chamber to obtain the maximal state IV $\Delta\Psi_m$ and JO_2. An ADP titration (25, 50, 100, 250, 500, 1000, 2000μM) was followed to obtain the kinetics of state III $\Delta\Psi_m$ and JO_2. Finally, 2μM FCCP was added to collapse $\Delta\Psi_m$ driven TPP^+ uptake. The criteria of steady state $pTPP^+$ signal (gain of 10) in each condition is defined as below: raw $pTPP^+$ slope = 0 to 0.003 $mpTPP^+$/s during TPP^+ titration; 0 to -0.002 $mpTPP^+$/s in 0-250μM ADP; 0 to -0.003 $mpTPP^+$/sec in 500μM ADP; 0 to -0.006 $mpTPP^+$/sec in 1000 and 2000μM ADP. The mathematics of $\Delta\Psi_m$ is based on classical Nernst equation with binding correction factors and assumed mitochondrial protein content to freeze dried muscle fiber weight ratio. Oroboros TPP^+-$\Delta\Psi_m$ calculation template (http://www.oroboros.at for detail) was used with minor modifications in order to apply the internal chemical background correction factor. This correction factor is defined as the instantaneous difference of stable signal between immediately before and 4-8 seconds following the chemical addition, which causes an artificial signal spike. It is based on 2 observations: 1) Due to the structure nature of PmFB, it appears that the re-distribution of TPP^+ upon substrate addition is much slower (than cell or isolated mitochondria) although the change in $\Delta\Psi_m$ may occur sooner, 2) ADP instantly causes a dose-dependent steady chemical

background effect (small reduction) on $pTPP^+$ signal in a system without biological sample. Equation as below:

$$\Delta\Psi = \frac{RT}{zF} \cdot \ln\left(\frac{\frac{n_{\mathrm{add}}}{c_{\mathrm{ext,free}}} - V_{\mathrm{ext}} - K_{\mathrm{O}}^{'} \cdot P_{\mathrm{C}}}{V_{\mathrm{mt}}(\mathrm{spec}) \cdot P_{\mathrm{mt}} + K_{\mathrm{i}}^{'} \cdot P_{\mathrm{mt}}} \right)$$

- n_{add}: total amount of probe ions added to the system.
- $C_{ext,free}$: free concentration of probe ion outside mitochondria.
- V_{ext}: external volume: total solution volume outside mitochondria.
- V_{mt}(spec): mass specific mitochondrial matrix volume (per mass of mitochondrial protein) = 1µl/mg[216-218].
- K_i': apparent partition coefficient describing internal binding = 7.9µl/mg[216].
- K_o': apparent partition coefficient describing external binding = 14.3µl/mg[216].
- P_{mt}: total mitochondrial protein content (as a marker for mitochondrial membrane content). Assumed to be 15% of freeze dried muscle fiber weight.
- P_c: total cellular protein content (as a marker for cellular membrane and other material content) = freeze dried muscle fiber weight.

Measuring Mitochondrial H_2O_2 Emitting Potential in PmFBs

The $_mE_{H2O2}$ of PmFBs (~0.3mg after freeze-dried) was measured by continuously monitoring fluorescence probe Amplex Ultra-Red (Invitrogen, A36006; excitation/emission: 568/581nm) using Fluorolog-3 (Horiba Jobin Yvon, Edison, NJ) spectrofluorometers with temperature control at 25°C and magnetic stirring. $_mE_{H2O2}$ protocol 1 is a parallel protocol of JO_2 & $\Delta\Psi_m$ protocol. The assay buffer condition is the

same with additional 2U/ml HK/ 5mM 2-DOG/ 6 U/ml HRP/ 25 U/ml CuZn-SOD/ 50μM Amplex Ultra-Red. After establishing a background fluorescence rate in the presence of a PmFB, the reaction is initiated by the addition of sequential substrates, G/Pyr/M/G3P/S+ADP titration (same concentration as in JO_2 & $\Delta\Psi_m$ protocol). For $_mE_{H2O2}$ protocol 2 and 3 the assay buffer condition is the same as JO_2 & $\Delta\Psi_m$ protocols with additional 6U/ml HRP/ 25U/ml CuZn-SOD/ 50μM Amplex Ultra-Red. After establishing a background fluorescence rate in the presence of a PmFB, the reaction is initiated by either 10mM G3P + 25μM PC in protocol 2 or 10mM S + 10mM G3P in protocol 3. $_mE_{H2O2}$ production rate is calculated from the slope of ΔF/min, after subtracting background, using a standard curve established for each reaction condition.

Measuring Mitochondrial Calcium Retention Capacity ($_mCa^{2+}_{RC}$) in PmFBs

The PmFBs (~0.2mg after freeze-dried) $_mCa^{2+}_{RC}$ were measured by continuously monitoring fluorescence probe calcium green 5N salt (Ca5N, Invitrogen, C3737; excitation/emission: 506/532 nm) using Spex Fluoromax 3 (Horiba Jobin Yvon, Edison, NJ) spectrofluorometers with temperature control at 25°C and magnetic stirring. The assay buffer condition is the same as JO_2 & $\Delta\Psi_m$ protocol with only 40μM EGTA and additional 2U/ml HK/ 5mM 2-DOG/ 1μM Ca5N/ 1.5 μM thapsigargin (sarco/endoplasmic reticulum Ca^{2+}-ATPase inhibitor). The assays were started with the G/Pyr/M/G3P/S (same concentration as in JO_2 & $\Delta\Psi_m$ protocol) plus 0, 25 or 500μM ADP in each individual experiment. After a steady background fluorescence intensity is obtained (~5min), the first pulse $CaCl_2$ of 75μM is added followed by 50μM pulses of $CaCl_2$ at the time interval of 15-30min/pulse based on the Ca^{2+} uptake rate. The fluorophore fluoresces in the presence of extra-mitochondrial Ca^{2+}, so that a decline in fluorescence intensity is indicative of mitochondrial Ca^{2+} uptake. PTP opening is evident when

mitochondria start to no longer take-up or rapidly release Ca^{2+}. In the end, 2.5mM $CaCl_2$ was added followed by 1~2 additions of 0.67mM $CaCl_2$ to obtain fluorescence of the calcium-saturated probe in order to quantify the total Ca^{2+} uptake.

At the conclusion of each experiment, PmFB were washed in ddH_2O to remove salts and then freeze-dried in a lyophilizer (LabConco). JO_2, $_mE_{H2O2}$ and $_mCa^{2+}{}_{RC}$ were normalized to dry tissue weight.

Statistics

All statistical analysis was performed using GraphPad Prism 5.02 (GraphPad software, San Diego, California). Unless specified otherwise, data are presented as mean ± S.E.M. from n=8~10/group. The statistical differences among groups under the same substrate or ADP concentration condition in each experiment was analyzed using the independent one-way ANOVA with Tukey post-hoc test. Statistical significance power was set at $p<0.05$. Since the "ceiling effect" was observed, independent T-tests were used for $\Delta\Psi_m$ data with statistical significance power set at $p<0.1$.

Results

Neither Single Lipid Loading nor Low Intensity Exercise Affect Mitochondrial Respiration Capacity

To determine if a single lipid loading or exercise has an effect on mitochondrial respiration (JO_2) capacity in skeletal muscle of rats, we measured JO_2 in PmFBs from the red gastrocnemius muscle. Neither single lipid loading nor exercise had a significant effect on palmitoyl-carnitine-supported maximal JO_2 capacity in combination with complex I (malate/ glutamate) or complex II substrate (succinate), nor maximal uncoupled FCCP-stimulated JO_2 (Fig. 2-2).

Low Intensity Exercise Attenuates Elevated State IV $_mE_{H2O2}$ Associated with Single Lipid Loading

It is not clear if single lipid loading induced ROS production potential can be attenuated by a post-meal low intensity exercise, although indirect data from single moderate exercise are available[193]. In this study, state IV ROS production mediated by succinate-induced reverse electron flux and/or lipid based substrates including glycerol-3-phosphate and palmitoyl-L-carnitine were measured from PmFBs. As shown in figure 2-3, single lipid loading caused a two fold increase in $_mE_{H2O2}$ versus untreated rats ($P<0.05$) in each substrate condition. This effect was nearly or completely normalized under all substrate conditions when low intensity exercise was performed after lipid ingestion.

Low Intensity Exercise Attenuates the Single Lipid Loading-Induced Increase $_mE_{H2O2}$ and Reduction in $_mCa^{2+}_{RC}$ with Slight Increase in JO_2 and Reduction in $\Delta\Psi_m$ in State III Condition

To further test whether low intensity exercise attenuates the single lipid loading-induced $_mE_{H2O2}$ under more physiological respiratory conditions, a series of kinetic experiments were performed in PmFBs across a wide range JO_2 levels (clamped state III).

JO_2 and $\Delta\Psi_m$ in both state IV and III conditions. The control experiment, figure 2-4 (A), showed no inhibition of 1.5μM TPP^+ on PmFB JO_2 under the same substrate protocols as in figure 2-5 or 2-6 (A). The TPP^+ electrode used showed a relatively high sensitivity (53.56±3.03mV/Decade, mean±SD, n=36; 59.13mV/Decade in theory) under our experimental conditions (Fig. 2-4 (B)). Shown in figure 2-5 are the representative traces from the control experiment. We simultaneously measured JO_2 and $\Delta\Psi_m$

supported by multiple substrates across a wide range of state III respiration levels (ADP titration). The quantified data (Fig. 2-6. (A)) show a single lipid loading slightly increases $\Delta\Psi_m$ with very little effect on JO_2 while low intensity exercise performed after lipid loading causes a mild increase in JO_2 and normalizes the single lipid loading-induced increase in $\Delta\Psi_m$ across multiple [ADP] conditions. It appears mitochondria are operating in a relatively tight $\Delta\Psi_m$ range (-145 to -170mV) across different JO_2 states.

$_mE_{H2O2}$ in both state IV and III conditions. As expected, $_mE_{H2O2}$ decreased rapidly in the transition from State IV to State III respiration. In addition, consistent with the $\Delta\Psi_m$ data (Fig. 2-6. (A)), $_mE_{H2O2}$ was highest after lipid loading but was normalized to at or below control rates when low intensity exercise was performed after the lipid loading (Fig. 2-6. (B)). A slightly higher JO_2 with the similar $\Delta\Psi_m$ may explain the observation of lower $_mE_{H2O2}$.

$_mCa^{2+}_{RC}$ in both state IV and III conditions. The mitochondrial permeability transition pore is sensitive to various cellular stresses including calcium[219-221] and ROS[222,223]. Figure 2-6 (C) shows low intensity exercise partially attenuated the single lipid loading-induced reduction in $_mCa^{2+}_{RC}$ under state III but not state IV conditions.

Discussion

Although postprandial systemic oxidative stress has long been observed following a lipid rich meal[202], the potential acute impact of lipid rich meals on mitochondrial function has not been studied. Furthermore, the benefits of regular exercise on metabolism, as well as mitochondria related effects, have been greatly acknowledged. Whether post-meal mild exercise may ameliorate the lipid induced postprandial oxidative stress and related defects is still not clear. More direct and

physiological evidence from mitochondria in working skeletal muscle is required to establish this relationship. In this context, our results provide evidence that, in the absence of mitochondrial dysfunction (in terms of JO_2 kinetics and maximal capacity) skeletal muscle $_mE_{H2O2}$, $\Delta\Psi_m$ and $_mCa^{2+}_{RC}$ are acutely sensitive to changes in metabolic status. There are several important and novel findings from the present study. *First*, acute lipid overloading induced by oral gavage of ~12% of daily total caloric intake (when fed with high fat diet) increased state IV $_mE_{H2O2}$ under multiple substrate conditions. This change in $_mE_{H2O2}$ occurred in the absence of any change in respiratory function. *Second,* mild exercise performed after the lipid load completely prevented the increase in $_mE_{H2O2}$. *Third*, consistent with the $_mE_{H2O2}$ data, state IV $\Delta\Psi_m$ was highest after acute lipid loading and lowest when exercise was performed after lipid loading. State IV JO_2 was also slightly elevated in the lipid plus exercise group. *Fourth*, as expected, transitioning to state III respiration sharply decreased both $\Delta\Psi_m$ and $_mE_{H2O2}$. However, the greater $\Delta\Psi_m$ and $_mE_{H2O2}$ induced by lipid load and apparent protection afforded by exercise present under state IV was also evident under mild to moderate state III respiratory conditions. *Fifth*, also under mild to moderate state III conditions, acute lipid load decreased $_mCa^{2+}_{RC}$, indicative of altered permeability transition pore function. Together, these findings provide strong evidence that mitochondrial oxidant production and related effects are very sensitive and dynamically regulated by metabolic status. It suggests an increase in $\Delta\Psi_m$ for a given substrate condition may be a primary factor driving the downstream cellular consequences of lipid loading, and that the increase in $\Delta\Psi_m$ is attenuated by mild exercise. Although further work is certainly required, it is tempting to speculate that the cumulative effects of transient increases in oxidant production following lipid meals may be responsible for the loss of mitochondria

density observed in long-term substrate oversupply conditions, ultimately leading to the mitochondrial dysfunction associated with metabolic diseases (e.g. diabetes). At the mitochondrial level, the balance of substrate supply and energy demand on a daily basis is likely critical for maintaining proper cellular redox environment and therefore cellular function and whole body health.

Several studies have observed an increase in oxidative stress with obesity, diabetes[21,63,64,224], and a number of other diseases[225-227]. The common $_{m}E_{H2O2}$[62-64,228-230], $\Delta\Psi_m$[231] and $_{m}Ca^{2+}_{RC}$[232-235] measurements are frequently performed under state IV respiration conditions. However, experimental state IV mitochondrial respiration does not exist *in vivo*, as different levels of state III respiration, based on metabolic status, are closer to the physiological condition *in vivo*. Thus, further evidence from state III respiration is required to examine the potential link between metabolic disease and mitochondrial ROS production, as well as $\Delta\Psi_m$ and $_{m}Ca^{2+}_{RC}$ in a more physiological manner. With the newly developed hexokinase dependent ADP regeneration system[81,85,86,236,237] in PmFBs[64,228,229], *in situ* state III "clamp" technique was successfully developed in our laboratory[236]. A second ADP regeneration system (endogenous mitochondrial creatine kinase and additional creatine[81,86,238]) was also applied in this study to maximize efficiency. We used this technique to investigate the relationship between substrate supply and metabolic demand on $\Delta\Psi_m$ and ROS production across different JO_2 levels which mimic different metabolic/physical activity states. Contrary to the widely held belief that electron leak and $O2^{\bar{}}\bullet$ formation occur only under state IV conditions, our findings (Fig. 2-6. (B)) reveal relatively low but appreciable $_{m}E_{H2O2}$ even under moderate-high state III conditions. These findings suggest that ROS production does occur *in vivo* and studies should be conducted under state III more typical of the

condition present *in vivo*. Based on the kinetics' relationship (Fig. 2-6), by clinically manipulating different mitochondrial respiratory levels, the energy expenditure level required to normalize the over nutrition induced oxidative stress can be revealed at the mitochondrial level.

The present data shows that acute lipid loading had no clear effect on mitochondrial OXPHOS capacity, while it elevated the $\Delta\Psi_m$, $_mE_{H2O2}$ and reduced $_mCa^{2+}_{RC}$. These findings suggest that reduced OXPHOS capacity is less likely the preceding factor of long-term HFD induced mitochondrial defect and related metabolic diseases. Evidence for reduced mitochondrial OXPHOS activity or respiration[16,17,27,28] has been shown to associate with long-term substrate oversupply such as occurs with IR or T2D. However, mounting evidence also suggests that mitochondrial dysfunction represents a secondary event in the development of IR or T2D[35-37,63,64]. In fact, short-term or early stage HFD feeding could actually promote mitochondrial density and fatty acid oxidation activity due to a prompt adaptive response[19,42,44,51]. Our mitochondrial respiration data support this idea in which significantly reduced mitochondrial OXPHOS capacity is less likely to occur in the beginning, at least, of lipid loading. Instead, our data further indicate that oxidative stress and related parameters can be elevated very quickly by lipid overloading and could be the preceding or among the primary factors that leads to metabolic diseases.

The treatment effect on $_mE_{H2O2}$ is clear. However, whether the $_mE_{H2O2}$ change was contributed by the treatment effect on mitochondrial oxidant production and/or anti-oxidant scavenging/buffering system (i.e., GSH/GSSG, thioredoxin and others) is unknown. Previous findings from our group provide evidence showing that skeletal muscle intracellular redox environment was acutely shifted to a more oxidized state

(reduced GSH/GSSG ratio) by an acute glucose injection[64] with a lower caloric loading compare with this study. In addition, it was shown that lipid rich meal acutely cause more oxidative stress than iso-caloric CHO rich meal[202]. With these, the GSH/GSSG ratio after lipid loading may be reduced and indicates a reduced anti-oxidant scavenging/buffering capacity. Further, since the $\Delta\Psi_m$ was affected by the treatments, this may indicate a change in oxidant production potential as well. Further study is required to confirm it.

Although ROS production and OXPHOS capacity have been well studied, the impact of metabolic imbalance on $\Delta\Psi_m$, which is the fundamental control of ROS production, is relatively less understood. Despite data from cell or isolated mitochondria using fluorescent imaging and/or flow cytometry, the evidence from *in situ* or even *in vivo* experiments show the metabolic intervention on $\Delta\Psi_m$ under state III condition without using any mitochondrial complex inhibitor is still very limited. In this study, the $\Delta\Psi_m$ and the rate of oxygen consumption were simultaneously measured by Oroboros oxygraph with newly developed TPP^+-selective electrode. Not only does the TPP^+ method provide better sensitivity and quantification, the $\Delta\Psi_m$ data in this study also has higher physiological relevance since it was measured from PmFBs *in situ*, the first such data reported under state IV-III respiration kinetic conditions.

Prior research shows that a 6hr lipid infusion decreases $\Delta\Psi_m$ by 33% of non-energized resting human intact skeletal muscle fibers by using TMRE stain and confocal[239]. However the better quantified $\Delta\Psi_m$ under energized status is unknown. The present data show slightly increased energized state III $\Delta\Psi_m$ in acute lipid loaded rats which was prevented by exercise. Interestingly, $\Delta\Psi_m$ during low JO_2 states was not affected by lipid loading but tended to be lower when followed with exercise. The lipid

group had the highest $\Delta\Psi_m$ without affecting JO_2. The state III $\Delta\Psi_m$ was similar between control, exercise, and lipid+exercise groups, but JO_2 tended to be higher in the exercise group. Our data indicate higher $\Delta\Psi_m$ and ROS production can be caused in a short time by lipid loading if no increased in energy demand. Although it was shown that skeletal muscle uncoupling protein 2 (UCP2) and UCP3 mRNA levels was enhanced in lean Zucker rats after 24h intralipid continuously infusion[240], the protein level is unlikely be different within 2h after the lipid loading in our study. Further, it was shown that fatty acid promote UCP2 and 3 activity[241,242] which should attenuate the $_mE_{H2O2}$, $\Delta\Psi_m$ and maybe even reduce JO_2 in some degree. In our study, however it seems that uncoupling protein (UCP) activity is less likely a significant contributing factor since both $_mE_{H2O2}$ and $\Delta\Psi_m$ are still high while JO_2 is unaffected. On the other hand, it seems exercise activates respiratory enzymes which make the mitochondria more coupled and therefore more able to maintain $\Delta\Psi_m$ when subjected to a given substrate stress under state III condition. Similar lipid effects were found from other laboratories. A trend for an increase in succinate supported state IV $\Delta\Psi_m$ or proton leak kinetics (the kinetic relationship of H^+ flux to $\Delta\Psi_m$ through simultaneous recording of oxygen consumption and potential) has been reported in isolated skeletal muscle mitochondria of C57BL/6 mice[243] and S-D rats[244] on a long term HFD. Isolated liver mitochondria from diabetic Goto-Kakizaki (GK) rats show higher $\Delta\Psi_m$ under both energized state IV[245,246] and low state III[245] respiration when compared with control Wistar rats[245], although no $\Delta\Psi_m$ difference was found in isolated brain, kidney, skeletal muscle mitochondria in the same animal model[246] or isolated cardiac mitochondria from streptozotocin-induced diabetic rat model[247]. However, some neutral or opposite results were also found. Isolated liver mitochondria from rats fed a HFD for 7 weeks show no change in succinate supported

state IV $\Delta\Psi_m$, proton leak rate/kinetics, and maximal state III $\Delta\Psi_m$, although increased oxidative stress and impaired glucose tolerance were observed[237]. In addition, despite increased oxidative or nitrosative stress, high glucose and/or high FFA cultured adipocytes[248] and isolated liver mitochondria from 16 weeks HFD fed mice[249] both show decreased $\Delta\Psi_m$ in an energized state[248]. Collectively, the development of oxidative stress is very consistent, but the impact of lipid loading on $\Delta\Psi_m$ is less predictable depending on the: energy status or substrate condition, duration of the metabolic intervention, and method of $\Delta\Psi_m$ measurement. Even though inconsistent data has been found, $\Delta\Psi_m$ appears to operate within a small range in a given substrate condition and is less easily affected by a metabolic intervention (i.e., a ceiling effect). In the short-term, when substrate supply is high without an increase in energy expenditure, it tends to cause high $\Delta\Psi_m$. However, if the high lipid is continued, $\Delta\Psi_m$ and ROS may cause lipid-enriched mitochondrial membrane composition modifications and structural damage, which could impair the ability of mitochondria to develop a sufficient $\Delta\Psi_m$ and eventually cause reduced $\Delta\Psi_m$, OXPHOS capacity and mitophagy although ROS production is still high.

Reduced mitochondrial density is a prominent characteristic of skeletal muscle from obese/diabetic individuals. The implication is that prolonged nutritional overload leads to mitochondrial degeneration and loss of mitochondrial content due to mitophagy and/or mitoptosis. The mPTP is a large conductance channel in the mitochondrial inner membrane comprised of multiple proteins which have not been fully identified. mPTP is sensitive to various cellular stresses, including calcium[219-221,250] and ROS[222,223,250]. The opening of the mPTP triggers the collapse of $\Delta\Psi_m$, release of pro-apoptotic factors, and mitochondrial degeneration. ${}_mCa^{2+}{}_{RC}$ is a negative indicator of the susceptibility of

permeability transition pore opening, or apoptosis upon matrix Ca^{2+} accumulation. An increase in $\Delta\Psi_m$ and reduced cell viability have been shown in cells either cultured with high glucose or fructose[233]. However, the direct evidence of substrate acute or over supply on ${}_mCa^{2+}{}_{RC}$ is limited, not to mention *in vivo* or *in situ* conditions. Although partial negative effects have been reported[251], both single bout endurance exercise[218] and long-term regular endurance training[252] have been shown to improve ${}_mCa^{2+}{}_{RC}$ under different stress states. Our data further show that under clamped state III respiratory conditions, supported by multiple substrates, low intensity exercise attenuates the single lipid loading mediated reduction (~35%) in skeletal muscle ${}_mCa^{2+}{}_{RC}$ *in situ*. This is the condition predominantly stressed by Ca^{2+}. During state IV, however, there is no clear treatment effect on ${}_mCa^{2+}{}_{RC}$. It may be due to the synergized effect of the Ca^{2+} stress and relatively high state IV $\Delta\Psi_m$ and ${}_mE_{H2O2}$ that exceed a certain threshold regardless of the treatment effect. In addition, a striking ${}_mCa^{2+}{}_{RC}$ difference between state IV and state III respiration condition was also observed. Under low state III condition (50μM ADP), ${}_mCa^{2+}{}_{RC}$ is dramatically increased when compared with state IV. However, there was only a minimal difference in ${}_mCa^{2+}{}_{RC}$ between low and high state III respiration conditions. It has been previously reported that the sensitivity of the mPTP opening to matrix Ca^{2+} accumulation can be greatly reduced by ATP and ADP due to their ability to act as substrates of the adenine nucleotide translocase (ANT)[250,253,254]. By default, reduction in $\Delta\Psi_m$ and ROS production under state III respiration also plays a role. This exponential relationship between ADP levels (or JO_2 levels) and Ca^{2+}-induced mPTP opening sensitivity brings up the physiological concern of experimental conditions similar to the ROS production measurements. Similar ${}_mCa^{2+}{}_{RC}$ experiments were often performed under state IV condition supported with multiple substrates or even solely

with high superoxide-causing succinate. However, a more preferred condition to evaluate the $_{m}Ca^{2+}_{RC}$ should be performed under “clamped” moderate state III condition supported with multiple substrates which mimic the more physiological substrate condition and the levels of JO_2, $\Delta\Psi_m$ and $_{m}E_{H2O2}$. It is well known that both high $\Delta\Psi_m$ and ROS trigger mitochondrial permeability transition although the mechanism is still largely unknown. Recent advances in redox biology identified the structure and enzymatic activity of proteins within the mPTP complex that are capable of undergoing reversibe redox modification could be responsible for mPTP opening[255-257]. Collectively, these findings suggest that exercise may ameliorate the higher level of mitophagy and/or mitoptosis normally associated with long-term substrate oversupply (e.g., obesity and diabetes) by preserving the reduced redox status of the mPTP complex due to the exercise-induced increase in JO_2 and the associated reduction in $\Delta\Psi_m$ and ROS production.

It has been shown long-term over nutrition, particularly lipid, is associated with oxidative stress and could causally lead to insulin resistance and mitochondrial dysfunction[63,64]. It is less appreciated how a single metabolic challenge could dynamically affect the control of mitochondria, (e.g. JO_2, $\Delta\Psi_m$, ROS production and apoptosis susceptibility). Our data suggest that $\Delta\Psi_m$ is in a constant state of flux during the day, depending on 1) the local intracellular rate of ATP utilization and 2) the rate at which reducing equivalents are presented to the mitochondria relative to energy demand (e.g., low ATP demand and high intracellular energy supply raise $\Delta\Psi_m$, high ATP demand lowers $\Delta\Psi_m$). Keeping in mind that the $\Delta\Psi_m$ at which superoxide begins to form significantly is fairly high (i.e., more negative than about -160mV), we envision (Fig. 2-8) that $\Delta\Psi_m$ oscillates above and below this threshold during the course of the day,

particularly in skeletal muscle. The more time spent inactive and under a positive energy balance, the more time $\Delta\Psi_m$ is likely to exceed the threshold, thus favoring mitochondrial ROS production and apoptosis susceptibility. Conversely, the more time spent active and in metabolic balance, the less $\Delta\Psi_m$ will rise above the threshold at which electrons leak to oxygen.

Conclusion

The interplay between substrate supply and metabolic demand is at the heart of cellular metabolic balance and the consequences of metabolic imbalance. This study provides mechanistic insights on the acute impact of cellular energy supply relative to demand on the control of $\Delta\Psi_m$, ROS production, and apoptosis susceptibility. Our data emphasize the deleterious effects of acute lipid oversupply at the mitochondrial and cellular level can occur rapidly, but can be sufficiently counterbalanced by mild increase in energy demand (low intensity exercise). Increased energy expenditure is fundamental to the preservation of mitochondrial function/integrity and/or for preventing oxidative stress on a daily basis.

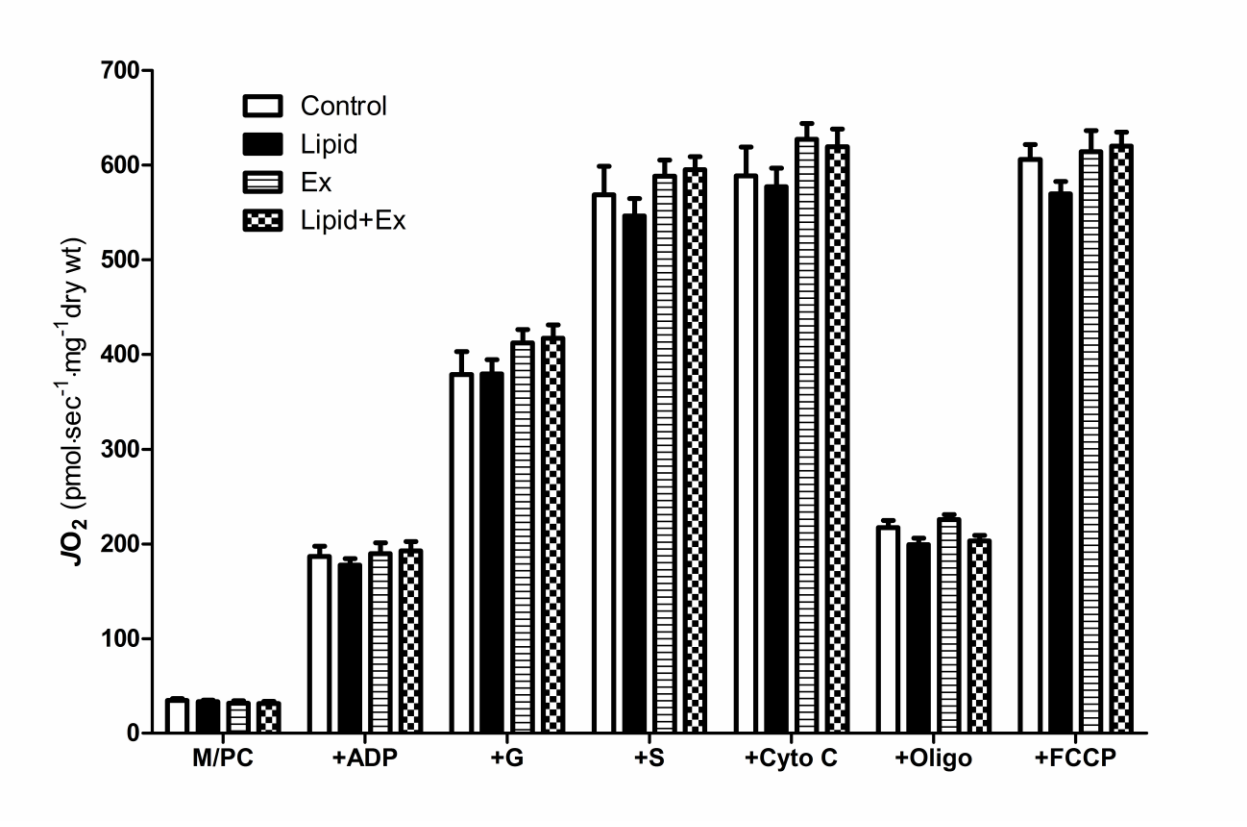

Figure 2-2. A single lipid loading or low intensity exercise has no effect on muscle mitochondrial respiration capacity. PmFBs mitochondrial respiration capacity was supported by: 2mM malate/ 25μM palmitoyl-L-carnitine (M/PC) + 2mM ADP + 5mM glutamate (G) + 10mM succinate (S) + 10μM cytochrome C (Cyto C) + 10μg/ml oligomycin (Oligo) + 4μM FCCP.

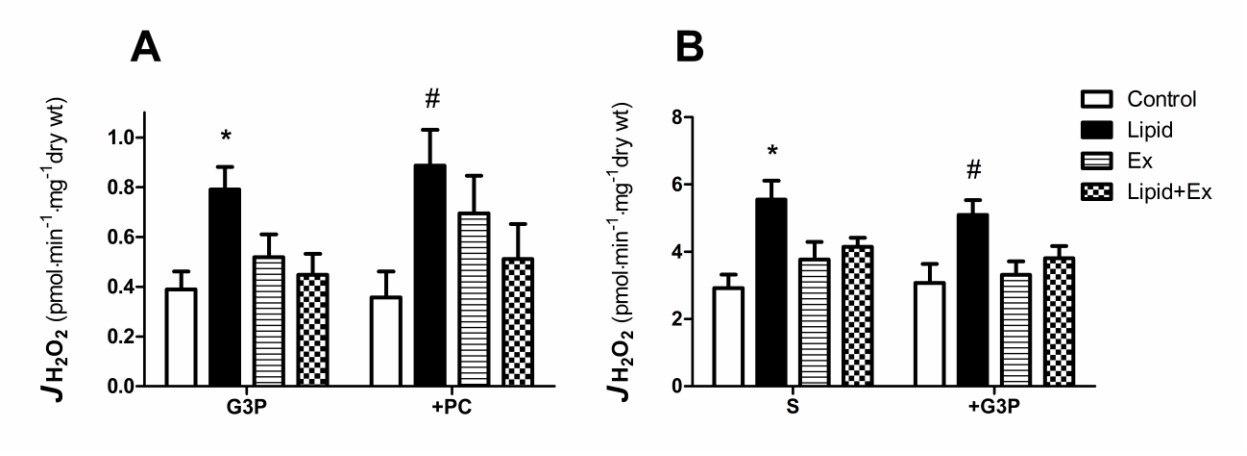

Figure 2-3. Low intensity exercise attenuates the single lipid loading-induced increase in mitochondrial H2O2 emitting potential ($_mE_{H2O2}$) during state IV respiration. (A) Muscle $_mE_{H2O2}$ in response to lipid based substrates 10mM glycerol-3-phosphate (G3P) + 25μM palmitoyl-L-carnitine (PC). G3P stresses the system by feeding electron into Q cycle via mitochondrial glycerol-3-phosphate dehydrogenase in the form of $FADH_2$. PC provides electrons in the form of NADH and $FADH_2$ via β-oxidation. * $p<0.05$ vs Control & Lipid+Ex. # $p<0.05$ vs Control. (B) Muscle $_mE_{H2O2}$ in response to complex I reverse electron flux by complex II substrate 10mM succinate (S). 10mM G3P was further added to provide additional strain. * $p<0.05$ vs Control. # $p<0.05$ vs Control & Ex.

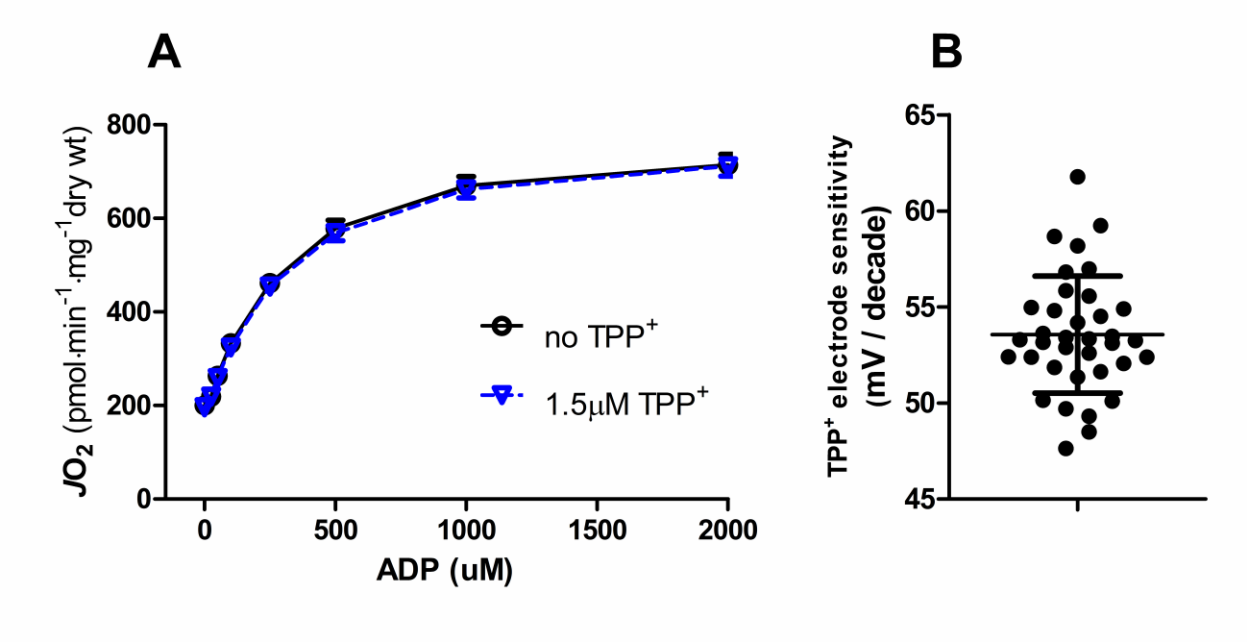

Figure 2-4. TPP^+ (1.5μM) has no affect on mitochondrial respiration but provides high TPP^+ electrode sensitivity. (A) In PmFBs, a control experiment shows no inhibition of mitochondrial respiration by 1.5 μM TPP+ using the same substrate protocol as in figure 2-5 or figure 2-6 (A). n= 8-10/condition evenly obtain from 2 rats. (B) The TPP^+ electrode sensitivity obtained from the experiment in figure 2-6 (A) is 53.56±3.034 mV/Decade (mean±SD, n=36).

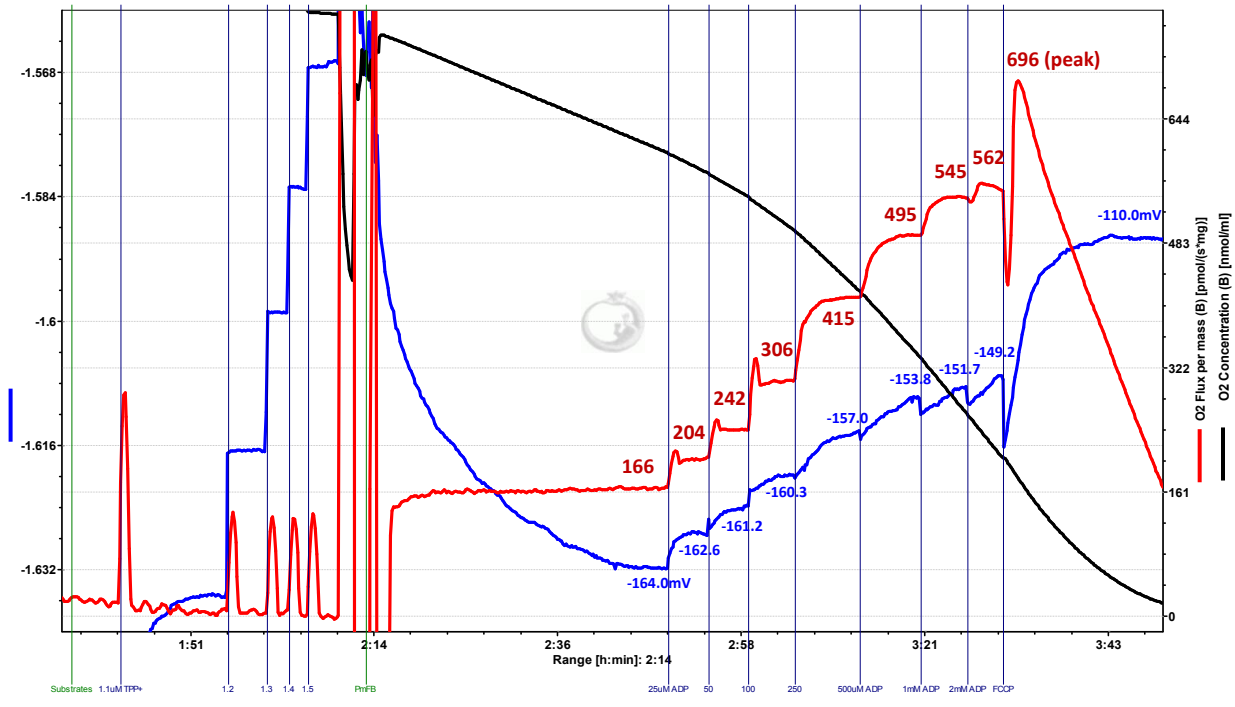

Figure 2-5. Representative experimental trace of $\Delta\Psi_m$ & JO_2. Reagents added at the start of the experiment include State III respiration "clamping" reagents: 2U/ml hexokinase and 5mM 2-deoxyglucose; mitochondrial substrates: 10mM glutamate/ 15mM pyruvate/ 2mM malate/ 10mM glycerol-3-phosphate/ 10mM succinate. After the $pTPP^+$ signal reaches a steady state, the TPP^+-selective electrode was calibrated by a 5 point TPP^+ titration range from 1.1 to 1.5μM TPP^+. The calibration and sensitivity calculation was based on the actual TPP^+ working range. PmFBs were added into the chamber to obtain the maximal state IV $\Delta\Psi_m$ and JO_2. An ADP titration (25, 50, 100, 250, 500, 1000, 2000μM) followed to obtain the kinetics of state III $\Delta\Psi_m$ and JO_2. 2μM FCCP was added in the end to prove the concept that TPP^+ uptake is $\Delta\Psi_m$ driven. The calculated steady state $\Delta\Psi_m$ and JO_2 is indicated. The experiment was performed at 25ºC. Blue line: $pTPP^+$. Red line: JO_2. Black line: $[O_2]$.

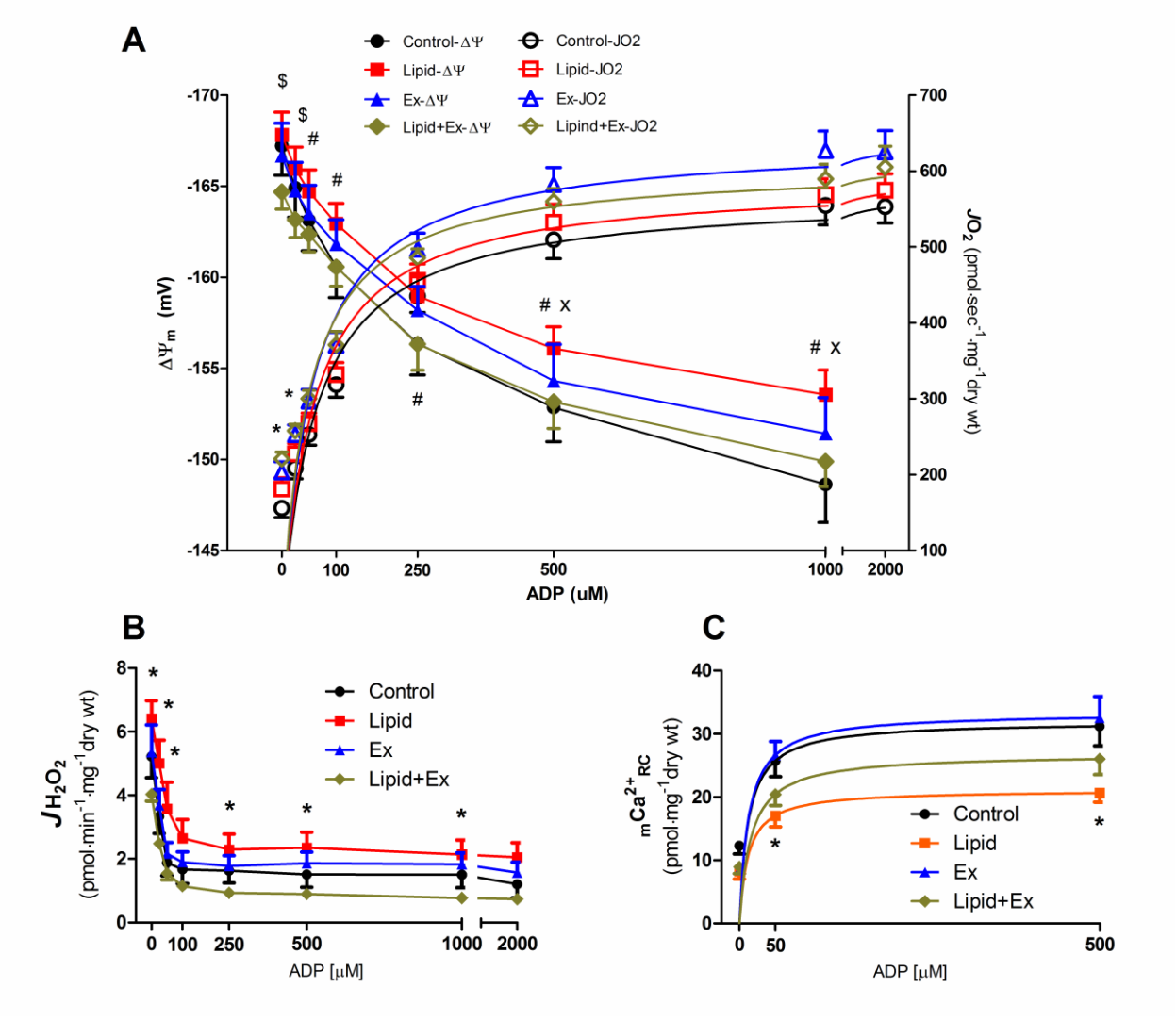

Figure 2-6. Low intensity exercise attenuates the single lipid loading-induced increase in $_mE_{H2O2}$ and reduction in $_mCa^{2+}{}_{RC}$, with increasing JO_2 and reducing $\Delta\Psi_m$. To determine if low intensity exercise is sufficient to attenuate the potential negative effect on JO_2, $\Delta\Psi_m$, $_mE_{H2O2}$ and $_mCa^{2+}{}_{RC}$ by single lipid loading in skeletal muscle from rats, the kinetics of these parameters under state IV-III conditions from PmFBs mitochondria were measured. Each experiment was performed essentially in parallel under similar buffering conditions supported with the same substrate protocol. 2U/ml hexokinase and 5mM 2-deoxyglucose were included in the system to "clamp" different level

physiological state III respiration states. Multiple substrates including10mM glutamate/ 15mM pyruvate/ 2mM malate/ 10mM glycerol-3-phosphate/ 10mM succinate were added in the beginning of the protocol to obtain a maximal state IV response. An ADP titration (25, 50, 100, 250, 500, 1000, 2000μM) followed to obtain the state III kinetics response in panel (A) and (B). In panel (C), data from each ADP concentration represents each individual experiment/PmFB under the same buffer and substrate background as panel (A) and (B). (A) JO_2 and $\Delta\Psi_m$. JO_2 and $\Delta\Psi_m$ were simultaneously measured from the same PmFB. Single lipid loading has very little effect on JO_2 while low intensity exercise causes a mildly increased JO_2 across different [ADP] conditions. In JO_2: * $p<0.05$ Lipid+Ex vs Control at 0 and 25μM ADP. Slightly increased $\Delta\Psi_m$ by single lipid loading was normalized by exercise. A less conservative statistics method was applied and significance power was set at $p<0.05$ or $p<0.1$. $\Delta\Psi_m$ at 2000μM was not reported since many of the raw pTPP+ signal above 1000μM ADP were not very steady and did not meet the steady status criteria. In $\Delta\Psi_m$: $ $p<0.05$ Lipid vs Lipid+Ex; # $p<0.1$ Lipid vs Lipid+Ex; x $p<0.1$ Lipid vs control; T-test. (B) Low intensity exercise maintain lower $_mE_{H2O2}$ after rats received single lipid loading in both state IV and state III condition. * $p<0.05$ Lipid vs Lipid+Ex. (C) Exercise attenuate the single lipid loading-induced reduction in calcium retention capacity under state III but not state IV condition. * $p<0.05$ Lipid vs Control & Ex. Each data set was examed by one-way ANOVA + Tukey in each [ADP] condition expect panel (A) $\Delta\Psi_m$ data was examed by t-test.

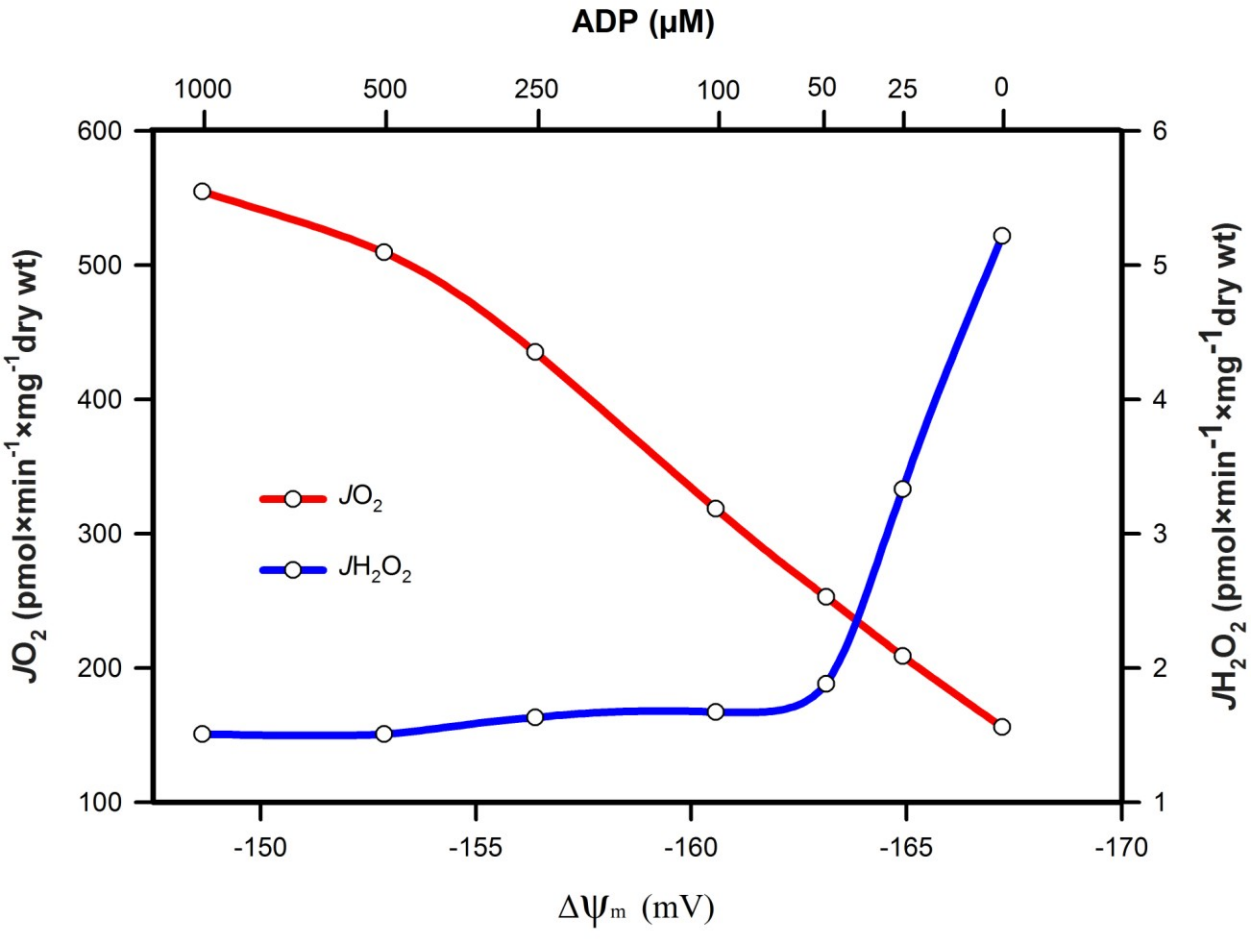

Figure 2-7. Mitochondrial membrane potential, OXPHOS and H_2O_2 emission kinetics. The control group $\Delta\Psi_m$, JO_2 and JH_2O_2 kinetics data from figure 2-6 was further plotted. Mitochondria of permeabilized rat red gastrocnemius muscle was supported by 10mM Glutamate/ 15mM Pyruvate/ 2mM Malate/ 10mM Glycerol-3-Phosphate/ 10mM Succinate. It was followed by ADP titration. Assays were performed in 25ºC with 25uM blebbstatin to prevent muscle contraction and with 2U/ml hexokinase/ 5mM 2-deoxyglucose/ 20mM creatine to "clamp" the [ADP] level. This proves the concept of bioenergetics principle that mild increase in mitochondrial respiration (energy expenditure) from idling reduces mitochondrial membrane potential ($\Delta\Psi_m$) and exponentially reduces H_2O_2 emission rate. N = 8.

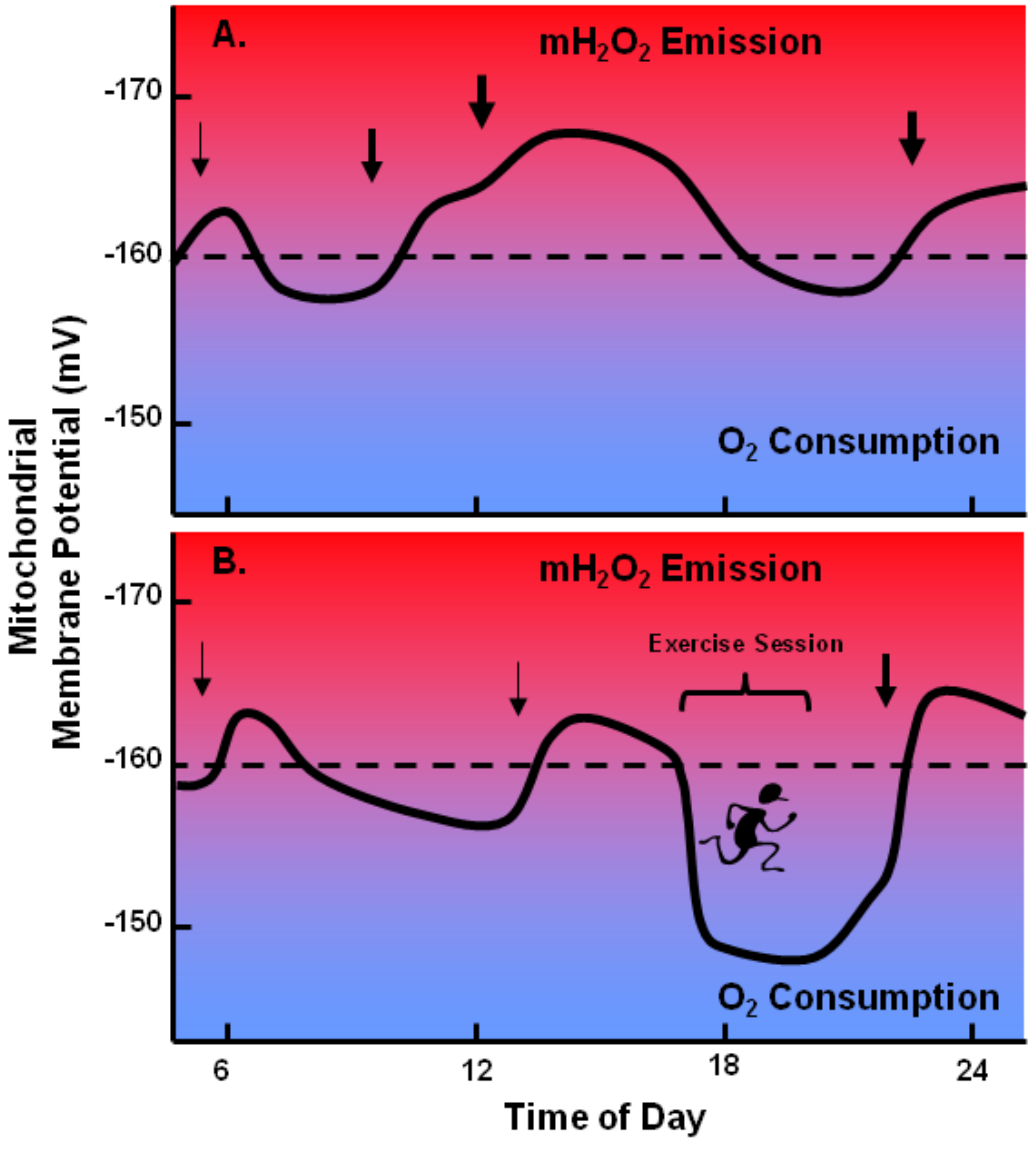

Figure 2-8. Schematic illustration showing predicted fluctuations in $\Delta\Psi_m$. (A) An individual out of metabolic balance due to excess caloric intake, particularly HFD, and sedentary lifestyle. (B) An individual in metabolic balance due to appropriate caloric intake and active lifestyle. Dotted line indicates approximate threshold $\Delta\Psi_m$ at which electrons begin to leak to from superoxide significantly. Arrows signify calorie intake. Red indicates progressively increasing mitochondrial H_2O_2 emission. Blue indicates progressively increasing mitochondrial O_2 consumption.

CHAPTER 3: Mildly Increased Energy Expenditure by either Exercise or β-GPA Sufficiently Prevent Increased Mitochondrial H_2O_2 Emission Potential and Insulin Resistance Induced by High Fat Diet in Rodents

Abstract

High fat diet (HFD)-induced mitochondrial H_2O_2 emission has been suggested as a primary factor linking excess fat intake to the development of insulin resistance (IR). Mitigating HFD-induced H_2O_2 emission may be a potential strategy to treat and/or prevent type II diabetes. Mitochondrial reactive oxygen species production is favored when cellular substrate supply is high and energy demand is low, and vice versa. The objective of this study was to determine if a daily mild increase in energy expenditure by either low intensity exercise or treatment with β-guanidinopropionic acid (β-GPA), a creatine analogue, is sufficient to prevent the increase in skeletal muscle mitochondrial H_2O_2 emitting potential ($_mE_{H2O2}$), and the decrease in insulin sensitivity induced by HFD in rodents. HFD increased $_mE_{H2O2}$ and decreased insulin action whereas both were preserved by either exercise or β-GPA. The protective effects of exercise or β-GPA were independent of mitochondrial respiratory function, fatty acid oxidation rate and AMPKα2 genotype. These data demonstrate that a small increase in energy expenditure prevents the increase in $_mE_{H2O2}$ potential and development of insulin resistance, supporting the concept that the governance of mitochondrial H_2O_2 emission is a primary factor regulating insulin sensitivity in skeletal muscle.

Introduction

A considerable body of research has reported consistent elevations in oxidative stress in both animal and human models of obesity and type II diabetes (T2D)[21,63,64,224]. Furthermore, a cause and effect relationship between mitochondrial reactive oxygen species (ROS) production and insulin resistance (IR) has recently been suggested[62-65]. In this context, mitigating oxidative stress may be a potential strategy to treat and/or prevent diabetes. Disruptions in whole body metabolic balance, in which substrate supply far exceeds energy demand on a consistent basis is believed to be the driving force behind this aforementioned relationship between mitochondrial ROS and metabolic disease. Previous work by our group has demonstrated that acute and chronic nutritional oversupply increases muscle mitochondrial H_2O_2 emitting potential ($_mE_{H2O2}$), a phenomenon that is causally linked to IR[64]. The interplay between metabolic supply and ROS production is well established, yet the extent to which energy expenditure can compensate for the deleterious effects of over-nutrition on ROS production, cellular redox state and insulin sensitivity is currently unknown. Based on fundamental principles of bioenergetics, when the rate of ADP supply to mitochondria is very low (state IV or close to state IV respiration), the mitochondrial membrane potential ($\Delta\Psi_m$) is high and an exponential increase in superoxide ($O_2^{-}\bullet$) generation occurs within a small range of $\Delta\Psi_m$ values exceeding about -160mV[79,81-84]. The inverse occurs when the mitochondrial ADP levels rise (i.e., ↑energy turnover or ↑energy expenditure) which lead to a reduction in $\Delta\Psi_m$ through F_1F_0 ATP synthase complex activity[85,86] and dramatically reduced $O_2^{-}\bullet$ generation. Therefore, increased energy expenditure (↑ADP/ATP) or reduced substrate supply (↓NADH/NAD^+) can reduce $O_2^{-}\bullet$ generation, decrease oxidative damage, and potentially attenuate IR. Therefore, we hypothesized that chronic mild increases in energy expenditure by either low intensity exercise or

β-guanidinopropionic acid (β-GPA) treatment could sufficiently prevent the increase in mitochondrial oxidant emitting potential and the decrease in insulin sensitivity that is normally induced by a high fat diet (HFD).

Increasing physical activity represents one of the most effective means of reversing IR in skeletal muscle of overweight/obese patients at high risk for T2D. However, it is generally believed that moderate-high intensity aerobic exercise is required to have a positive outcome on IR. However, if oxidative stress is a primary factor causing insulin resistance, then even a mild increase in energy expenditure should be sufficient to prevent diet induced IR as it should, in theory, reduce $O_2^{-}\bullet$ generation significantly.

β-GPA is a non-metabolized creatine analog that cannot be used to regenerate ATP. β-GPA feeding in rodents chronically decreases skeletal muscle ATP, phosphocreatine, creatine and total creatine content by about 50%, 90%, 80% and 85%, respectively[185]. In other words, cellular energy charge is decreased, which causes an increase in cellular metabolic demand (ATP synthesis) to compensate for the decrease in energy availability. Consistent with work showing an increase in mitochondrial biogenesis during conditions of high metabolic demand, β-GPA feeding has also been shown to induce mitochondrial biogenesis in rodent skeletal muscle[189,258], while attenuating IR and T2D[182-184] although the exact mechanism is unclear. The overriding hypothesis of this project is that a mild increase in energy expenditure in cells will significantly decrease $_{m}E_{H2O2}$ and thereby prevent the development of IR induced by a HFD. However, an increase in energy expenditure and associated decrease intracellular energy charge (i.e., ATP/ADP ratio) may also activate 5'-AMP-activated protein kinase (AMPK). AMPK-mediated signaling is known to stimulate glucose uptake independent

of insulin[192]. Both exercise[186-188] and β-GPA[185,189-191] have also been shown to activate AMPK. This suggests any metabolic effects induced by exercise or β-GPA, if occurring, may be mediated by AMPK and/or mH_2O_2. AMPKα2 is the main AMPK catalytic subunit dominant in skeletal muscle, heart, and liver[259-261]. Therefore, to better define the role of AMPKα2 signaling under β-GPA feeding, we tested whether β-GPA treatment normalized HFD induced IR and elevated $_mE_{H2O2}$ in the AMPKα2-DN mice. The AMPKα2-DN mice[262] express a dominant negative mutant (non-functional) form of the AMPK alpha2 catalytic subunit specifically in both skeletal and cardiac muscle.

The results show that a daily mild increase in energy expenditure, independent of AMPK activation, is sufficient to prevent the increase in skeletal muscle $_mE_{H2O2}$, and decrease in insulin sensitivity induced by metabolic oversupply (HFD).

Methods

Rat Study

Young male Sprague-Dawley rats (4 groups, n=10/ group, ~200g bodyweight) were maintained on a standard 12h/12h light/dark cycle (7:00 am light). Rats were fed a standard chow (Chow) or high fat diet (HF, rodent diet with 60% of total calorie from fat, Research Diets D12492) for seven weeks. The animals given a high fat diet were also administered either low intensity exercise (HF-EX, treadmill, 15m/min, 0 grade, 2h/d, 3-5pm, 7d/wk, 7wks) or β-GPA (HF-GPA, 2 times of 200mg/kg whole body mass/day, 8:30am & 5:00pm, 7d/wk, the final 5 wks only, by oral gavage). β-GPA was administered twice a day to account for the metabolic clearance. A water gavage (1ml) control was performed in Chow, HF and HF-EX groups every 3 days. Body weight was recorded weekly. The rats were acclimated to procedure conditions every 2 weeks

including restraining/handling. A 10h fasting blood sample from the tail vain followed for blood glucose and serum insulin level determination. There was no difference in fasting glucose and insulin level over the time course of treatment or between groups (data not shown). Oral glucose tolerance tests (OGTT, 2g/ kg whole body mass) were conducted during week 6 in the morning following an overnight fast (10h). Blood samples from OGTT were analyzed for glucose using a handheld glucometer (OneTouch Ultra) and serum insulin levels using a commercially available ELISA kit (Millipore). In the morning during week 7, five rats from each group were sacrificed after either a 4h fast (n=5/ group) or 1h after a glucose gavage (2g/ kg whole body mass) performed after a 3h fast to examine mitochondrial function, oxidative stress and insulin signaling in muscle. Insulin sensitivity index was calculated as the inverse of the area under the curve for glucose x area under the curve for insulin[263]. Muscle fiber samples from fresh red gastrocnemius (RG) were obtained and trimmed of connective tissue. A portion of muscle (~20mg) was immediately used for the preparation of small fiber bundles (each ~0.8-1.5mg wet weight, ~100 muscle fibers/bundle) under a dissecting scope. Fiber bundles were immediately saponin-permeabilized and maintained in buffer at 4ºC until used to assess mitochondrial oxygen respiration (JO_2) and $_mE_{H2O2}$. Fresh mixed gastrocnemius muscle and liver tissue were also obtained to determine FAO rate. The remainder of the fresh RG was frozen by liquid nitrogen and stored in -80^oC for later analysis of AMPK and insulin signaling proteins (total and phosphorylated $AMPK_{Thr172}$ and Akt_{Ser473} by Western Blot).

AMPKα2-DN Mouse Study

AMPKα2-DN mice were kindly provided by Morris Birnbaum[262]. Male AMPKα2-DN mice and their wild-type (WT) littermates (5 groups, n=9-18/group) were

fed standard chow diet or HFD with or without β-GPA started at 13-18 weeks of age. Mice were maintained on a standard 12h/12h light/dark cycle (7:00 am light). WT mice were fed standard chow (WT-Chow) or HFD for 10 weeks (Research Diets D12492) (WT-HF), or HFD plus β-GPA oral gavage for 10 weeks (WT-HF-GPA, 2 times of 250mg/ kg whole body mass/day, 8:30am & 5:00pm, 7d/wk). AMPKα2-DN mice were fed HFD for 10 weeks (DN-HF), or HFD plus β-GPA oral gavage for 10 weeks (DN-HF-GPA). A water gavage (0.4ml) was performed on all non-β-GPA fed groups every 3 days. Body weight was recorded weekly. In week 8, whole body metabolic state was assessed via an indirect calorimetry system. Body composition was determined immediately after the mice came out of the calorimetry system. In week 9, after the mice acclimated to surgery room and restrainers/handling for 2 days, intraperitoneal glucose tolerance tests (IPGTT, 1.5g dextrose/kg whole body mass) were performed following a 4h fast that began at 4:00 am (last 3h of dark cycle). Blood samples from the IPGTT were analyzed for blood glucose and plasma insulin level (fasting and 30 minutes after the glucose injection). Mice were sacrificed on the 10^{th} week after a 4h fast in the morning. Soleus & EDL muscle strips from both legs were obtained for the measurement of basal and insulin stimulated ^{3}H-2-deoxyglucose (^{3}H-2-DOG) uptake. A portion of fresh RG was immediately saponin-permeabilized and maintained (4ºC) in buffer for the determination of JO_2 and $_mE_{H2O2}$. Body composition was determined again the day prior to sacrifice.

Permeabilized Myofibers (PmFBs) Preparation

Animals were anaesthetized by IP injection of ketamine/xylazine (9:1) mixture. The same portion of fresh RG muscle from each animal was harvested, trimmed of connective tissue, and fresh muscle fiber bundles (~2 x 7mm, 2-3mg wet weight) were

gently separated to maximize the exposure surface using fine forceps under a binocular dissecting microscope in ice-cold buffer X containing (in mM) 60 K-MES, 35 KCl, 7.23 K_2EGTA, 2.77 CaK_2EGTA, 20 imidazole, 0.5 dithiothreitol, 20 taurine, 5.7 ATP, 15 phosphocreatine 6.56 $MgCl_2 \cdot 6H_2O$ (pH adjusted to 7.10) plus 0.5 glutamate (G) and 0.2 malate (M). After separation, the plasma membrane of myofiber bundles were permeabilized in buffer X with 0.5mM G, 0.2mM M and 50µg/ml saponin while gently shaking on a rocker at 4ºC for 30min. To wash out the extra-mitochondrial components, the PmFBs were subsequently washed in buffer Z containing (in mM) 105 K-Mes, 30 KCl, 10 K_2HPO_4, 5 $MgCl_2 \cdot 6H_2O$ and 5mg/ml bovine serum albumin (pH adjusted to 7.40) plus freshly added 1 EGTA, 0.5 G and 0.2 M with gently shaking on a rocker at 4ºC for 15 min.

Measuring JO_2 in PmFBs

JO_2 was measured in PmFBs (~0.4mg after freeze-dried) using high-resolution respirometry (Oroboros Oxygraph-2 K (O2K) Innsbruck, Austria) at 30ºC in assay buffer containing buffer Z plus 1mM EGTA, 20mM creatine (to saturate endogenous creatine kinase) and 50µM N-benzyl-p-toluene sulphonamide (a muscle contraction inhibitor[264]). After establishing a background JO_2 rate in the presence of a PmFB, the reaction was initiated by the addition of sequential substrates.

Measuring $_mE_{H2O2}$ in PmFBs

Washed PmFBs (~0.2mg after freeze-dried) were rinsed with 10mM sodium pyrophosphate in ice-cold Buffer Z for three minutes prior to $_mE_{H2O2}$ measuring to deplete the fibers of endogenous adenine nucleotides and to prevent calcium-independent contraction of the fibers during the assay. $_mE_{H2O2}$ was measured by continuously monitoring the fluorescence probe Amplex Red (Invitrogen, A22188;

excitation/emission: 563/587nm) using spectrofluorometers (In rat study: Spex Fluoromax 3, Horiba Jobin Yvon; in mice study: Fluorolog-3, Horiba Jobin Yvon) with temperature control at 30ºC and magnetic stirring. The assay buffer contained buffer Z plus 10U/ml CuZn-superoxide dismutase, 10μM Amplex Red, 1.5U/ml horseradish peroxidase and 10μg/ml oligomycin (state IV respiration condition). After establishing a background fluorescence rate in the presence of a PmFB, the experiment was initiated by the addition of sequential substrates. $_{m}E_{H2O2}$ rate was calculated from the slope of ΔF/min, after subtracting background, using a standard curve established for each reaction condition.

At the conclusion of each experiment, PmFBs were washed in ddH_2O to remove salts and then freeze-dried in a lyophilizer (LabConco). JO_2 and $_{m}E_{H2O2}$ were normalized to dry tissue weight since a functional index of mitochondria density (FCCP uncoupled JO_2, figure 3-4, 3-5 (non glucose challenged state) & figure 3-12) was not significantly different between groups in either rat or mouse study.

Indirect Calorimetry and Locomotor Activity

Mouse whole body metabolic state at week 8 of treatment was measured in a Calorimetry Module (CaloSys V2.1, TSE Systems) with the relevant software (ActiMot2, TSE Systems) for two complete light-dark cycles (48h) after 4 days of acclimation. Parameters measured included whole body oxygen consumption, CO_2 expiration, respiratory exchange ratio (RER), food intake and X+Y+Z axis locomotor activity.

Body Composition

Whole body composition of live mice was determined using the Echo Magnetic Resonance Imaging (EchoMRI-900™, Echo Medical System, Houston, TX), a QNMR system used to precisely measure whole body composition parameters including total

body fat, lean mass, body fluids, and total body water in live rats/mice without the need for anesthesia or sedation.

^{3}H-2-DOG Uptake

Muscle strip ^{3}H-2-DOG uptake assay was modified from previously described methods[265,266]. Immediately after excision from the animal, muscle samples were placed in a sealed container with 1.5ml of oxygenated (95% O_2 & 5% CO_2) Krebs-Henseleit buffer (KHB), containing (mM): 2.52 $CaCl_2$, 4.73 KCl, 1.18 $MgSO_4$, 118 NaCl, 1.17 KH_2PO_4 and 25 $NaHCO_3$ with 25μM blebbistatin (Bleb, an inhibitor of myosin II crossbridge formation[212-215]) in room temperature for transport. Each experiment was 60 min in total duration. Muscle strips were first pre-incubated for 30min under basal conditions (oxygenated KHB+Bleb). Where appropriate, muscle strips were pre-incubated with insulin (100nM) for the last 10min of this pre-incubation period. Following the pre-incubation period, muscle strips were then transferred to incubation wells containing identical conditions with the exception that the incubation media contained 10mM 2-DOG, 40mM mannitol, 2.0μCi/ml ^{3}H-2-DOG (to quantify glucose transport), 0.1μCi/ml ^{14}C-D-mannitol (as an extracellular space marker), and with or without insulin (100nM) where appropriate. Pre-incubation and incubation volumes were 2ml. Samples were continuously gassed with 95% O_2 & 5% CO_2. Incubation temperature was maintained at 29ºC in a gentle shaking water bath. After incubation period, muscle strips were washed in ice-cold KHB gently twice for 5 minutes each to wash off excess 2-DOG and mannitol from the samples. After washing, muscle strips were blotted, weighed, and then solubilized in 0.5ml of 0.5N NaOH. Solubilized muscle strips and incubation media samples (specific activity determination) were then

stabilized in scintillation fluid for 7 days before being counted in a Beckman LS 5000 TD liquid scintillation counter preset to count ^{14}C and ^{3}H channels simultaneously.

Preparation of Skeletal Muscle Homogenates and Western Blotting

Frozen muscles were powdered under liquid N_2 and 50-80mg of powdered tissue was homogenized in ice-cold lysis buffer [50mM HEPES, 50mM Na^+ pyrophosphate, 100mM Na^+ fluoride, 10mM EDTA, 10mM Na^+ orthovanadate, 1% Triton X-100, and protease and phosphatase (1 and 2) inhibitor cocktails (Sigma, St. Louis, MO)]. Homogenates were sonicated for 10sec then rotated for 2h at 4ºC. After centrifugation for 25min at 15,000g, supernatants were extracted and protein content was detected using a BCA protein assay (Pierce, Rockford, IL) and individual homogenate volumes were separated into 50µg of protein before being frozen in liquid nitrogen and stored at -80ºC until used for immunoblotting. Conventional immunoblotting techniques were employed using antibodies specific for total AMPK, phosphorylated $AMPK_{Thr172}$, total Akt and phosphorylated Akt_{Ser473} (Cell Signaling 2532, 2531, 9272 and 9271, respectively). Homogenates were subjected to monoclonal IP antibody overnight then coupled to protein A sepharose beads and rotated for 2 hours (Amersham Biosciences, Uppsala Sweden) and eluted with sample buffer. Samples were separated by SDS-PAGE using 7.5% or 10% Tris-HCl gels and then transferred to PVDF membranes for probing by appropriate antibodies. Following incubation with primary antibodies, blots were incubated with appropriate horseradish peroxidase-conjugated secondary antibodies. Horseradish peroxidase activity was assessed with ECL solution (Thermo Scientific, Rockford, IL), and exposed to film. The image was scanned and band densitometry was assessed with Gel Pro Analyzer software (Media Cybernetics, Silver Spring, MD). Content of phospho-proteins (using phosphor-specific antibodies) was calculated from

the density of the band of the phospho-protein divided by the density of the protein using the appropriate antibody.

Muscle and Liver Fatty Acid Oxidation

With minor modifications from previous[267], experiment utilizing [1-^{14}C]palmitate was performed to study the mitochondrial fatty acid oxidation rate of fresh liver and mixed gastrocnemius muscle tissue homogenate. Palmitate (200μM) was bound to 0.5% bovine serum albumin (3.3 molar ratio of fatty acid:albumin). Specific activities for [1-^{14}C]palmitate (200μM) were ~8,000-10,000dpm/nmol (0.5μCi/ml). Once solubilized, fatty acid substrate were brought up in reaction buffer to yield the following final concentrations (mM): 100 sucrose, 10 Tris·HCl, 10 KPO_4, 100 KCl, 1 $MgCl_2 \cdot 6H_2O$, 1 L-carnitine, 0.1 malate, 2 ATP, 0.05 coenzyme A, and 1 dithiothreitol (pH adjusted to 7.40). Oxidation studies measured ^{14}C-labeled CO_2 and acid-soluble metabolite (ASM) production over the course of 30 min. Radioactivity of CO_2 and ASM fractions was determined by liquid scintillation counting using 4ml of Uniscint BD (National Diagnostics, Atlanta, GA). Fatty acid oxidation was quantified using the following formula: 60 min/h x [(dpm – BL)/SA]/[g of tissue wet wt/well x time (min) of reaction incubation], where BL is dpm of blank wells and SA is fatty acid-specific radioactivity. Data are expressed as nano moles of substrate oxidized per gram tissue wet weight per hour.

Statistical Analysis

A monoexponential fitting of the Michaelis-Menten kinetic curve was computed using GraphPad Prism software 5.02 (San Diego, CA) to determine the Km and Vmax of the respirometric substrate titration data. Independent student's t-tests, one way ANOVA + Tukey or two-way ANOVA + Bonferroni (as appropriate) were performed as

dictated by the design of the study. All values are reported as Mean ± SEM. Statistical significance was set at $p<0.05$.

Results

HFD-Induced Insulin Resistance is Attenuated by β-GPA and Exercise in Rats Independent of Changes in Fatty Acid Oxidation

Body weight increased over the duration of the study but did not differ among treatment groups (Fig. 3-1F). To determine if daily treatment with β-GPA or low intensity daily treadmill exercise is sufficient to preserve insulin action in rats consuming a HFD, whole body glucose tolerance and skeletal muscle insulin signaling were measured. As expected, the areas under the curve for both glucose and insulin were elevated in HFD-fed rats. Both β-GPA treatment and exercise preserved whole body insulin sensitivity (Fig. 3-1A-E). Interestingly, the increase in Akt phosphorylation, a marker of insulin signaling, 1h following a glucose challenge was blunted in animals fed the HFD, consistent with the development of insulin resistance. However, Akt phosphorylation was partially restored only in the β-GPA treated animals (Fig. 3-2A). Interestingly, the improved glucose clearance in the β-GPA-, but not low intensity exercise-, treated animals occurred concurrent with increased AMPK phosphorylation ratio, an index of AMPK activation (Fig. 3-2B). To determine if potential treatment effects on insulin sensitivity paralleled changes in FAO, palmitate oxidation was measured from fresh mixed gastrocnemius muscle and liver tissue homogenates. HFD did not cause any change in FAO in either skeletal muscle or liver homogenates. In fact, a trend of increased FAO in HFD fed rats was observed in muscle (Fig. 3-3).

β-GPA and Exercise Improve Mitochondrial OXPHOS Capacity in Rats

To determine if HFD alone or coupled with daily β-GPA treatment or low intensity exercise alters mitochondrial respiratory sensitivity and capacity, JO_2 in PmFBs was assessed under both basal (4h fast) and 1h after glucose challenge. Mitochondrial respiratory control indices which indicate the quality of mitochondria OXPHOS capacity were also calculated. During respiration supported only by the complex I substrates glutamate + malate, no differences were detected in either mitochondrial respiratory sensitivity or capacity under basal (no glucose challenge) or glucose challenge conditions with the exception of a decrease in sensitivity to ADP (increased Km) in HF-GPA rats in the basal state (Fig. 3-4). During respiration supported by multiple substrates, maximal ADP-stimulated respiration was increased by HF-GPA in the basal condition. Interestingly, in the glucose challenged condition, maximal respiration was elevated by HFD treatment and further elevated in HF-GPA and HF-EX (Fig. 3-5). The mitochondrial respiratory control indices showed no treatment effect on the ADP titration protocol in both basal and glucose challenged states or basal states using multiple substrates (Fig. 3-6). Under glucose challenged state in multiple substrate condition, HFD induced improvements in both respiration control ratio (increased) and adenylate control ratio (decreased) independent of β-GPA or exercise treatment (Fig. 3-6F).

β-GPA and Exercise Prevent HFD-Induced $_mE_{H2O2}$ and $_mFRL\%$ in Rats

To determine if daily treatment with β-GPA or low intensity exercise may attenuate or prevent HFD induced elevations in $_mE_{H2O2}$[64], $_mE_{H2O2}$ was assessed under both basal and glucose challenge conditions. During succinate-supported respiration which induces high rates of H_2O_2 emission due to reverse electron flux back through complex I, HFD-induced a >2-fold increase in $_mE_{H2O2}$ under basal conditions that was

prevented by both β-GPA and exercise treatments (Fig. 3-7). Nearly identical responses, including protection by β-GPA and exercise treatments, were seen during respiration supported by multiple substrates (Fig. 3-8). In the glucose challenged condition, $_{m}E_{H2O2}$ was increased in the chow fed animals during both succinate and multi-substrate conditions, illustrating the acute impact of metabolic overload on mitochondrial H_2O_2 emission. Mitochondrial free radical leak percentage ($_{m}$FRL%), an index of H_2O_2 emission per O_2 consumed, was also increased in HF animals and in chow fed animals in response to the glucose challenge (Fig. 3-9). Interestingly, the glucose challenge did not induce a further increase in $_{m}$FRL% in HF animals, implying a ceiling effect. Both β-GPA and exercise treatments prevented the HFD-induced increase $_{m}$FRL% in both the basal and glucose challenge conditions.

β-GPA effects on Body Composition, Metabolic State and Locomotor Activity in Mice are independent of AMPKα2 Genotype

To further test whether improvements in whole body metabolic profile, cellular oxidative stress and insulin sensitivity in response to β-GPA treatment during a HFD may be mediated by AMPK (suggested in Fig. 3-2B), young male AMPKα2-DN and their wild-type (WT) littermates were fed a HFD with or without β-GPA. The whole body metabolic state of these mice was monitored. Regardless of AMPKα2 genotype, β-GPA prevented HFD-induced body weight gain while both food intake and energy expenditure were significantly increased (Fig. 3-10). Importantly, total locomotor activity was not affected by β-GPA treatment, indicating that the increase in energy expenditure with β-GPA treatment was likely due to an increase in basal oxidative metabolism due to creatine depletion. Furthermore, respiratory exchange ratio was lower in β-GPA fed mice indicating a greater reliance on lipid metabolism. All metabolic parameters were

normalized to lean body mass to eliminate bias introduced by differences in total body weight between groups.

β-GPA Maintains Insulin Sensitivity in Mice Fed a HFD Independent of AMPKα2 Genotype

IPGTT and muscle ^{3}H-2-DOG uptake were conducted to determine if the effects of β-GPA on insulin sensitivity may be mediated by AMPK (Fig. 3-11). β-GPA treatment completely normalized both whole body glucose and insulin responses to the IPGTT and muscle-specific insulin-stimulated glucose uptake rates regardless of AMPKα2 genotype. These findings indicate that the protective effects of β-GPA on HFD-induced insulin resistance are not mediated by AMPKα2. Interestingly, insulin-stimulated glucose uptake was higher in the EDL muscle of HF β-GPA treated as compared with chow fed wild-type mice.

β-GPA Prevents HFD-Induced $_{m}E_{H2O2}$ and $_{m}$FRL% Regardless of AMPKα2 Genotype

As expected, HFD significantly increased $_{m}E_{H2O2}$ under multiple substrate conditions (Fig. 3-12). By contrast, neither mitochondrial respiratory capacity nor various indices of respiratory control were affected by the dietary regimen (Fig. 3-12 and 3-13), indicating “normal” mitochondrial respiratory function. Regardless of AMPKα2 genotype, β-GPA treatment completely prevented the HFD-induced increase in $_{m}E_{H2O2}$ and $_{m}$FRL% (Fig. 3-12), again in the absence of any change in respiratory function. In fact, β-GPA treated mice on HFD displayed lower $_{m}E_{H2O2}$ and $_{m}$FRL% compared with the standard chow diet fed mice.

Discussion

In the present study, chronic elevations in energy expenditure by either low intensity exercise or β-GPA treatment in both rats and AMPKα2-DN mice, resulted in the following major findings. *First*, aside from conventional wisdom that moderate-high energy expenditure is required, our results indicate a mild increase in energy demand by daily low intensity exercise or β-GPA treatment is sufficient to attenuate the HFD-induced $_{m}E_{H2O2}$ and IR. It follows from the principles of bioenergetics that a small reduction in $\Delta\Psi_m$ caused by a mild increase in respiration from idling (close to state IV respiration condition) can sufficiently lower "the reducing pressure of electron transport system (ETS)" and oxidant production that is otherwise causally linked to IR. *Second*, these data provide further support for the idea that elevated mitochondrial $_{m}E_{H2O2}$ (and/or downstream oxidative stress) is likely to be one of the primary factors contributing to HFD-induced IR. Importantly, these findings demonstrate that the protective effects induced by an increase in energy expenditure are not mediated by activation of AMPKα2. *Third*, skeletal muscle $_{m}E_{H2O2}$ and $_{m}$FRL%, but not OXPHOS capacity, are acutely sensitive to metabolic state. Glucose loading caused a 30~108% increase in $_{m}E_{H2O2}$ and $_{m}$FRL%, even in chow fed rats. Acute glucose loading however did not further increase $_{m}E_{H2O2}$ and $_{m}$FRL% in HF fed animals, providing evidence of a ceiling effect of metabolic overload on factors governing mitochondrial oxidant emission. Collectively, these findings provide clear evidence that metabolic oversupply induces elevated $_{m}E_{H2O2}$ and IR while the other side of the balance equation, energy expenditure, reduces both. These findings are consistent with the hypothesis that mitochondrial H_2O_2 production is very sensitive to cellular metabolic state, the emission of which under metabolic overload is at least one of the preceding/primary factors ultimately leading to IR. The balance of substrate supply and energy expenditure is critical for

maintaining proper cellular redox environment and therefore cellular function and whole body health.

The benefits of regular moderate-high intensity aerobic exercise on metabolic diseases, as well as mitochondria related effects, are well known. The higher the aerobic exercise intensity, the greater the adaptive response (e.g. cardiovascular adaptation). However, the idea that a threshold level of activity may exert a protective effect against metabolic imbalance has not been previously explored. A "minimal" mitochondrial respiratory activity stimulus was selected by the design in the present study based on the bioenergetics principle that only a slight increase in mitochondria respiratory activity from idling should be sufficient to alleviate the pressure leading to elevated mitochondrial H_2O_2 emission caused by HFD-induced metabolic overload. Our data show that only a mild increase in energy expenditure is sufficient to prevent the development of insulin resistance in the setting of a HFD. This protective effect occurred with minimal increase in energy expenditure, as none of the adaptations typically associated regular higher intensity exercise training (e.g., mitochondrial biogenesis, cardiovascular adaptations, etc.) were found. However, whether the $_mE_{H2O2}$ change was contributed by the treatment effect on mitochondrial oxidant production and/or anti-oxidant scavenging/buffering system (i.e., GSH/GSSG, thioredoxin and others) is unknown although it was shown that HFD reduce skeletal muscle GSH/GSSG ratio acutely and chronically[64,268].

β-GPA is an antidiabetic/antihyperglycemic agent[182-184] with unclear mechanism. In a dose and duration dependent manner, β-GPA induces a chronic reduction in cellular energy level and therefore activation of AMPK which is thought in turn to coordinate the activation of catabolic pathways and inactivation of anabolic pathways,

as well as activate pathways leading to the transcriptional activation of mitochondria biogenesis. These same effects were believed to mediate the improvements in insulin sensitivity induced by β-GPA[182-184]. However, many of these observations were from animals fed with 1~2% of β-GPA in the diet. Since eating behavior can potentially be changed by the drug, it is difficult to evaluate the effective β-GPA dose and its potential relationship to the metabolic outcomes in these studies. In the present study, β-GPA was administered by oral gavage, thus insuring stable and consistent dosing. Our data show in mice β-GPA treatment caused an increase in energy expenditure and compensatory increase in food intake despite no change in locomotor activity or HFD-induced weight gain, providing evidence of a decrease in metabolic efficiency as a consequence of the treatment. These findings are therefore consistent with the interpretation that β-GPA accelerated energy synthesizing demand in muscle, thereby relieving the elevated mitochondrial reducing pressure and $_{m}E_{H2O2}$ created by a HFD. However, β-GPA treatment also elicited an increase in muscle AMPKα2 activity, raising the possible alternative interpretation that the protective effects of the drug may be mediated simply by the activation of this energy sensing kinase. AMPKα2 is well known to stimulate muscle glucose uptake. However, when repeated in AMPKα2-DN mice, β-GPA treatment protected against the HFD-induced increase in $_{m}E_{H2O2}$ and loss of insulin sensitivity in both AMPKα2-DN and wild-type mice, suggesting the effects of β-GPA are not mediated by AMPKα2 activation. However, we cannot exclude a potential compensatory increase in AMPKα1 activity in response to β-GPA treatment. In a different muscle-specific AMPKα2-DN line of mice however, no compensatory increase in α1 was found under either basal or 5-aminoimidazole-4-carboxamide-ribonucleoside (AICAR) -stimulated conditions[269].

β-GPA also activates mitochondrial biogenesis, and an increase in mitochondrial content could account for an increase in basal energy requirements and thus energy expenditure. However, β-GPA treatment increased OXPHOS capacity in the rat study but not in the mouse study while both mice and rats were protected from HFD-induced IR. We also found no clear increase in the functional index of mitochondrial content (FCCP uncoupled respiration) in both mice and rats treated with β-GPA. Similarly, low intensity exercise maintained the insulin sensitivity under the HFD condition without an increase AMPK phosphorylation ratio or consistent increase in OXPHOS capacity. Thus, neither AMPK activity nor OXPHOS/mitochondrial content tracked consistently with insulin sensitivity in both rat and mouse studies. In contrast, the increase in energy expenditure and decreases in $_{m}E_{H2O2}$ and $_{m}$FRL% induced by β-GPA treatment, in the absence of any change in locomotor activity, consistently tracked with protection from HFD-induced insulin resistance. Although these findings cannot establish cause and effect, they support the concept that mitochondrial H_2O_2 is a major sensor of intracellular energy balance and a primary signal regulating insulin sensitivity[64].

Studies in which reduced FAO rates or mitochondrial OXPHOS capacity observed in muscle from elderly individuals, family offspring of diabetics, or obese/diabetic have been interpreted as indicative of a diminished FAO capacity[17,18,23]. The diminished FAO or OXPHOS capacity has been suggested to be a primary cause of IR due to the inappropriate cellular lipid accumulation which activates DAG-PKC-IRS pathway and results in the blockage of insulin signaling cascade[8,9,11,17,270]. Evidence for reduced mitochondrial function has been shown to associate with long-term substrate oversupply such as occurs with IR or T2D[19-22]. These include reduced mitochondrial content[23], size[23], enzyme activity[24-26], ETS complexes and OXPHOS activity or

respiration[16,17,27,28], TCA cycle flux rates[29], ATP production[25,26], and decreased expression of OXPHOS related genes[15,30,31]. However in the present study, IR was induced by 7-10 weeks of HFD in rodents in the absence of any change in mitochondrial FAO/OXPHOS capacity. It should be appreciated that mitochondrial H_2O_2 production and emission are extremely sensitive to acute metabolic balance as evidenced by the impact of acute glucose ingestion on $_mE_{H2O2}$ and GSH/GSSG ratios in muscle (Fig. 3-7, 3-8 and Anderson et al[64]). Elevated $_mE_{H2O2}$ and consequent shifting to a more oxidized redox environment has been linked to development of IR and, under persistent metabolic oversupply states, is likely contributing to mitochondrial OXPHOS deficiencies and eventual mitoptosis[63].

Mounting evidence also suggests that mitochondrial dysfunction represents a secondary event in the development of IR or T2D[35-37,63,64]. Reports from animal and human studies have shown long-term HFD may not affect[38-40,64] or may even promote[41-45] skeletal muscle mitochondrial function while IR may already exist. Although oversupply of fuel can over-ride mitochondrial compensation[19], short-term or early stage HFD feeding could actually promote mitochondrial density and FAO activity due to a prompt adaptive response[19,42,44,51]. Our data support this idea in which significantly reduced FAO and mitochondrial OXPHOS capacity are unlikely the only primary cause of over-nutrition induced IR. In fact, a decrease in mitochondrial function observed in insulin-resistant humans may not even limit muscle FAO and lead to lipid accumulation[22]. It is of importance to recognize the muscle mitochondrial FAO/OXPHOS capacity, such as during maximal exercise, is far in excess of the rate measured under resting conditions when energy demand, and thus the rate of FAO/OXPHOS, is low. In other words, it is questionable whether mitochondrial

FAO/OXPHOS deficiencies would have a considerable limitation on the rate of FAO/OXPHOS under normal resting conditions when energy demand is low[22]. In this context, the imbalance of substrate supply and consumption capacity (i.e., energy demand) of mitochondria should be the primary factor leading to IR and lipid accumulation. Most importantly, and perhaps most germane, it is imperative to recognize that the rate of mitochondrial respiration (i.e., oxidative metabolism) in cells is governed mainly by energy demand (basal + ADP-driven)[52,53]. Thus, based on principles of mitochondrial bioenergetics, intramyocellular lipid accumulation will occur whenever the supply of lipids exceeds the energy needs of the cell, independent of mitochondrial content or capacity. A reduction in mitochondrial density, if it does occur, will reduce overall basal non-ADP driven state IV respiration (i.e., basal energy demand) since mitochondria account for approximately 25% of basal metabolic rate[54,55], but the underlying mechanism accounting for lipid accumulation is still supply outpacing demand.

Compelling evidence is also accumulating to suggest a cause and effect relationship between mitochondrial H_2O_2 emission/oxidative stress and IR[62-65]. However, the detailed molecular pathway as to how ROS leads to IR is still largely unknown. Other than causing oxidative damage (e.g., lipids, proteins or DNA), what is the mechanism makes signaling pathways redox-sensitive and insulin sensitivity potentially redox-regulated? Both mitochondrial proteins and insulin signaling proteins appear to be regulated by redox-sensitive protein modification which alters protein activity/function. Redox regulation of cell function is mainly mediated by thiol (-SH) redox circuits, which normally reversibly control the intracellular localization and activity of many cell signaling and physiological regulation proteins[90,105,114,115]. Protein thiols are rich in

mitochondrial ETS proteins[271,272] and the reactive/regulatory protein thiols that are believed to have physiological functions are mainly found within complex I[273-277]. Oxidative stress causes multiple types of redox-sensitive protein modifications in complex I proteins[274,276-278]. This could further lead to complex I O_2^{-}• production increase[276,279] and oxidative activity reduction[274,278,279]. These data raise the possibility that the metabolic oversupply induced increase in ${}_mE_{H2O2}$ may be related to a change of redox state of mitochondria proteins in a vicious cycle manner. Further, oxidation of some insulin signaling proteins might lead to suppression of insulin signaling. These proteins include IRS[121-124], Ras[125], PI3 kinase[130], PKC and Akt (PKB). Many PKC isoforms appear to be sensitive to redox inhibition by S-glutathionylation or unknown protein modification[114,126-128]. Purified human recombinant aPKC-ζ is subject to oxidative inactivation by S-glutathiolation induced by the concentration-dependent thiol-specific oxidant diamide, which induces disulfide bridge formation[129]. In addition, H_2O_2 exposure results in impaired Akt activation[131,132], while lipoic acid, by its capacity to maintain intracellular redox state, protects against oxidative stress induced impairment in Akt activity[133]. Akt is reversibly inactivated by S-nitrosylation[135] specifically in Cys224[136] or Cys296[137]. Nevertheless, sirtuin 1[176], a key protein involved in metabolism, is also redox-sensitive although no direct evidence has shown active site specific redox-sensitive cysteine residues yet. Together, the redox-sensitive protein modification mechanism of IR is circumstantially compelling. However, most of the redox-sensitive protein modification studies on mitochondrial or insulin signaling were performed based on *in vitro* treatment. How does over-nutrition actually affect it and link to the development of IR in an animal or human model *in vivo* has not been determined and is of future directions.

Conclusion

These data demonstrate that a daily mild increase in energy expenditure induced by either low intensity exercise or β-GPA treatment sufficiently prevents the increase in $_{m}E_{H2O2}$ and the development of IR induced by HFD, supporting the idea that the governance of $_{m}E_{H2O2}$ is a primary factor regulating insulin sensitivity in skeletal muscle.

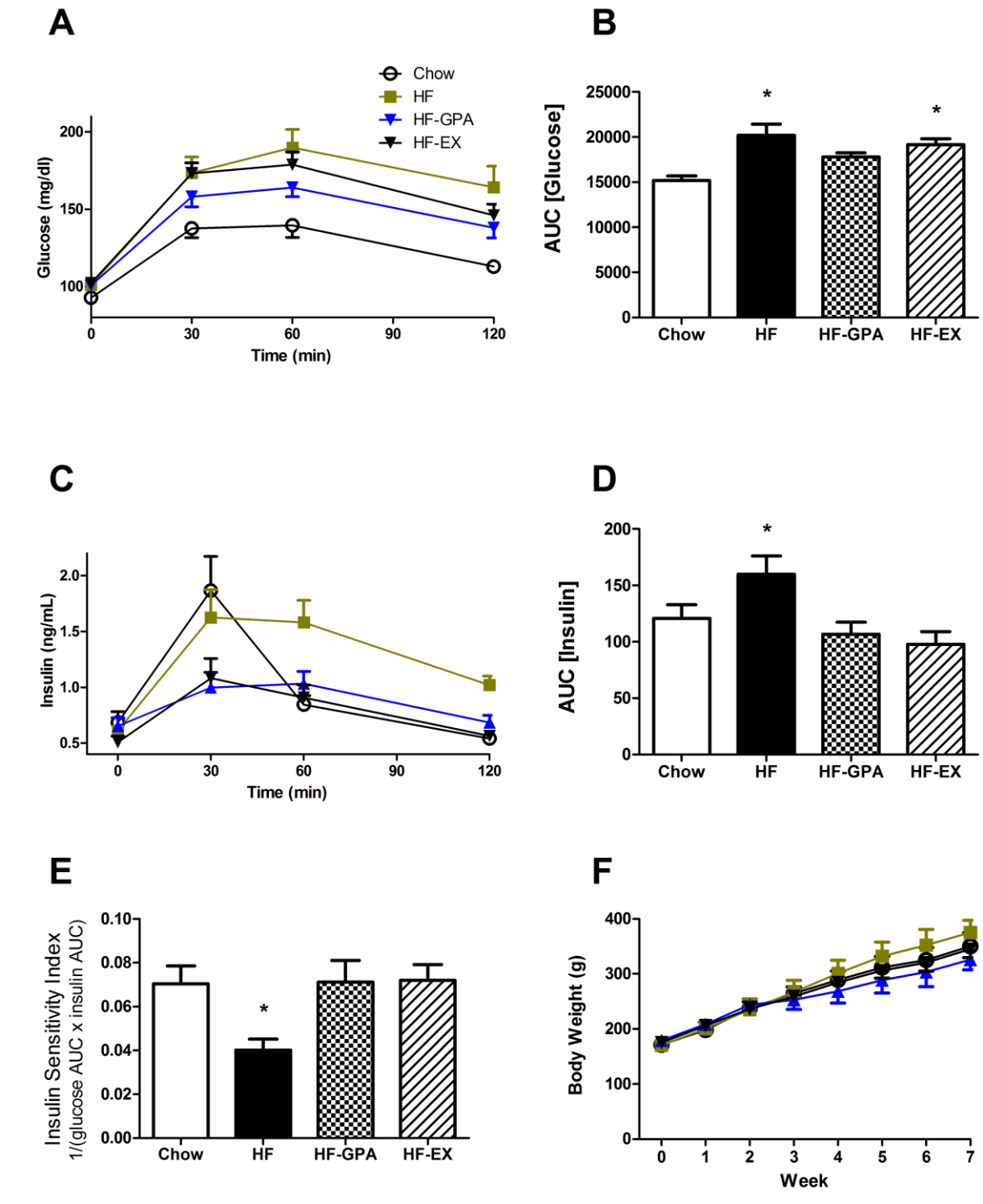
A
Chow
HF
HF-GPA
HF-EX
Glucose (mg/dl)
200
150
100
0
30
60
90
120
Time (min)
B
AUC [Glucose]
25000
20000
15000
10000
5000
0
*
*
Chow
HF
HF-GPA
HF-EX
C
Insulin (ng/mL)
2.0
1.5
1.0
0.5
0
30
60
90
120
Time (min)
D
AUC [Insulin]
200
150
100
50
0
*
Chow
HF
HF-GPA
HF-EX
E
Insulin Sensitivity Index
1/(glucose AUC x insulin AUC)
0.10
0.08
0.06
0.04
0.02
0.00
*
Chow
HF
HF-GPA
HF-EX
F
Body Weight (g)
400
300
200
100
0
0
1
2
3
4
5
6
7
Week

Figure 3-1. β-GPA and exercise prevent insulin resistance induced by HFD in rats without affecting body weight.

Young male S-D rats fed (7 weeks) with standard chow (Chow group), 60% HFD (HF group), HFD plus β-GPA for the final 5 weeks (HF-GPA, 2x200 mg/kg/d, 8:30am & 5:00pm, 7d/wk, by oral gavage), or HFD plus low intensity treadmill exercise (HF-EX group, 15m/min, 0 grade, 2 h/d). To determine if daily treatment with β-GPA or low intensity daily treadmill exercise are sufficient to preserve insulin sensitivity in rats consuming a HFD, OGTT (2g/ kg whole body mass) were conducted during week 6 in the morning following an overnight fast (10h). Rats were studied ~16 hours after the final β-GPA or exercise treatment. (A) Serum glucose level from OGTT. (B) Area under the curve (AUC) of serum glucose level from OGTT. * $p<0.05$ vs Chow (C) Serum insulin level from OGTT. (D) AUC of serum insulin level from OGTT. * $p<0.05$ vs HF-GPA or HF-EX (E) Insulin Sensitivity Index = 1/(glucose AUC x insulin AUC) from OGTT. * $p<0.05$ vs all other groups. (F) Rats' body weight over the treatment duration. Mean ± SEM. N=10/ group. one-way ANOVA, Tukey.

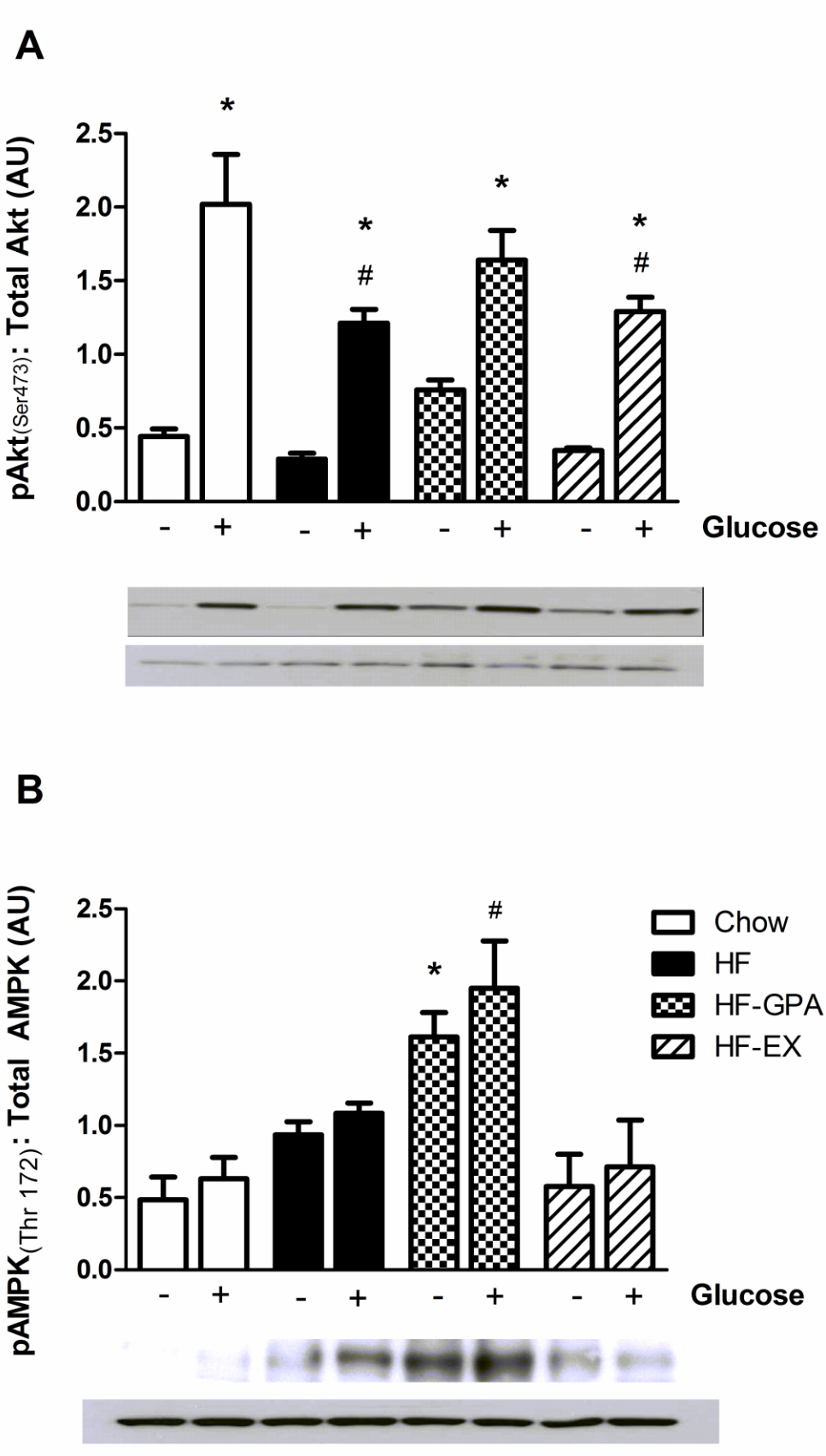
A
pAkt(Ser473): Total Akt (AU)
2.5
2.0
1.5
1.0
0.5
0.0
*
*
#
*
*
#
- + - + - + - +
Glucose
B
pAMPK(Thr 172): Total AMPK (AU)
2.5
2.0
1.5
1.0
0.5
0.0
*
#
Chow
HF
HF-GPA
HF-EX
- + - + - + - +
Glucose

Figure 3-2. β-GPA treatment attenuated HFD impairment in insulin signaling but also activate AMPK pathway.

To determine the treatment effect on insulin signaling and AMPK pathway, phosphorylated/total Akt or AMPK were examined by western blotting. Rats were studied ~16 hours after the final β-GPA or exercise treatment at week 7. After either a 4h fast or 1h after a glucose gavage (2g/ kg body weight) performed after a 3h fast, rats' red gastrocnemius were harvested for western blotting. β-GPA treatment attenuated HFD impairment in insulin signaling. However, unlike the low intensity exercise group, AMPK pathway may be involved in the β-GPA mediated effect in glucose clearance. (A) The ratio of phosphorylated (Ser473) and total Akt protein level. * $p<0.05$ vs no glucose challenged condition within the same treatment. # $P<0.05$ vs Chow in glucose challenged condition. (B) The ratio of phosphorylated (Thr172) and total AMPK protein level. * $P<0.05$ vs Chow or HF-EX in no glucose challenge condition. # $P<0.05$ vs all other groups in glucose challenged condition. Mean ± SEM. N=5/ group. Glucose(2) X Treatment(4) two-way ANOVA, Bonferroni.

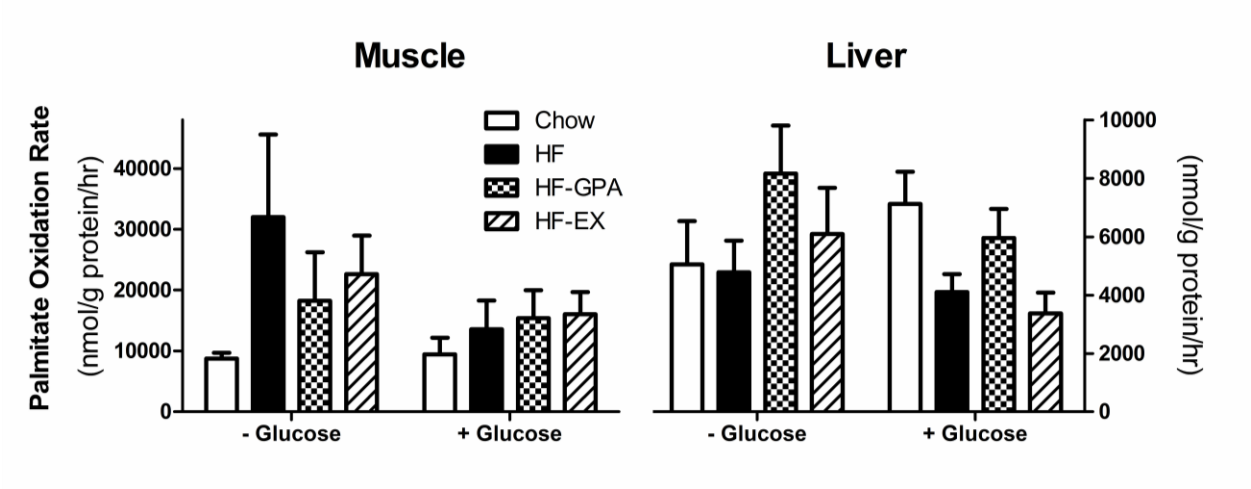

Figure 3-3. No HFD or acute glucose loading caused FAO defect in either skeletal muscle or liver of rats.

To determine if HFD or acute high glucose intake influences FAO rate, 7 weeks treated rats were sacrificed after a 4h fast or 1h after a single glucose challenge (2g/ kg body weight) performed after a 3h fast. Fresh mix gastrocnemius muscle and liver tissue homogenate were obtained for palmitate oxidation rate measurement utilizing [1-^{14}C]palmitate. The data indicate no HFD or acute glucose loading caused FAO defect. Mean ± SEM. N=5/ group. Glucose(2) X Treatment(4) two-way ANOVA, Bonferroni.

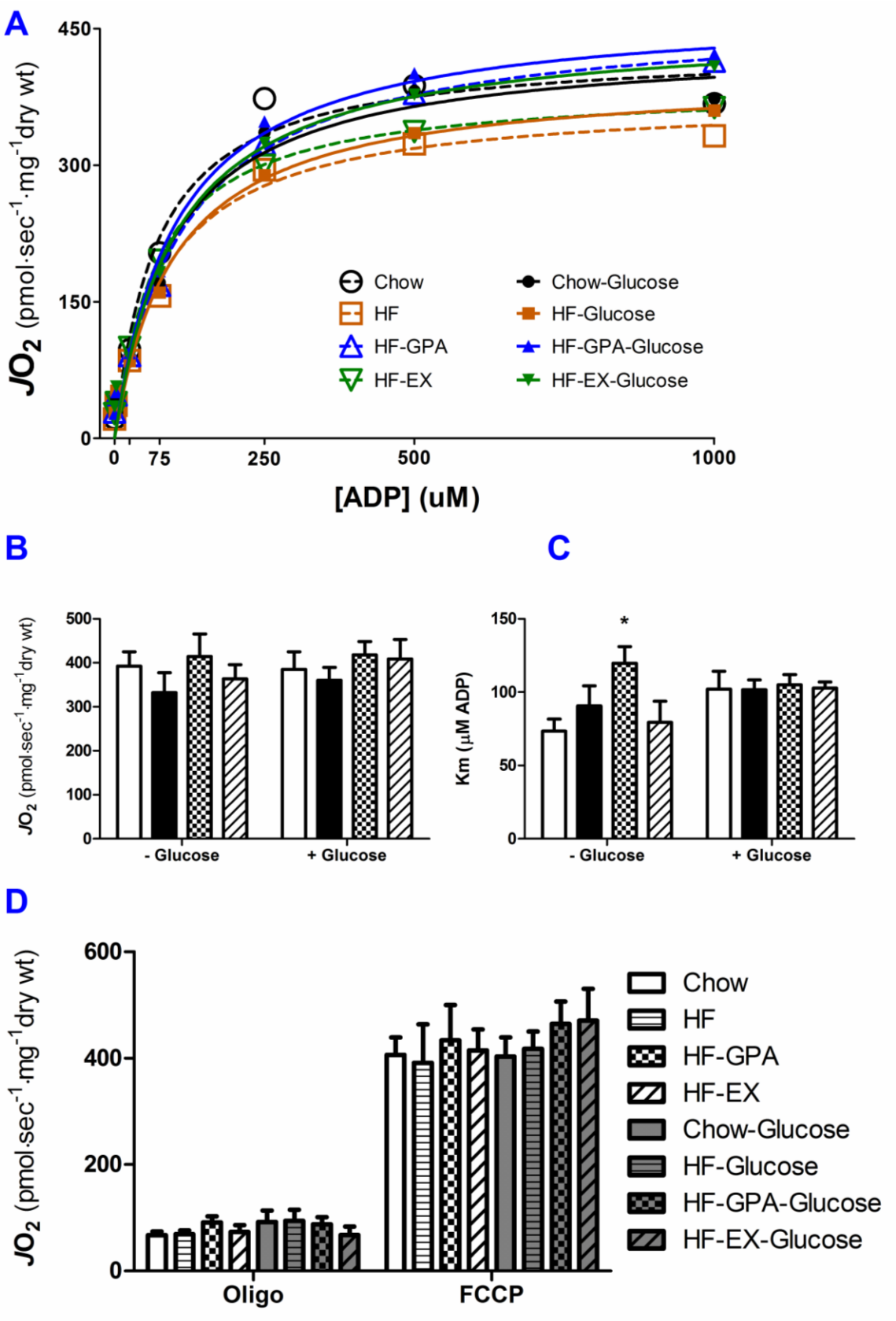
A
450
300
150
0
JO2 (pmol·sec-1·mg-1dry wt)
0
75
250
500
1000
[ADP] (uM)
Chow
HF
HF-GPA
HF-EX
Chow-Glucose
HF-Glucose
HF-GPA-Glucose
HF-EX-Glucose
B
500
400
300
200
100
0
JO2 (pmol·sec-1·mg-1dry wt)
- Glucose
+ Glucose
C
150
100
50
0
Km (μM ADP)
*
- Glucose
+ Glucose
D
600
400
200
0
JO2 (pmol·sec-1·mg-1dry wt)
Oligo
FCCP
Chow
HF
HF-GPA
HF-EX
Chow-Glucose
HF-Glucose
HF-GPA-Glucose
HF-EX-Glucose

Figure 3-4. Little effect of β-GPA and exercise on mitochondria respiration kinetics in response to ADP titration in rats.

Rats‘ PmFBs mitochondria respiration kinetics in response to ADP titration was measured in the presence of 5mM glutamate + 2mM malate. Oligomycin and FCCP were added subsequently in the end of the ADP titration protocol. Michaelis-Menten enzyme kinetics curve was fitted. Other than the decreased sensitivity (increased Km) by β-GPA, little treatment effect on the respiration kinetics was found. (A) The quantified kinetics trace. (B) Maximal mitochondria respiration capacity from panel A. (C) Mitochondria respiration sensitivity (Km) in response to ADP obtained from Michaelis-Menten enzyme kinetics. (D) 10μg/ml Oligomycin-inhibited and 4μM FCCP-uncoupled respiration rate. *P<0.05 vs Chow or HF-EX. Mean ± SEM. N=5/ group. Glucose(2) X Treatment(4) two-way ANOVA, Bonferroni.

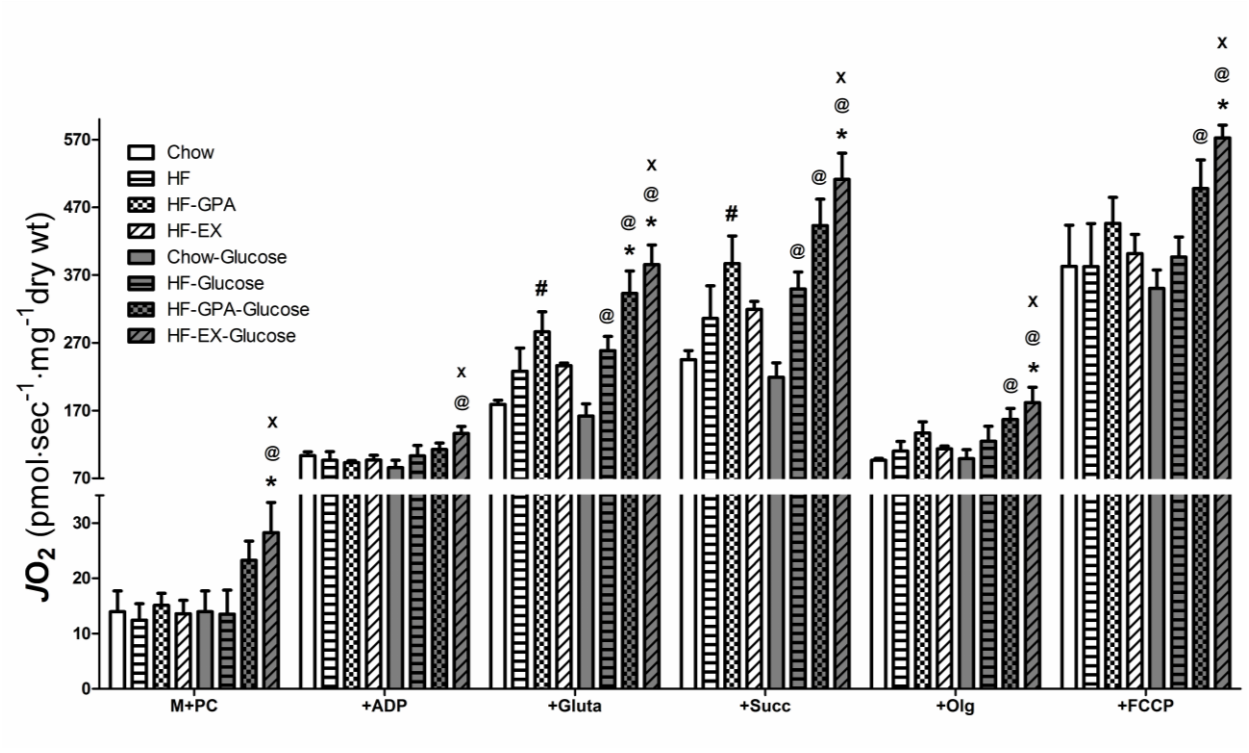

Figure 3-5. β-GPA and exercise increase mitochondria respiration capacity in response to multiple substrates in rats.

Rats‘ PmFBs mitochondria respiration capacity was measured in response to sequential addition of the following substrates. 1mM malate + 25μM palmitoyl-L-carnitine (M+PC) + 2mM ADP + 2mM glutamate (+Gluta) + 3mM succinate (+Succ) + 10μg/ml oligomycin (+Olg) + 4μM FCCP. The data indicate β-GPA and exercise increase mitochondria respiration capacity in response to multiple substrates. # P<0.05 vs Chow. @ P<0.05 vs Chow-Glucose. *P<0.05 vs HF-Glucose. x P<0.05 vs HF-EX. Mean ± SEM. N=5/ group. Glucose(2) X Treatment(4) two-way ANOVA, Bonferroni.

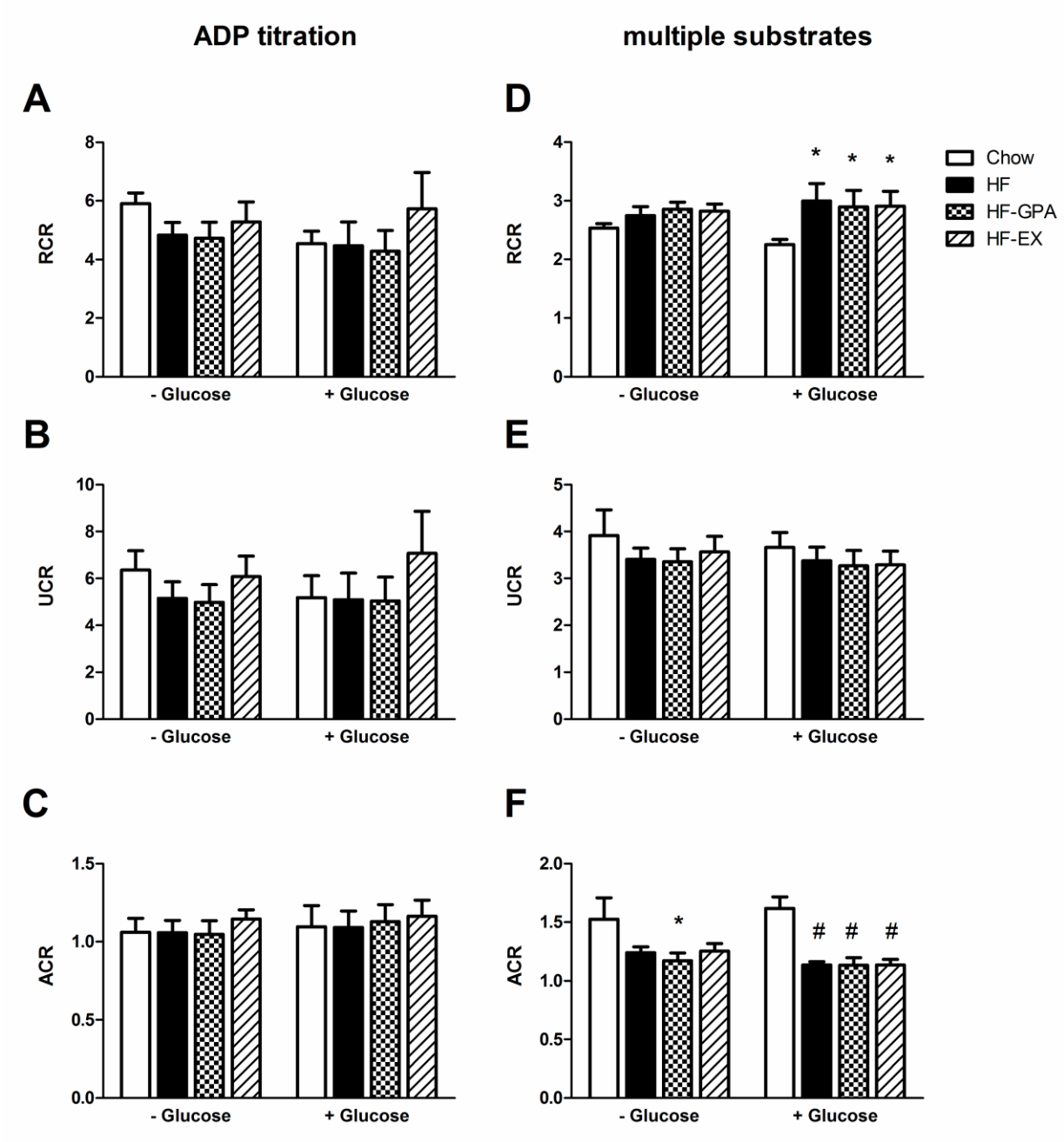
ADP titration
multiple substrates
A
B
C
D
E
F
RCR
UCR
ACR
- Glucose
+ Glucose
Chow
HF
HF-GPA
HF-EX
*
#

Figure 3-6. Little effect of β-GPA and exercise on mitochondria respiratory control indices of rats.

Mitochondria respiratory control indices which indicate the quality of mitochondria OXPHOS capacity were calculated from ADP titration protocol (Fig. 3-4) or multiple substrates protocol (Fig. 3-5). Respiration control ratio (RCR) is the quotient of maximal state III to oligomycin-inhibited state IV respiration. Uncoupling control ratio (UCR) is the quotient of FCCP-uncoupled respiration to oligomycin-inhibited state IV respiration. Andenylate control ratio (ACR) is the quotient of FCCP-uncoupled respiration to maximal state III respiration. No treatment effect was found expect that, under glucose challenged state in multiple substrate condition, an improvement in both RCR (increased) and ACR (decreased) by HFD independent of β-GPA or exercise treatment. (A) RCR from ADP titration protocol. (B) UCR from ADP titration protocol. (C) ACR from ADP titration protocol. (D) RCR from multiple substrates protocol. * $P<0.05$ vs all other groups in glucose challenged condition. (E) UCR from multiple substrates protocol. (F) ACR from multiple substrates protocol. * $P<0.05$ vs Chow in no glucose challenge condition. # $P<0.05$ vs Chow in glucose challenged condition. Mean ± SEM. N=5/ group. Glucose(2) X Treatment(4) two-way ANOVA, Bonferroni.

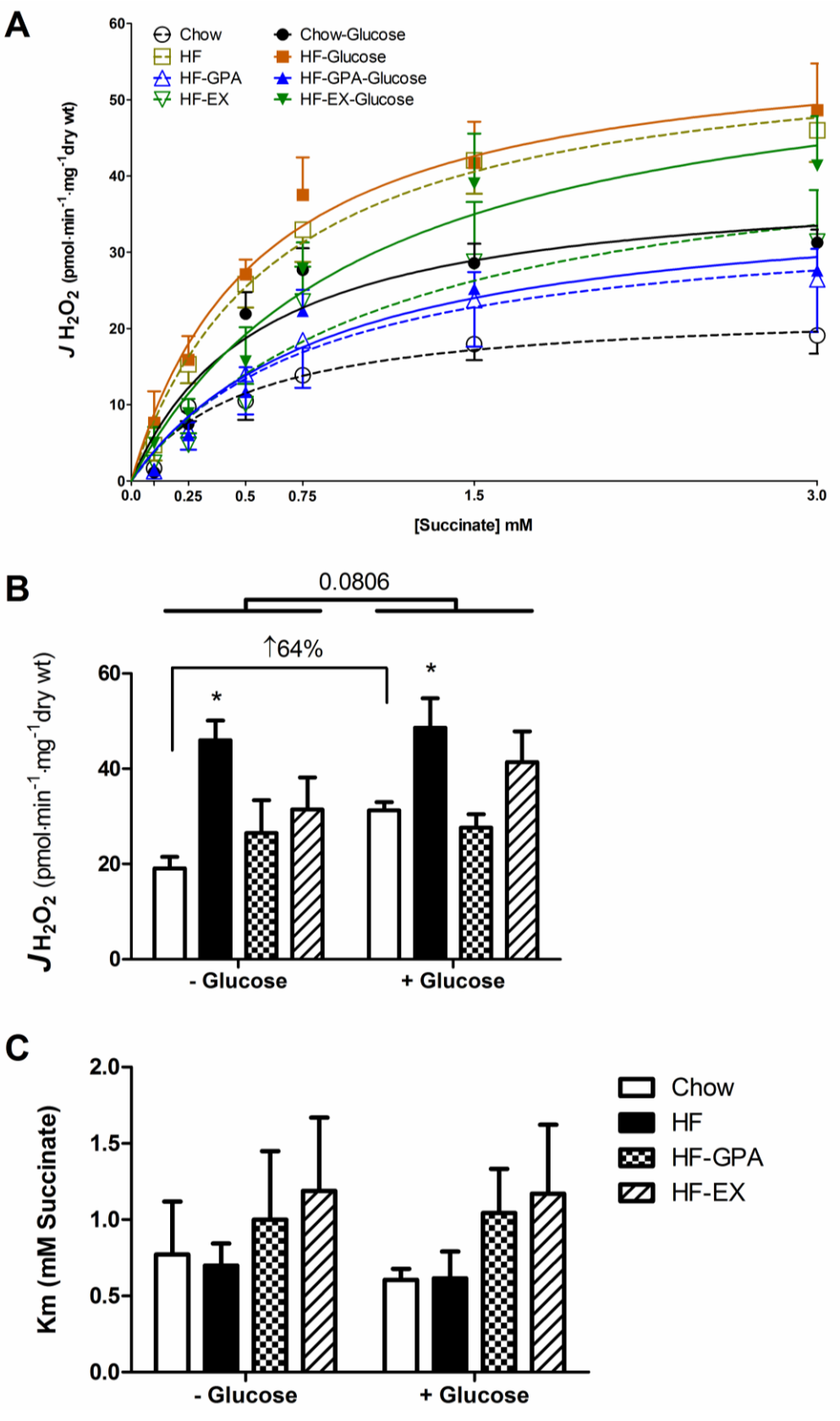
A
Chow
HF
HF-GPA
HF-EX
Chow-Glucose
HF-Glucose
HF-GPA-Glucose
HF-EX-Glucose
J H2O2 (pmol·min-1·mg-1dry wt)
[Succinate] mM
0.0
0.25
0.5
0.75
1.5
3.0
B
0.0806
↑64%
*
*
J H2O2 (pmol·min-1·mg-1dry wt)
- Glucose
+ Glucose
C
Km (mM Succinate)
Chow
HF
HF-GPA
HF-EX
- Glucose
+ Glucose

Figure 3-7. β-GPA and exercise attenuated HFD caused $_{m}E_{H2O2}$ challenged by complex I reverse electron flux in rats.

To determine if high caloric intake acutely and chronically influences $_{m}E_{H2O2}$, 7 week treated rats were sacrificed after a 4h fast or 1h after a single glucose challenge (2g/ kg body weight) performed after a 3h fast. The kinetics of PmFBs state IV $_{m}E_{H2O2}$ in response to succinate titration was measured in the presence of 5μM glutamate + 2μM malate. Michaelis-Menten enzyme kinetics curve was fitted. The results indicate β-GPA and exercise attenuated HFD caused $_{m}E_{H2O2}$. Further, $_{m}E_{H2O2}$ are remarkably sensitive to acute high glucose intake. (A) The kinetics response. (B) Maximal $_{m}E_{H2O2}$ (at 3mM succinate) from panel A. * $P<0.05$ vs Chow or HF-GPA. $p=.0806$ main factor effect with vs without glucose challenge. Note that a single glucose challenge on chow diet fed rats 1h before sacrifice increase 64% of $_{m}E_{H2O2}$ although it does not reach statistical significance. (C) $_{m}E_{H2O2}$ sensitivity (Km) in response to succinate titration obtained from Michaelis-Menten enzyme kinetics. Mean ± SEM. N=5/ group. Glucose(2) X Treatment(4) two-way ANOVA, Bonferroni.

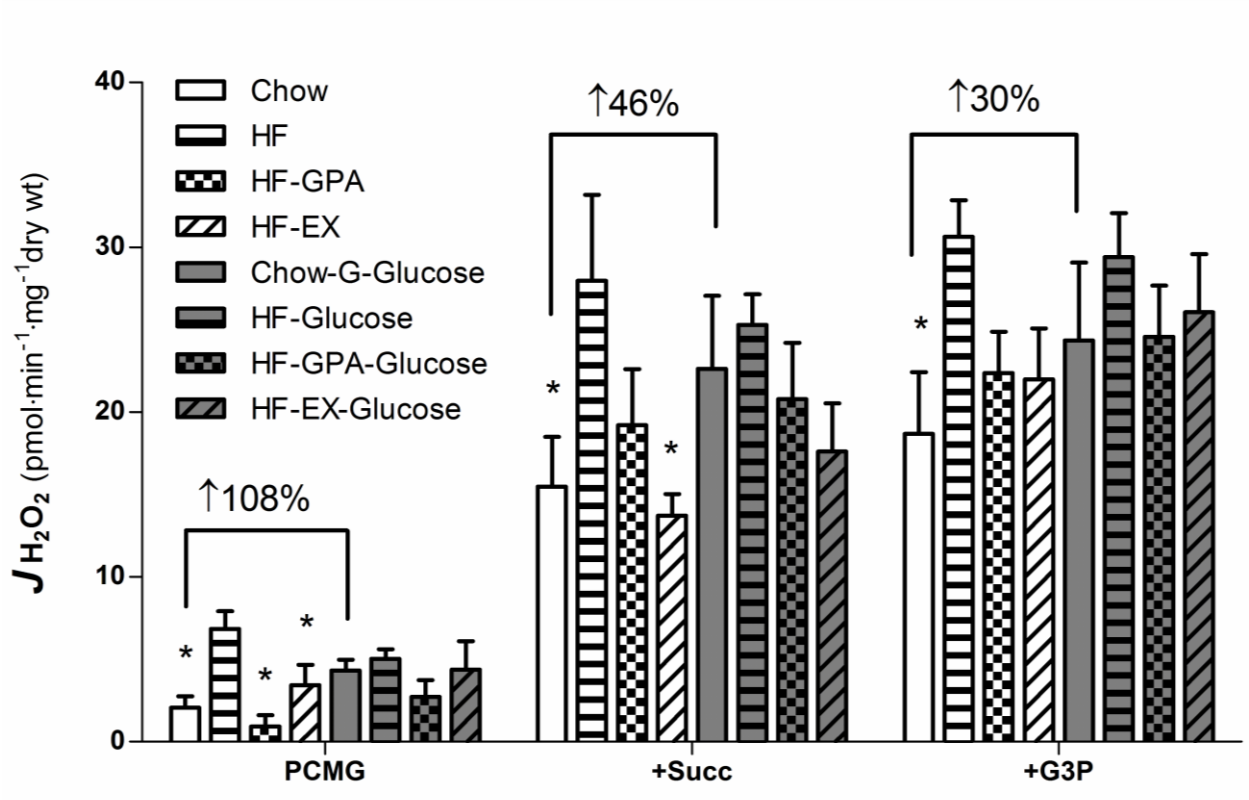

Figure 3-8. β-GPA and exercise attenuated HFD caused $_mE_{H2O2}$ challenged by multiple substrates in rats.

Rats' PmFBs state IV $_mE_{H2O2}$ in oxidizing 25μM palmitoyl-L-carnitine + 1mM malate + 2mM glutamate (PCMG), + 3mM succinate (+Succ), and + 10mM Glycerol-3-Phosphate (+G3P). The result indicate both β-GPA and exercise treatment sufficiently normalize the HFD caused $_mE_{H2O2}$ under multiple substrate conditions. Note that a single glucose challenge (2g/ kg body weight) on chow diet fed rats 1h before sacrifice increase 30-108% of $_mE_{H2O2}$ * $P<0.05$ vs HF in each substrate condition either with or without glucose challenge. Mean ± SEM. N=5/ group. Glucose(2) X Treatment(4) two-way ANOVA, Bonferroni.

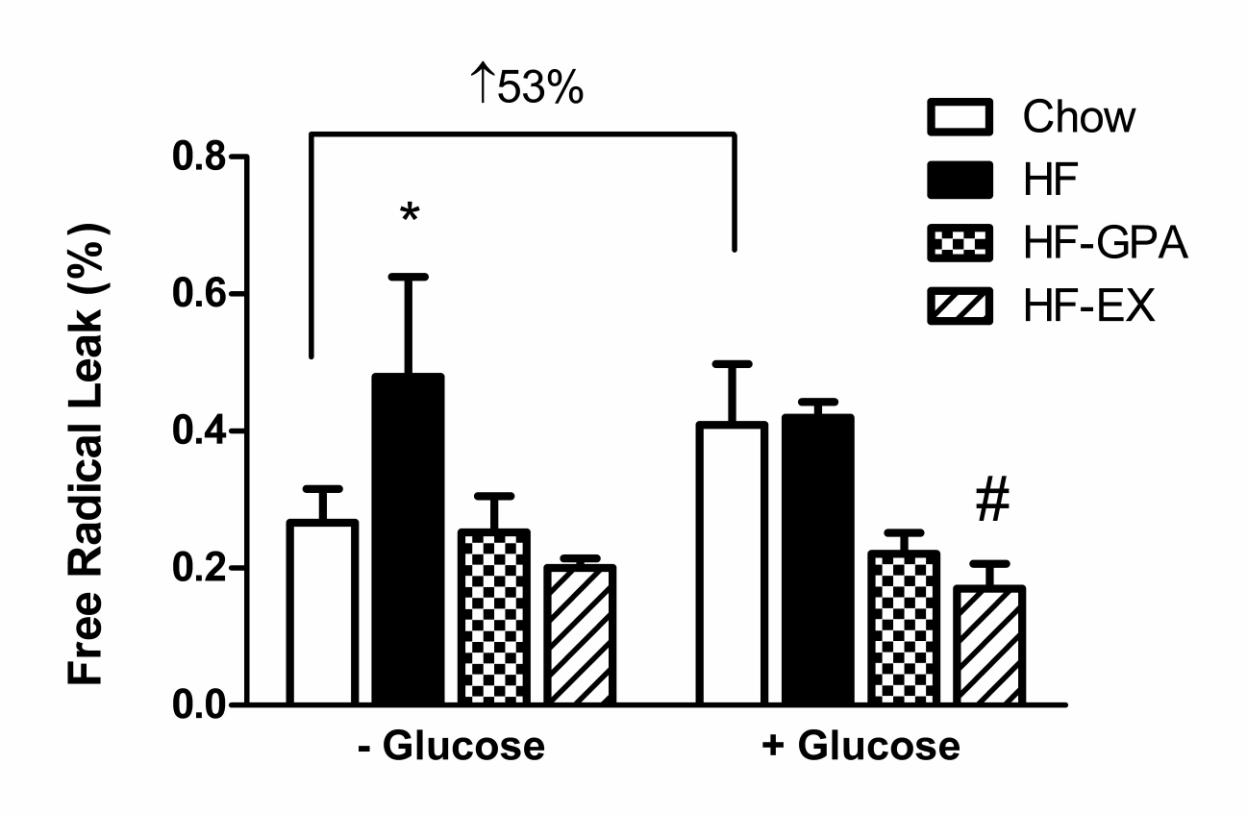

Figure 3-9. β-GPA and exercise attenuated HFD caused mitochondria $_{m}$FRL% in rats. Mitochondrial $_{m}$FRL% was calculated from H_2O_2 generated per O_2 consumed. H_2O_2 generation (Fig. 3-8) and O_2 consumption (Fig. 3-5) were under the condition mitochondria oxidizing 25μM palmitoyl-L-carnitine + 1mM malate + 2mM glutamate + 3mM succinate in state IV (with oligomycin). * $P<0.05$ vs HF-EX. # $P<0.05$ vs Chow or HF. Mean ± SEM. N=5/ group. Glucose(2) X Treatment(4) two-way ANOVA, Bonferroni.

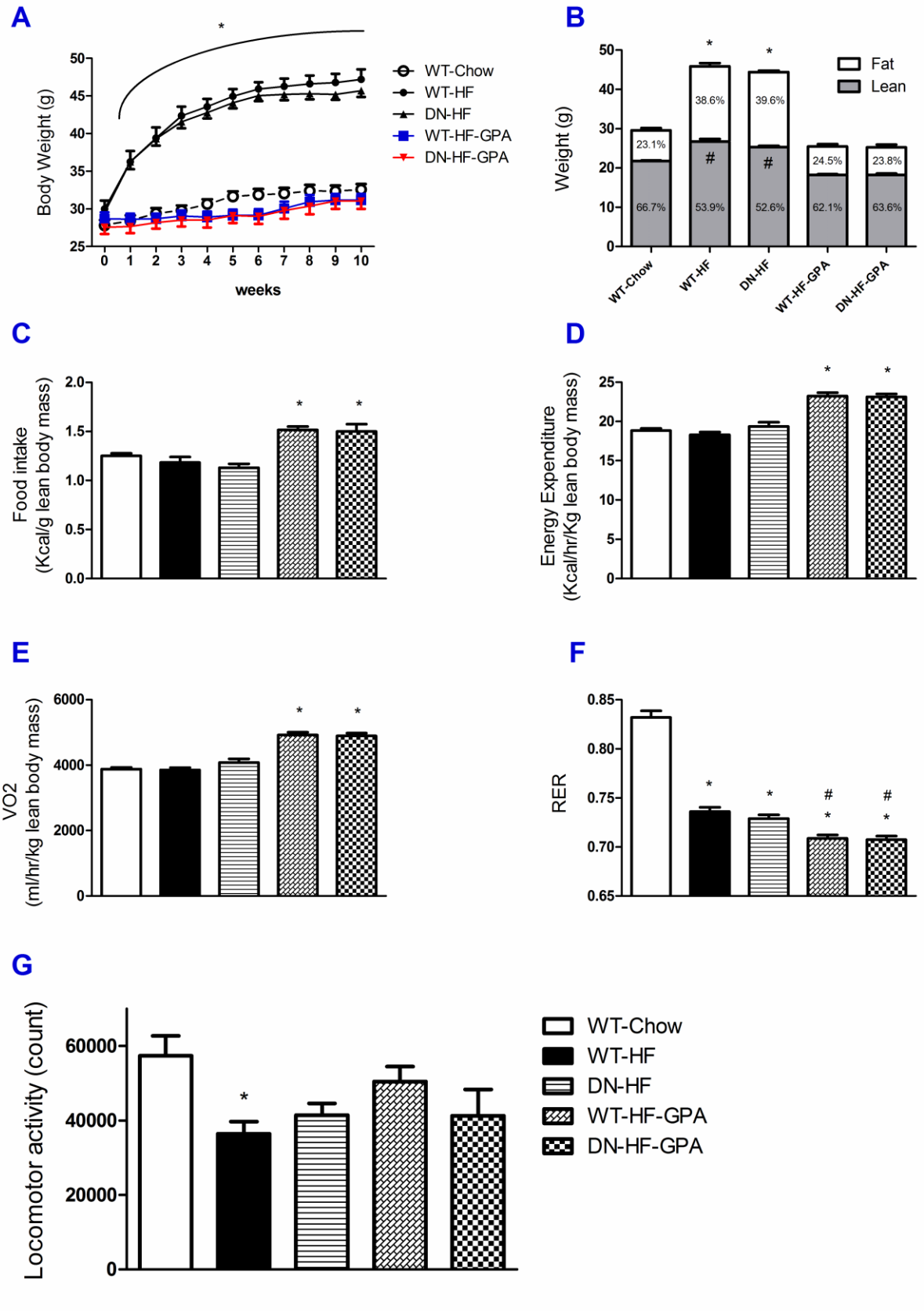
A
Body Weight (g)
weeks
WT-Chow
WT-HF
DN-HF
WT-HF-GPA
DN-HF-GPA
B
Weight (g)
Fat
Lean
23.1%
38.6%
39.6%
24.5%
23.8%
66.7%
53.9%
52.6%
62.1%
63.6%
WT-Chow
WT-HF
DN-HF
WT-HF-GPA
DN-HF-GPA
C
Food intake
(Kcal/g lean body mass)
D
Energy Expenditure
(Kcal/hr/Kg lean body mass)
E
VO2
(ml/hr/kg lean body mass)
F
RER
G
Locomotor activity (count)
WT-Chow
WT-HF
DN-HF
WT-HF-GPA
DN-HF-GPA

Figure 3-10. AMPKα2 genotype did not affect the β-GPA effect on body composition, metabolic state and locomotor activity in mice.

To determine if AMPKα2 genotype influences the β-GPA effects on metabolism, AMPKα2-DN mice and its WT littermates were monitored for two complete light-dark cycles (48h) via an indirect calorimetry system after 4 days of acclimation during week 8 of diet treatment. Body composition was determined right after the calorimetry system using the Echo Magnetic Resonance Imaging system. The data of metabolic state had a very similar trend when normalized to either lean body mass (shown) or whole body mass. Regardless of the AMPKα2 genotype, β-GPA treatment increases energy expenditure without affecting locomotor activity, and prevents HF-induced body weight gain despite higher food intake. (A) Body weight over the 10 weeks of diet treatment. * $P<0.05$ vs Chow, WT-HF-GPA or DN-HF-GPA. (B) Body composition. # $P<0.05$ vs Chow, WT-HF-GPA or DN-HF-GPA in lean body mass. * $P<0.05$ vs Chow, WT-HF-GPA or DN-HF-GPA in fat body mass. The total body mass percentage of lean or fat was indicated. (C) Food intake (48h total). * $P<0.05$ vs WT-Chow, WT-HF or DN-HF. (D) Energy expenditure rate (48h average). * $P<0.05$ vs WT-Chow, WT-HF or DN-HF. (E) Oxygen consumption rate (48h average). * $P<0.05$ vs WT-Chow, WT-HF or DN-HF. (F) RER (48h average). * $P<0.05$ vs WT-Chow. # $P<0.05$ vs WT-HF or DN-HF. (G) Locomotor activity (sum of X, Y, Z axis count/activity, 48h total). * $P<0.05$ vs WT-Chow. Mean ± SEM. N=9~18/ group. One-way ANOVA + Tukey.

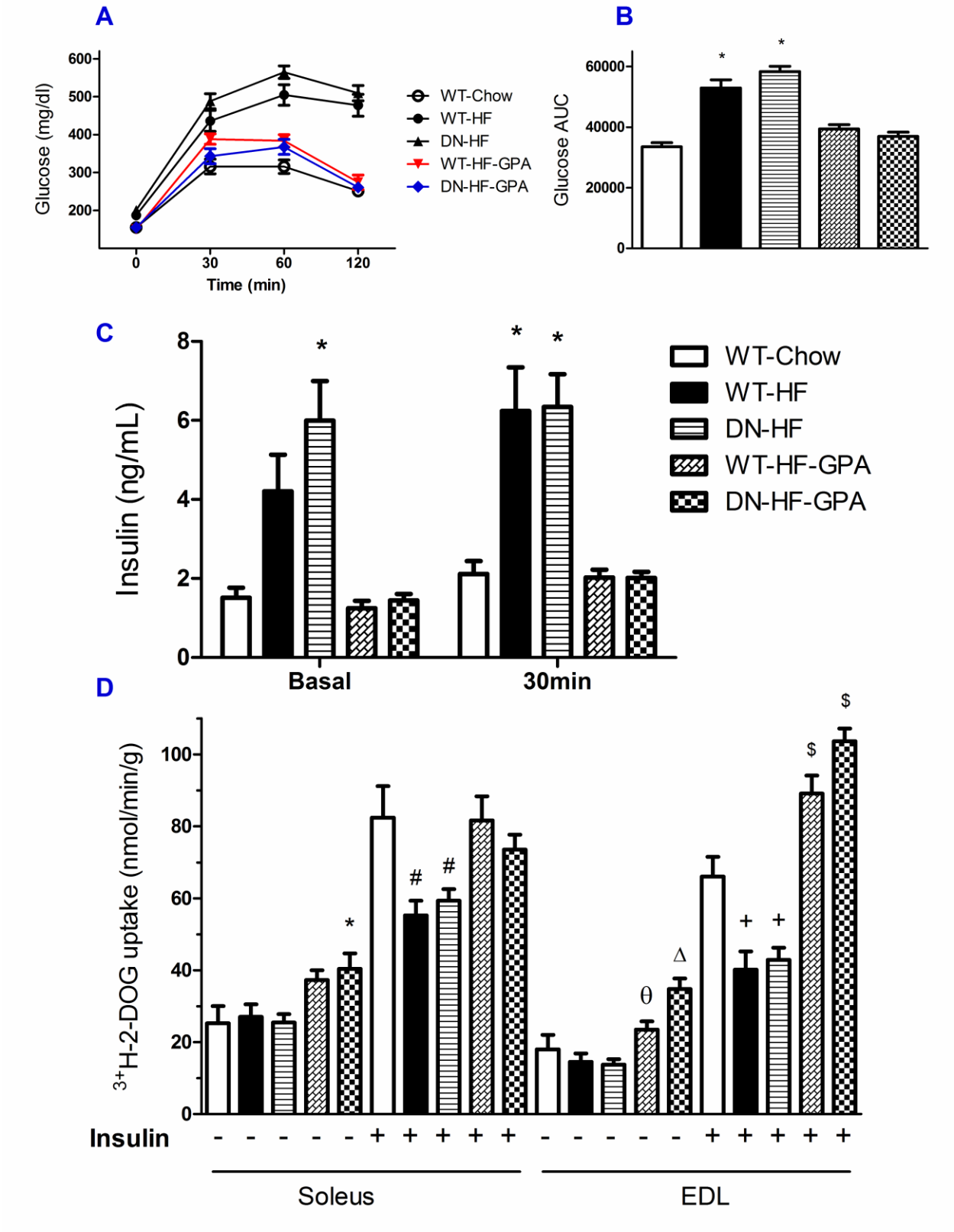
A
Glucose (mg/dl)
600
500
400
300
200
0
30
60
120
Time (min)
WT-Chow
WT-HF
DN-HF
WT-HF-GPA
DN-HF-GPA
B
Glucose AUC
60000
40000
20000
0
*
*
C
Insulin (ng/mL)
8
6
4
2
0
*
*
*
Basal
30min
WT-Chow
WT-HF
DN-HF
WT-HF-GPA
DN-HF-GPA
D
3+H-2-DOG uptake (nmol/min/g)
100
80
60
40
20
0
*
#
#
θ
Δ
+
+
$
$
$
Insulin
- - - - - + + + + +
- - - - - + + + + +
Soleus
EDL

Figure 3-11. β-GPA prevented HFD caused IR regardless of the AMPKα2 genotype in mice.

To determine if mice AMPKα2 genotype affect the effects of β-GPA on insulin sensitivity after HFD, IPGTT (1.5g/ kg body weight) was conducted in the morning following a 4h fasting in mice at week 9 of treatment. Plasma for [insulin] measurement was collected from the tail vein in the basal state and 30min after the glucose injection. Mice were further sacrificed in the morning following a 4h fasting at week 10 of treatment. Soleus (slow twitch) and EDL (fast twitch) muscle were harvested for in vitro determination of muscle $^{3+}$H-2-DOG uptake. Mice were studied ~16 hours after the last β-GPA treatment in both IPGTT and $^{3+}$H-2-DOG uptake experiments. The data indicate there was no AMPKα2 genotype effect. (A) [Glucose] from IPGTT. (B) Area under the curve (AUC) of [Glucose] from IPGTT. * P<0.05 vs WT-Chow, WT-HF-GPA or DN-HF-GPA. (C) [Insulin] from baseline and 30 min after glucose injection. * P<0.05 vs WT-Chow, WT-HF-GPA or DN-HF-GPA. (D) Muscle $^{3+}$H-2-DOG uptake. * P<0.05 vs WT-Chow or DN-HF. # P<0.05 vs WT-Chow or WT-HF-GPA. ∆ P<0.05 vs all other groups. ɵ P<0.05 vs DN-HF. + P<0.05 vs all other groups but not the other HF without GPA treated group. $ P<0.05 vs all other groups but not the other GPA treated group. Mean ± SEM. N=9~18/ group. One-way ANOVA + Tukey.

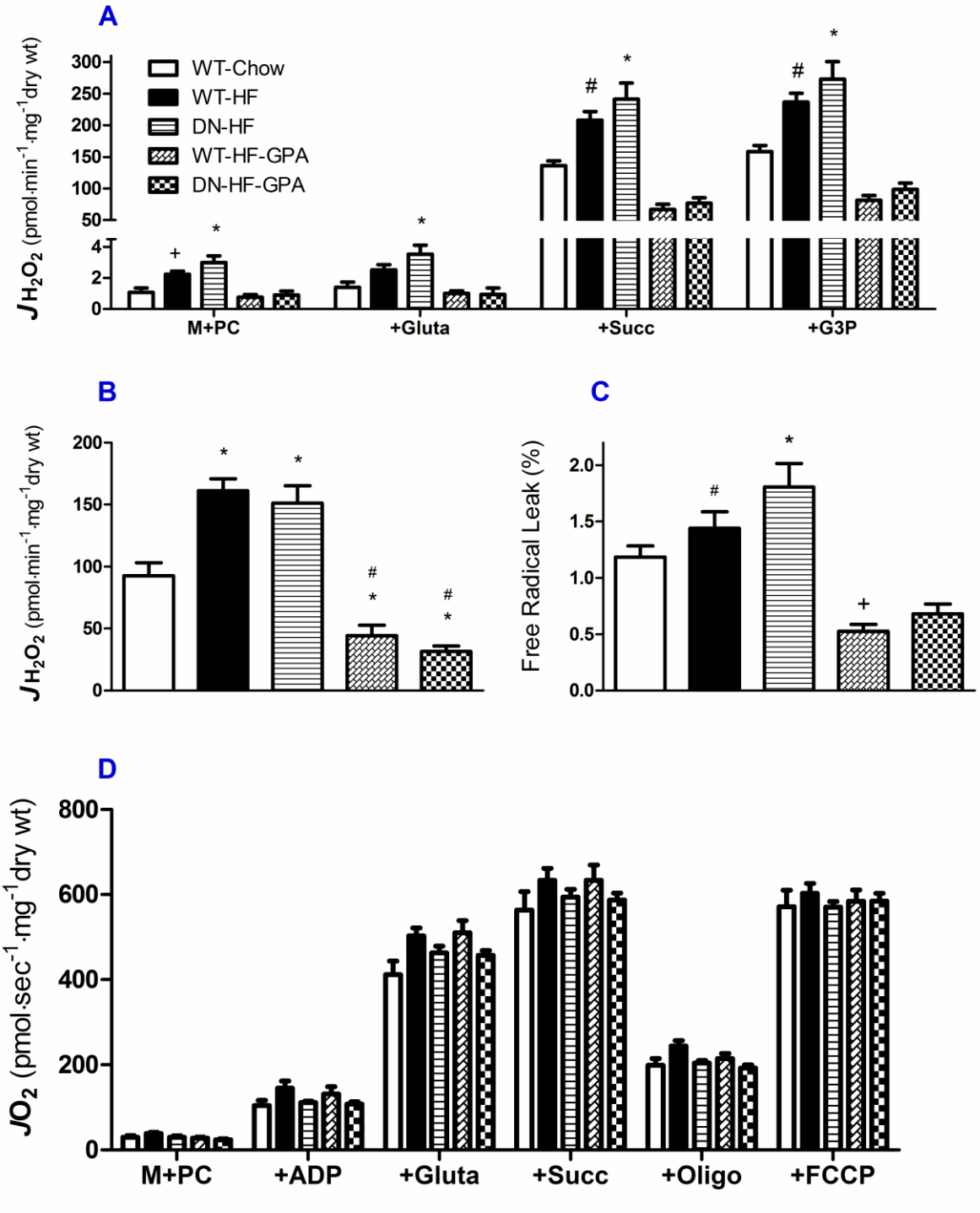
A
WT-Chow
WT-HF
DN-HF
WT-HF-GPA
DN-HF-GPA
$J_{H_2O_2}$ (pmol·min^{-1}·mg^{-1}dry wt)
M+PC
+Gluta
+Succ
+G3P
B
$J_{H_2O_2}$ (pmol·min^{-1}·mg^{-1}dry wt)
C
Free Radical Leak (%)
D
JO_2 (pmol·sec^{-1}·mg^{-1}dry wt)
M+PC
+ADP
+Gluta
+Succ
+Oligo
+FCCP

Figure 3-12. β-GPA prevented the HFD caused $_{m}E_{H2O2}$ and $_{m}$FRL% regardless of AMPKα2 genotype in mice.

To determine if AMPKα2 genotype affect the β-GPA treatment effect in mitochondrial respiration and state IV $_{m}E_{H2O2}$ of HFD fed mice, assays were performed in PmFBs prepared from 4h fasted AMPKα2-DN mice and its wild type littermates after 10 weeks of HFD feeding. The data indicated, without affecting mitochondria respiration capacity, β-GPA prevents the HFD-induced increase in $_{m}E_{H2O2}$ and $_{m}$FRL% regardless of AMPKα2 genotype. (A) Muscle $_{m}E_{H2O2}$ in response to 1mM malate + 25μM palmitoyl-L-carnitine (M+PC) + 2mM glutamate (+Gluta), + 9mM succinate (+Succ), and + 10mM Glycerol-3-Phosphate (+G3P). * P<0.05 vs W-Chow, WT-HF-GPA or DN-HF-GPA. # P<0.05 vs WT-HF-GPA or DN-HF-GPA. + P<0.05 vs WT-HF-GPA. (B) Muscle $_{m}E_{H2O2}$ in response to 9mM succinate. # P<0.05 vs WT-HF or DN-HF. * P<0.05 vs WT-Chow. (C) $_{m}$FRL% was calculated from H_2O_2 generated per O_2 consumed. H_2O_2 generation (panel A) and O_2 consumption (panel D) were under the condition mitochondria oxidizing M+PC+Gluta+Succ under state IV condition (with oligomycin). * P<0.05 vs WT-Chow, WT-HF-GPA or DN-HF-GPA. # P<0.05 vs WT-HF-GPA or DN-HF-GPA. + P<0.05 vs WT-Chow. (D) Muscle mitochondria respiration capacity in response to 1mM malate + 25μM palmitoyl-L-carnitine (M+PC) + 2mM ADP + 2mM glutamate (Gluta) + 9mM succinate (Succ) + 10μg/ml oligomycin (Oligo) + 4μM FCCP. Mean ± SEM. N=9~18/ group. One-way ANOVA + Tukey.

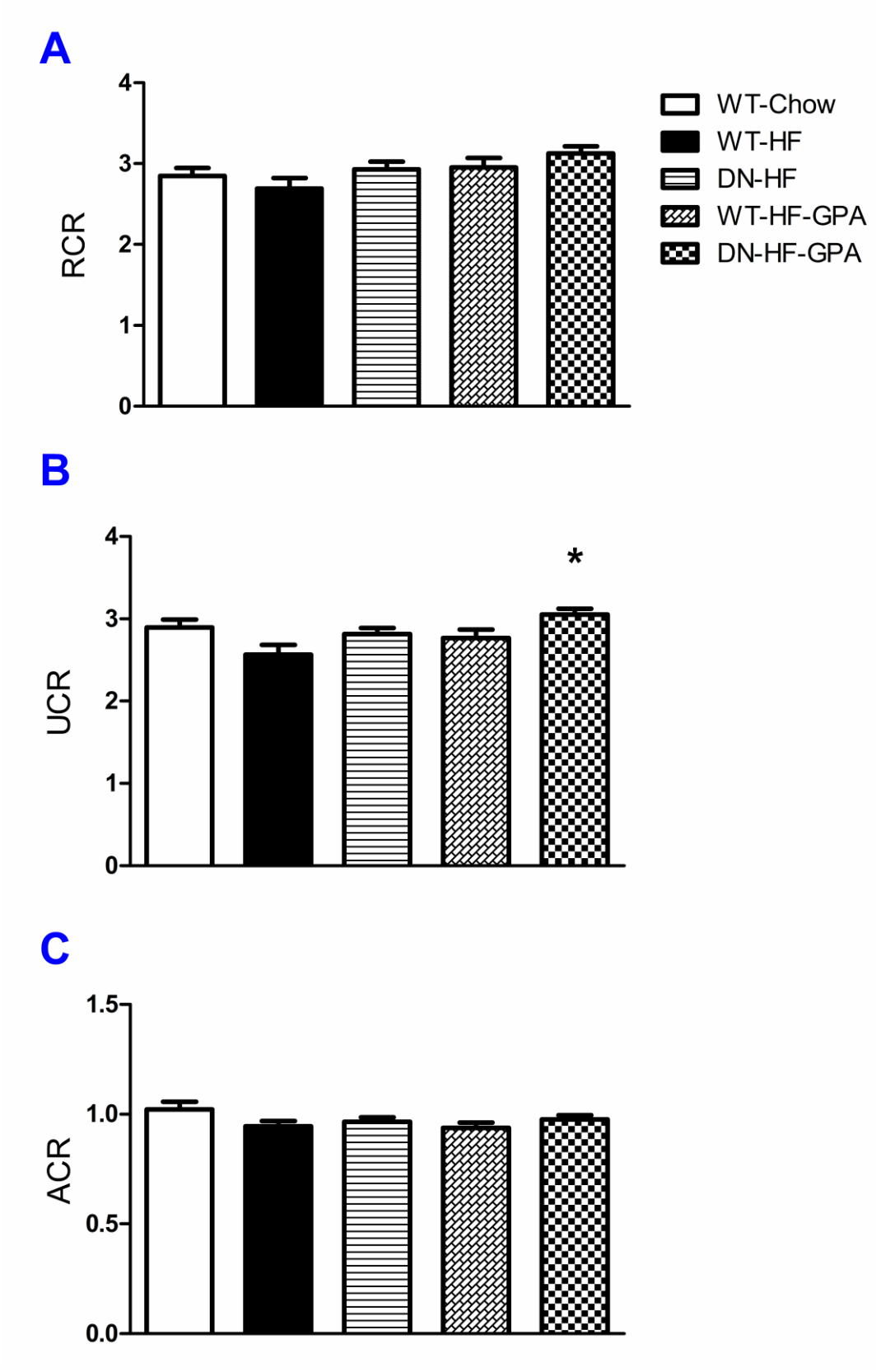
A
RCR
4
3
2
1
0
WT-Chow
WT-HF
DN-HF
WT-HF-GPA
DN-HF-GPA
B
UCR
4
3
2
1
0
*
C
ACR
1.5
1.0
0.5
0.0

Figure 3-13. No clear HFD, β-GPA or AMPKα2 genotype effect on mitochondria respiratory control indices of mice.

Mitochondria respiratory control indices (as explained in figure 3-6) were calculated from mitochondrial respiration capacity (Fig. 3-12 (D)). Overall, no treatment or genotype effect was found indicating no mitochondrial OXPHOS defect. (A) RCR. (B) UCR. * $P<0.05$ vs WT-HF. (C) ACR. Mean ± SEM. N=9~18/ group. One-way ANOVA + Tukey.

CHAPTER 4: Integrated Discussion

The roles of mitochondrial FAO/OXPHOS capacity and oxidative stress in the development of diabetes have recently gained considerable attention, and more specifically how insulin action is regulated in skeletal muscle (the main glucose disposal organ). In Chapter 1, review of the literature suggests a causative role of mitochondrial oxidative stress in the etiology of diet induced IR. It has been demonstrated that acute and chronic nutritional oversupply increases skeletal muscle $_{m}E_{H2O2}$, a phenomenon that is causally linked to IR[64]. Whole body metabolic imbalance is the underlying cause of metabolic diseases, and within cells metabolic balance is a function of how well substrate supply matches energy demand and vice versa. The interplay between metabolic supply and ROS production is well established, yet the extent to which energy expenditure can compensate for the deleterious effects of over-nutrition on ROS production, cellular redox state and insulin sensitivity is currently unknown. The studies described in chapter 2 and 3 were all conducted with hypotheses governed by the same theme: to examine the impact of a mild increase in energy expenditure on over-nutrition induced skeletal muscle mitochondrial oxidative stress and IR.

In chapter 2, an acute effect of metabolic oversupply (lipid loading) and energy expenditure (low intensity exercise) on the regulation of rat skeletal muscle mitochondria was examined. This study examed $_{m}E_{H2O2}$, $\Delta\Psi_{m}$ and $_{m}Ca^{2+}{}_{RC}$ under state IV and more physiological state III respiration conditions using a novel “clamp” technique. These data revealed a number of important findings. First, without affecting OXPHOS capacity, skeletal muscle $_{m}E_{H2O2}$, $\Delta\Psi_{m}$ and $_{m}Ca^{2+}{}_{RC}$ were extremely

sensitive to metabolic status. The lipid overloading of ~12% of the daily total caloric intake (when in HFD conditions) acutely caused an adverse effect of these 3 parameters of mitochondria while post-meal low intensity exercise nearly completely attenuated the response. This supports the idea that mitochondrial $_{m}E_{H2O2}$ emission is more likely the preceding and possibly primary underlying cause of IR. OXPHOS capacity, on the other hand, may play a secondary role. Furthermore, it is notable that low intensity exercise is sufficient to attenuate the acute lipid loading induced defects on $_{m}E_{H2O2}$, $\Delta\Psi_m$ and $_{m}Ca^{2+}_{RC}$. It follows the principle of bioenergetics that a reduction in $\Delta\Psi_m$ by mildly increasing energy demand and therefore JO_2 from idling (close to state IV) can significantly reduce "the reducing pressure of electron transport system (ETS)" and oxidant production.

In chapter 3, the impact of a mild daily increase in energy expenditure on $_{m}E_{H2O2}$ and the development of insulin resistance were examined in the context of chronic HF intake. The findings of this study provide further support for a causative role of mitochondrial H_2O_2 emission in the development of diet induced IR. This study again shows that a long term HFD causes an increased skeletal muscle $_{m}E_{H2O2}$, albeit state IV data only, in conjunction with the development of IR in rodents. Mildly increased energy expenditure by either exercise or β-GPA attenuated HFD caused both $_{m}E_{H2O2}$ elevation and IR development. The treatment effects of HFD, exercise or β-GPA appeared to be mitochondrial density, respiratory function, fatty acid oxidation rate and AMPKα2 genotype independent, leaving the reduction in mitochondrial oxidative stress as the most likely primary mechanism of exercise and β-GPA on attenuating HFD caused IR.

In the context of both acute and chronic manipulation of positive (oversupply) and negative (expenditure) cellular energy balance, together, these findings support the

mounting evidence favoring the causative role of skeletal muscle mitochondrial H_2O_2 emission/oxidative stress in the development of diet induced IR. These data demonstrated a mild increase in energy expenditure can sufficiently attenuate the HFD caused oxidative stress and IR. This is important because it not only supports the causative role of oxidative stress based on the known inverse exponential relationship of superoxide production and JO_2 under low respiration condition, but also provides a clinical and practical strategy (i.e., mild physical activity) to treat/prevent over-nutrition caused IR. These findings also provide evidence that mitochondrial oxidative stress and related effects are very sensitive and dynamically regulated by the metabolic status. $\Delta\Psi_m$ and oxidative stress are likely among the preceding factors acutely elevated by lipid loading and ultimately could lead to the development of IR and mitochondrial dysfunction (reduced density and respiration capacity). A shift in respiratory activity from idling to mild increase in state III respiration is sufficient to prevent/attenuate the oxidant production and related risks.

Given that the literature and the presenting data favor the causative role of mitochondrial oxidant production in the etiology of diet induced IR, the molecular mechanism of how mitochondrial H_2O_2 causes IR is still largely unknown and is of important direction of future studies. Redox-sensitive protein modifications may be a crucial mechanism of how oxidative stress regulates the insulin signaling cascade and causes IR. The reversible prosperity of redox-sensitive protein modifications may therefore allow increased energy expenditure (reduced oxidative stress) to dynamically compensate for the metabolic oversupply caused IR.

In the present studies, the potential influence of DAG-PKC-IRS pathway was not examined. Intracellular accumulation of DAG due to mitochondrial dysfunction has been

widely suggested as a primary cause of insulin resistance in skeletal muscle[280]. In the present study, HFD induced insulin resistance did not affect mitochondrial OXPHOS or content. Moreover, the improvements in insulin sensitivity found in HFD animals that were subjected to exercise or β-GPA treatment occurred in the absence of any change in "mitochondrial function". It is certainly possible that cytosolic lipid levels, and thus activity of DAG-induced signaling, decreased in the muscle of exercise and β-GPA treated animals due to the increase in energy demand. This would be entirely consistent with our hypothesis that the metabolic defect induced by a HFD is triggered by the imbalance in energy supply relative to demand and that increasing energy demand relieves this imbalance. Although the exercise and β-GPA treatment effect on $_{m}E_{H2O2}$ and IR is clear and supports our hypothesis that $_{m}E_{H2O2}$ is a key factor regulating insulin sensitivity, we cannot exclude the potential influence of the DAG-PKC-IRS pathway. However, arguing against a primary role for DAG-PKC-IRS pathway is the study by Finck et al[281] who found that muscle lipid accumulation was completely dissociated from muscle insulin sensitivity in transgenic mice with targeted PPARα knockout or overexpression. Nevertheless, whether the DAG-PKC-IRS pathway or ROS are the more dominate primary factor leading to the over-nutrition caused IR is still unknown, our data support the idea that the ROS-mediated effect is a primary factor controling insulin sensitivity in skeletal muscle.

REFERENCES

1. DeFronzo, R.A*., et al.* The effect of insulin on the disposal of intravenous glucose. Results from indirect calorimetry and hepatic and femoral venous catheterization. *Diabetes* **30**, 1000-1007 (1981).
2. Reaven, G.M. Pathophysiology of insulin resistance in human disease. *Physiol Rev* **75**, 473-486 (1995).
3. Cooney, G.J., Thompson, A.L., Furler, S.M., Ye, J. & Kraegen, E.W. Muscle long-chain acyl CoA esters and insulin resistance. *Ann N Y Acad Sci* **967**, 196-207 (2002).
4. McGarry, J.D. Banting lecture 2001: dysregulation of fatty acid metabolism in the etiology of type 2 diabetes. *Diabetes* **51**, 7-18 (2002).
5. Schmitz-Peiffer, C. Protein kinase C and lipid-induced insulin resistance in skeletal muscle. *Ann N Y Acad Sci* **967**, 146-157 (2002).
6. Rudich, A*., et al.* Prolonged oxidative stress impairs insulin-induced GLUT4 translocation in 3T3-L1 adipocytes. *Diabetes* **47**, 1562-1569 (1998).
7. Itani, S.I., Ruderman, N.B., Schmieder, F. & Boden, G. Lipid-induced insulin resistance in human muscle is associated with changes in diacylglycerol, protein kinase C, and IkappaB-alpha. *Diabetes* **51**, 2005-2011 (2002).
8. Samuel, V.T., Petersen, K.F. & Shulman, G.I. Lipid-induced insulin resistance: unravelling the mechanism. *Lancet* **375**, 2267-2277.
9. Erion, D.M. & Shulman, G.I. Diacylglycerol-mediated insulin resistance. *Nat Med* **16**, 400-402.
10. Lowell, B.B. & Shulman, G.I. Mitochondrial dysfunction and type 2 diabetes. *Science* **307**, 384-387 (2005).
11. Kim, J.K*., et al.* PKC-theta knockout mice are protected from fat-induced insulin resistance. *J Clin Invest* **114**, 823-827 (2004).
12. Gao, Z*., et al.* Inactivation of PKCtheta leads to increased susceptibility to obesity and dietary insulin resistance in mice. *Am J Physiol Endocrinol Metab* **292**, E84-91 (2007).
13. Bocher, V., Pineda-Torra, I., Fruchart, J.C. & Staels, B. PPARs: transcription factors controlling lipid and lipoprotein metabolism. *Ann N Y Acad Sci* **967**, 7-18 (2002).
14. Ling, C*., et al.* Multiple environmental and genetic factors influence skeletal muscle PGC-1alpha and PGC-1beta gene expression in twins. *J Clin Invest* **114**, 1518-1526 (2004).
15. Mootha, V.K*., et al.* PGC-1alpha-responsive genes involved in oxidative phosphorylation are coordinately downregulated in human diabetes. *Nat Genet* **34**, 267-273 (2003).
16. Patti, M.E. Gene expression in humans with diabetes and prediabetes: what have we learned about diabetes pathophysiology? *Curr Opin Clin Nutr Metab Care* **7**, 383-390 (2004).
17. Petersen, K.F*., et al.* Mitochondrial dysfunction in the elderly: possible role in insulin resistance. *Science* **300**, 1140-1142 (2003).
18. Petersen, K.F., Dufour, S., Befroy, D., Garcia, R. & Shulman, G.I. Impaired mitochondrial activity in the insulin-resistant offspring of patients with type 2 diabetes. *N Engl J Med* **350**, 664-671 (2004).
19. Cheng, Z., Tseng, Y. & White, M.F. Insulin signaling meets mitochondria in metabolism. *Trends Endocrinol Metab*.
20. Chow, L., From, A. & Seaquist, E. Skeletal muscle insulin resistance: the interplay of local lipid excess and mitochondrial dysfunction. *Metabolism* **59**, 70-85.
21. Dumas, J.F., Simard, G., Flamment, M., Ducluzeau, P.H. & Ritz, P. Is skeletal muscle mitochondrial dysfunction a cause or an indirect consequence of insulin resistance in humans? *Diabetes Metab* **35**, 159-167 (2009).

22. Turner, N. & Heilbronn, L.K. Is mitochondrial dysfunction a cause of insulin resistance? *Trends Endocrinol Metab* **19**, 324-330 (2008).
23. Kelley, D.E., He, J., Menshikova, E.V. & Ritov, V.B. Dysfunction of mitochondria in human skeletal muscle in type 2 diabetes. *Diabetes* **51**, 2944-2950 (2002).
24. Ritov, V.B.*, et al.* Deficiency of Electron Transport Chain in Human Skeletal Muscle Mitochondria in Type 2 Diabetes Mellitus and Obesity. *Am J Physiol Endocrinol Metab* (2009).
25. Asmann, Y.W.*, et al.* Skeletal muscle mitochondrial functions, mitochondrial DNA copy numbers, and gene transcript profiles in type 2 diabetic and nondiabetic subjects at equal levels of low or high insulin and euglycemia. *Diabetes* **55**, 3309-3319 (2006).
26. Stump, C.S., Short, K.R., Bigelow, M.L., Schimke, J.M. & Nair, K.S. Effect of insulin on human skeletal muscle mitochondrial ATP production, protein synthesis, and mRNA transcripts. *Proc Natl Acad Sci U S A* **100**, 7996-8001 (2003).
27. Mogensen, M.*, et al.* Mitochondrial respiration is decreased in skeletal muscle of patients with type 2 diabetes. *Diabetes* **56**, 1592-1599 (2007).
28. Petersen, K.F., Dufour, S., Befroy, D., Garcia, R. & Shulman, G.I. Impaired mitochondrial activity in the insulin-resistant offspring of patients with type 2 diabetes. *The New England journal of medicine* **350**, 664-671 (2004).
29. Befroy, D.E.*, et al.* Impaired mitochondrial substrate oxidation in muscle of insulin-resistant offspring of type 2 diabetic patients. *Diabetes* **56**, 1376-1381 (2007).
30. Patti, M.E.*, et al.* Coordinated reduction of genes of oxidative metabolism in humans with insulin resistance and diabetes: Potential role of PGC1 and NRF1. *Proc Natl Acad Sci U S A* **100**, 8466-8471 (2003).
31. Sparks, L.M.*, et al.* A high-fat diet coordinately downregulates genes required for mitochondrial oxidative phosphorylation in skeletal muscle. *Diabetes* **54**, 1926-1933 (2005).
32. Fleischman, A.*, et al.* Effects of a nucleoside reverse transcriptase inhibitor, stavudine, on glucose disposal and mitochondrial function in muscle of healthy adults. *Am J Physiol Endocrinol Metab* **292**, E1666-1673 (2007).
33. Patti, M.E. & Kahn, B.B. Nutrient sensor links obesity with diabetes risk. *Nat Med* **10**, 1049-1050 (2004).
34. Schrauwen, P. & Hesselink, M.K. Oxidative capacity, lipotoxicity, and mitochondrial damage in type 2 diabetes. *Diabetes* **53**, 1412-1417 (2004).
35. Nair, K.S.*, et al.* Asian Indians have enhanced skeletal muscle mitochondrial capacity to produce ATP in association with severe insulin resistance. *Diabetes* **57**, 1166-1175 (2008).
36. De Feyter, H.M.*, et al.* Early or advanced stage type 2 diabetes is not accompanied by in vivo skeletal muscle mitochondrial dysfunction. *European journal of endocrinology / European Federation of Endocrine Societies* **158**, 643-653 (2008).
37. De Feyter, H.M.*, et al.* Increased intramyocellular lipid content but normal skeletal muscle mitochondrial oxidative capacity throughout the pathogenesis of type 2 diabetes. *The FASEB journal : official publication of the Federation of American Societies for Experimental Biology* **22**, 3947-3955 (2008).
38. Helge, J.W. & Kiens, B. Muscle enzyme activity in humans: role of substrate availability and training. *Am J Physiol* **272**, R1620-1624 (1997).
39. Vogt, M.*, et al.* Effects of dietary fat on muscle substrates, metabolism, and performance in athletes. *Med Sci Sports Exerc* **35**, 952-960 (2003).
40. Goedecke, J.H.*, et al.* Metabolic adaptations to a high-fat diet in endurance cyclists. *Metabolism* **48**, 1509-1517 (1999).
41. Iossa, S.*, et al.* Skeletal muscle oxidative capacity in rats fed high-fat diet. *Int J Obes Relat Metab Disord* **26**, 65-72 (2002).

42. Turner, N.*, et al.* Excess lipid availability increases mitochondrial fatty acid oxidative capacity in muscle: evidence against a role for reduced fatty acid oxidation in lipid-induced insulin resistance in rodents. *Diabetes* **56**, 2085-2092 (2007).
43. Chanseaume, E.*, et al.* Enhanced muscle mixed and mitochondrial protein synthesis rates after a high-fat or high-sucrose diet. *Obesity (Silver Spring)* **15**, 853-859 (2007).
44. de Wilde, J.*, et al.* Short-term high fat-feeding results in morphological and metabolic adaptations in the skeletal muscle of C57BL/6J mice. *Physiol Genomics* **32**, 360-369 (2008).
45. Hancock, C.R.*, et al.* High-fat diets cause insulin resistance despite an increase in muscle mitochondria. *Proc Natl Acad Sci U S A* **105**, 7815-7820 (2008).
46. Wredenberg, A.*, et al.* Respiratory chain dysfunction in skeletal muscle does not cause insulin resistance. *Biochem Biophys Res Commun* **350**, 202-207 (2006).
47. Handschin, C.*, et al.* Abnormal glucose homeostasis in skeletal muscle-specific PGC-1alpha knockout mice reveals skeletal muscle-pancreatic beta cell crosstalk. *J Clin Invest* **117**, 3463-3474 (2007).
48. Vianna, C.R.*, et al.* Hypomorphic mutation of PGC-1beta causes mitochondrial dysfunction and liver insulin resistance. *Cell Metab* **4**, 453-464 (2006).
49. Calvo, J.A.*, et al.* Muscle-specific expression of PPARgamma coactivator-1alpha improves exercise performance and increases peak oxygen uptake. *J Appl Physiol* **104**, 1304-1312 (2008).
50. Handschin, C.*, et al.* Abnormal glucose homeostasis in skeletal muscle-specific PGC-1alpha knockout mice reveals skeletal muscle-pancreatic beta cell crosstalk. *The Journal of clinical investigation* **117**, 3463-3474 (2007).
51. Muoio, D.M. Intramuscular triacylglycerol and insulin resistance: guilty as charged or wrongly accused? *Biochim Biophys Acta* **1801**, 281-288.
52. Staples, J.F. & Buck, L.T. Matching cellular metabolic supply and demand in energy-stressed animals. *Comp Biochem Physiol A Mol Integr Physiol* **153**, 95-105 (2009).
53. Saks, V., Favier, R., Guzun, R., Schlattner, U. & Wallimann, T. Molecular system bioenergetics: regulation of substrate supply in response to heart energy demands. *J Physiol* **577**, 769-777 (2006).
54. Rolfe, D.F. & Brand, M.D. Contribution of mitochondrial proton leak to skeletal muscle respiration and to standard metabolic rate. *Am J Physiol* **271**, C1380-1389 (1996).
55. Rolfe, D.F. & Brown, G.C. Cellular energy utilization and molecular origin of standard metabolic rate in mammals. *Physiol Rev* **77**, 731-758 (1997).
56. Pospisilik, J.A.*, et al.* Targeted deletion of AIF decreases mitochondrial oxidative phosphorylation and protects from obesity and diabetes. *Cell* **131**, 476-491 (2007).
57. Awad, S., Constantin-Teodosiu, D., Macdonald, I.A. & Lobo, D.N. Short-term starvation and mitochondrial dysfunction - a possible mechanism leading to postoperative insulin resistance. *Clin Nutr* **28**, 497-509 (2009).
58. van Hoorn, D.E.*, et al.* Preoperative feeding preserves heart function and decreases oxidative injury in rats. *Nutrition* **21**, 859-866 (2005).
59. Vendemiale, G.*, et al.* Mitochondrial oxidative injury and energy metabolism alteration in rat fatty liver: effect of the nutritional status. *Hepatology* **33**, 808-815 (2001).
60. Jackson, M.J.*, et al.* Antioxidants, reactive oxygen and nitrogen species, gene induction and mitochondrial function. *Mol Aspects Med* **23**, 209-285 (2002).
61. Nakamura, S.*, et al.* Palmitate induces insulin resistance in H4IIEC3 hepatocytes through reactive oxygen species produced by mitochondria. *J Biol Chem* **284**, 14809-14818 (2009).
62. Houstis, N., Rosen, E.D. & Lander, E.S. Reactive oxygen species have a causal role in multiple forms of insulin resistance. *Nature* **440**, 944-948 (2006).

63. Bonnard, C*., et al.* Mitochondrial dysfunction results from oxidative stress in the skeletal muscle of diet-induced insulin-resistant mice. *J Clin Invest* **118**, 789-800 (2008).
64. Anderson, E.J*., et al.* Mitochondrial H2O2 emission and cellular redox state link excess fat intake to insulin resistance in both rodents and humans. *J Clin Invest* (2009).
65. Hoehn, K.L*., et al.* Insulin resistance is a cellular antioxidant defense mechanism. *Proceedings of the National Academy of Sciences of the United States of America* **106**, 17787-17792 (2009).
66. Foretz, M*., et al.* Metformin inhibits hepatic gluconeogenesis in mice independently of the LKB1/AMPK pathway via a decrease in hepatic energy state. *J Clin Invest* **120**, 2355-2369.
67. El-Mir, M.Y*., et al.* Dimethylbiguanide inhibits cell respiration via an indirect effect targeted on the respiratory chain complex I. *J Biol Chem* **275**, 223-228 (2000).
68. Owen, M.R., Doran, E. & Halestrap, A.P. Evidence that metformin exerts its anti-diabetic effects through inhibition of complex 1 of the mitochondrial respiratory chain. *Biochem J* **348 Pt 3**, 607-614 (2000).
69. Kane, D.A*., et al.* Metformin selectively attenuates mitochondrial H(2)O(2) emission without affecting respiratory capacity in skeletal muscle of obese rats. *Free Radic Biol Med*.
70. Barja, G. Mitochondrial oxygen radical generation and leak: sites of production in states 4 and 3, organ specificity, and relation to aging and longevity. *J Bioenerg Biomembr* **31**, 347-366 (1999).
71. Murrant, C.L. & Reid, M.B. Detection of reactive oxygen and reactive nitrogen species in skeletal muscle. *Microsc Res Tech* **55**, 236-248 (2001).
72. Turrens, J.F. Mitochondrial formation of reactive oxygen species. *J Physiol* **552**, 335-344 (2003).
73. Nathan, C. & Ding, A. SnapShot: Reactive Oxygen Intermediates (ROI). *Cell* **140**, 951-951 e952.
74. St-Pierre, J., Buckingham, J.A., Roebuck, S.J. & Brand, M.D. Topology of superoxide production from different sites in the mitochondrial electron transport chain. *J Biol Chem* **277**, 44784-44790 (2002).
75. Chance, B., Sies, H. & Boveris, A. Hydroperoxide metabolism in mammalian organs. *Physiol Rev* **59**, 527-605 (1979).
76. Kietzmann, T. Intracellular redox compartments: mechanisms and significances. *Antioxid Redox Signal* **13**, 395-398.
77. Murphy, M.P. How mitochondria produce reactive oxygen species. *The Biochemical journal* **417**, 1-13 (2009).
78. Boveris, A. & Chance, B. The mitochondrial generation of hydrogen peroxide. General properties and effect of hyperbaric oxygen. *Biochem J* **134**, 707-716 (1973).
79. Korshunov, S.S., Skulachev, V.P. & Starkov, A.A. High protonic potential actuates a mechanism of production of reactive oxygen species in mitochondria. *FEBS Lett* **416**, 15-18 (1997).
80. Cardenas, M.L., Cornish-Bowden, A. & Ureta, T. Evolution and regulatory role of the hexokinases. *Biochim Biophys Acta* **1401**, 242-264 (1998).
81. Meyer, L.E*., et al.* Mitochondrial creatine kinase activity prevents reactive oxygen species generation: antioxidant role of mitochondrial kinase-dependent ADP re-cycling activity. *J Biol Chem* **281**, 37361-37371 (2006).
82. Hansford, R.G., Hogue, B.A. & Mildaziene, V. Dependence of H2O2 formation by rat heart mitochondria on substrate availability and donor age. *J Bioenerg Biomembr* **29**, 89-95 (1997).
83. Starkov, A.A. & Fiskum, G. Regulation of brain mitochondrial H2O2 production by membrane potential and NAD(P)H redox state. *J Neurochem* **86**, 1101-1107 (2003).
84. Votyakova, T.V. & Reynolds, I.J. DeltaPsi(m)-Dependent and -independent production of reactive oxygen species by rat brain mitochondria. *J Neurochem* **79**, 266-277 (2001).
85. da-Silva, W.S*., et al.* Mitochondrial bound hexokinase activity as a preventive antioxidant defense: steady-state ADP formation as a regulatory mechanism of membrane potential and reactive oxygen species generation in mitochondria. *J Biol Chem* **279**, 39846-39855 (2004).

86. Santiago, A.P., Chaves, E.A., Oliveira, M.F. & Galina, A. Reactive oxygen species generation is modulated by mitochondrial kinases: correlation with mitochondrial antioxidant peroxidases in rat tissues. *Biochimie* **90**, 1566-1577 (2008).
87. Yu, T., Robotham, J.L. & Yoon, Y. Increased production of reactive oxygen species in hyperglycemic conditions requires dynamic change of mitochondrial morphology. *Proc Natl Acad Sci U S A* **103**, 2653-2658 (2006).
88. Bloch-Damti, A. & Bashan, N. Proposed mechanisms for the induction of insulin resistance by oxidative stress. *Antioxid Redox Signal* **7**, 1553-1567 (2005).
89. Yuan, M.*, et al.* Reversal of obesity- and diet-induced insulin resistance with salicylates or targeted disruption of Ikkbeta. *Science* **293**, 1673-1677 (2001).
90. Jones, D.P. Radical-free biology of oxidative stress. *American journal of physiology* **295**, C849-868 (2008).
91. Brandes, N., Schmitt, S. & Jakob, U. Thiol-Based Redox Switches in Eukaryotic Proteins. *Antioxid Redox Signal* (2008).
92. Giles, G.I., Tasker, K.M. & Jacob, C. Hypothesis: the role of reactive sulfur species in oxidative stress. *Free radical biology & medicine* **31**, 1279-1283 (2001).
93. Lohse, D.L., Denu, J.M., Santoro, N. & Dixon, J.E. Roles of aspartic acid-181 and serine-222 in intermediate formation and hydrolysis of the mammalian protein-tyrosine-phosphatase PTP1. *Biochemistry* **36**, 4568-4575 (1997).
94. Ma, L.H., Takanishi, C.L. & Wood, M.J. Molecular mechanism of oxidative stress perception by the Orp1 protein. *The Journal of biological chemistry* **282**, 31429-31436 (2007).
95. Rhee, S.G., Bae, Y.S., Lee, S.R. & Kwon, J. Hydrogen peroxide: a key messenger that modulates protein phosphorylation through cysteine oxidation. *Sci STKE* **2000**, PE1 (2000).
96. Zhang, Z.Y. & Dixon, J.E. Active site labeling of the Yersinia protein tyrosine phosphatase: the determination of the pKa of the active site cysteine and the function of the conserved histidine 402. *Biochemistry* **32**, 9340-9345 (1993).
97. Winterbourn, C.C. & Metodiewa, D. Reactivity of biologically important thiol compounds with superoxide and hydrogen peroxide. *Free radical biology & medicine* **27**, 322-328 (1999).
98. Cumming, R.C.*, et al.* Protein disulfide bond formation in the cytoplasm during oxidative stress. *The Journal of biological chemistry* **279**, 21749-21758 (2004).
99. Stadtman, E.R. & Berlett, B.S. Reactive oxygen-mediated protein oxidation in aging and disease. *Drug metabolism reviews* **30**, 225-243 (1998).
100. Stamler, J.S. Redox signaling: nitrosylation and related target interactions of nitric oxide. *Cell* **78**, 931-936 (1994).
101. Paget, M.S. & Buttner, M.J. Thiol-based regulatory switches. *Annual review of genetics* **37**, 91-121 (2003).
102. Ilbert, M.*, et al.* The redox-switch domain of Hsp33 functions as dual stress sensor. *Nature structural & molecular biology* **14**, 556-563 (2007).
103. Shenton, D. & Grant, C.M. Protein S-thiolation targets glycolysis and protein synthesis in response to oxidative stress in the yeast Saccharomyces cerevisiae. *The Biochemical journal* **374**, 513-519 (2003).
104. Yu, C.X., Li, S. & Whorton, A.R. Redox regulation of PTEN by S-nitrosothiols. *Molecular pharmacology* **68**, 847-854 (2005).
105. Gallogly, M.M. & Mieyal, J.J. Mechanisms of reversible protein glutathionylation in redox signaling and oxidative stress. *Current opinion in pharmacology* **7**, 381-391 (2007).
106. Matteucci, E., Malvaldi, G., Fagnani, F., Evangelista, I. & Giampietro, O. Redox status and immune function in type I diabetes families. *Clinical and experimental immunology* **136**, 549-554 (2004).

107. Beckett, G.J. & Arthur, J.R. Selenium and endocrine systems. *The Journal of endocrinology* **184**, 455-465 (2005).
108. Su, W.C.*, et al.* Differential activation of a C/EBP beta isoform by a novel redox switch may confer the lipopolysaccharide-inducible expression of interleukin-6 gene. *The Journal of biological chemistry* **278**, 51150-51158 (2003).
109. Seth, D. & Rudolph, J. Redox regulation of MAP kinase phosphatase 3. *Biochemistry* **45**, 8476-8487 (2006).
110. Li, X.*, et al.* Redox control of K+ channel remodeling in rat ventricle. *Journal of molecular and cellular cardiology* **40**, 339-349 (2006).
111. Dietrich, L.E., Teal, T.K., Price-Whelan, A. & Newman, D.K. Redox-active antibiotics control gene expression and community behavior in divergent bacteria. *Science (New York, N.Y* **321**, 1203-1206 (2008).
112. Osyczka, A., Moser, C.C., Daldal, F. & Dutton, P.L. Reversible redox energy coupling in electron transfer chains. *Nature* **427**, 607-612 (2004).
113. Wood, M.J., Storz, G. & Tjandra, N. Structural basis for redox regulation of Yap1 transcription factor localization. *Nature* **430**, 917-921 (2004).
114. Mieyal, J.J., Gallogly, M.M., Qanungo, S., Sabens, E.A. & Shelton, M.D. Molecular mechanisms and clinical implications of reversible protein S-glutathionylation. *Antioxidants & redox signaling* **10**, 1941-1988 (2008).
115. Dalle-Donne, I.*, et al.* Molecular mechanisms and potential clinical significance of S-glutathionylation. *Antioxidants & redox signaling* **10**, 445-473 (2008).
116. Burhans, W.C. & Heintz, N.H. The cell cycle is a redox cycle; linking phase-specific targets to cell fate. *Free radical biology & medicine* (2009).
117. Xie, Y., Kole, S., Precht, P., Pazin, M.J. & Bernier, M. S-glutathionylation impairs signal transducer and activator of transcription 3 activation and signaling. *Endocrinology* **150**, 1122-1131 (2009).
118. Hitchler, M.J. & Domann, F.E. An epigenetic perspective on the free radical theory of development. *Free radical biology & medicine* **43**, 1023-1036 (2007).
119. Hitchler, M.J. & Domann, F.E. Metabolic defects provide a spark for the epigenetic switch in cancer. *Free radical biology & medicine* **47**, 115-127 (2009).
120. Rajendrasozhan, S.*, et al.* Deacetylases and NF-kappaB in redox regulation of cigarette smoke-induced lung inflammation: epigenetics in pathogenesis of COPD. *Antioxidants & redox signaling* **10**, 799-811 (2008).
121. Bashan, N., Kovsan, J., Kachko, I., Ovadia, H. & Rudich, A. Positive and negative regulation of insulin signaling by reactive oxygen and nitrogen species. *Physiological reviews* **89**, 27-71 (2009).
122. Potashnik, R., Bloch-Damti, A., Bashan, N. & Rudich, A. IRS1 degradation and increased serine phosphorylation cannot predict the degree of metabolic insulin resistance induced by oxidative stress. *Diabetologia* **46**, 639-648 (2003).
123. Demozay, D., Mas, J.C., Rocchi, S. & Van Obberghen, E. FALDH reverses the deleterious action of oxidative stress induced by lipid peroxidation product 4-hydroxynonenal on insulin signaling in 3T3-L1 adipocytes. *Diabetes* **57**, 1216-1226 (2008).
124. Taniyama, Y., Hitomi, H., Shah, A., Alexander, R.W. & Griendling, K.K. Mechanisms of reactive oxygen species-dependent downregulation of insulin receptor substrate-1 by angiotensin II. *Arteriosclerosis, thrombosis, and vascular biology* **25**, 1142-1147 (2005).
125. Clavreul, N.*, et al.* S-glutathiolation of p21ras by peroxynitrite mediates endothelial insulin resistance caused by oxidized low-density lipoprotein. *Arteriosclerosis, thrombosis, and vascular biology* **26**, 2454-2461 (2006).

126. Shelton, M.D., Chock, P.B. & Mieyal, J.J. Glutaredoxin: role in reversible protein s-glutathionylation and regulation of redox signal transduction and protein translocation. *Antioxidants & redox signaling* **7**, 348-366 (2005).
127. Ward, N.E., Stewart, J.R., Ioannides, C.G. & O'Brian, C.A. Oxidant-induced S-glutathiolation inactivates protein kinase C-alpha (PKC-alpha): a potential mechanism of PKC isozyme regulation. *Biochemistry* **39**, 10319-10329 (2000).
128. Gopalakrishna, R., Gundimeda, U., Schiffman, J.E. & McNeill, T.H. A direct redox regulation of protein kinase C isoenzymes mediates oxidant-induced neuritogenesis in PC12 cells. *The Journal of biological chemistry* **283**, 14430-14444 (2008).
129. Chu, F., Ward, N.E. & O'Brian, C.A. Potent inactivation of representative members of each PKC isozyme subfamily and PKD via S-thiolation by the tumor-promotion/progression antagonist glutathione but not by its precursor cysteine. *Carcinogenesis* **22**, 1221-1229 (2001).
130. el-Remessy, A.B., Bartoli, M., Platt, D.H., Fulton, D. & Caldwell, R.B. Oxidative stress inactivates VEGF survival signaling in retinal endothelial cells via PI 3-kinase tyrosine nitration. *Journal of cell science* **118**, 243-252 (2005).
131. JeBailey, L*., et al.* Ceramide- and oxidant-induced insulin resistance involve loss of insulin-dependent Rac-activation and actin remodeling in muscle cells. *Diabetes* **56**, 394-403 (2007).
132. Tirosh, A., Potashnik, R., Bashan, N. & Rudich, A. Oxidative stress disrupts insulin-induced cellular redistribution of insulin receptor substrate-1 and phosphatidylinositol 3-kinase in 3T3-L1 adipocytes. A putative cellular mechanism for impaired protein kinase B activation and GLUT4 translocation. *The Journal of biological chemistry* **274**, 10595-10602 (1999).
133. Rudich, A., Tirosh, A., Potashnik, R., Khamaisi, M. & Bashan, N. Lipoic acid protects against oxidative stress induced impairment in insulin stimulation of protein kinase B and glucose transport in 3T3-L1 adipocytes. *Diabetologia* **42**, 949-957 (1999).
134. Murata, H*., et al.* Glutaredoxin exerts an antiapoptotic effect by regulating the redox state of Akt. *The Journal of biological chemistry* **278**, 50226-50233 (2003).
135. Kaneki, M., Shimizu, N., Yamada, D. & Chang, K. Nitrosative stress and pathogenesis of insulin resistance. *Antioxidants & redox signaling* **9**, 319-329 (2007).
136. Yasukawa, T*., et al.* S-nitrosylation-dependent inactivation of Akt/protein kinase B in insulin resistance. *The Journal of biological chemistry* **280**, 7511-7518 (2005).
137. Lu, X.M., Lu, M., Tompkins, R.G. & Fischman, A.J. Site-specific detection of S-nitrosylated PKB alpha/Akt1 from rat soleus muscle using CapLC-Q-TOF(micro) mass spectrometry. *J Mass Spectrom* **40**, 1140-1148 (2005).
138. Carvalho-Filho, M.A*., et al.* S-nitrosation of the insulin receptor, insulin receptor substrate 1, and protein kinase B/Akt: a novel mechanism of insulin resistance. *Diabetes* **54**, 959-967 (2005).
139. Pauli, J.R*., et al.* Acute physical exercise reverses S-nitrosation of the insulin receptor, insulin receptor substrate 1 and protein kinase B/Akt in diet-induced obese Wistar rats. *The Journal of physiology* **586**, 659-671 (2008).
140. Pessler-Cohen, D*., et al.* GLUT4 repression in response to oxidative stress is associated with reciprocal alterations in C/EBP alpha and delta isoforms in 3T3-L1 adipocytes. *Archives of physiology and biochemistry* **112**, 3-12 (2006).
141. Pessler, D., Rudich, A. & Bashan, N. Oxidative stress impairs nuclear proteins binding to the insulin responsive element in the GLUT4 promoter. *Diabetologia* **44**, 2156-2164 (2001).
142. Cooke, D.W. & Lane, M.D. A sequence element in the GLUT4 gene that mediates repression by insulin. *The Journal of biological chemistry* **273**, 6210-6217 (1998).
143. Johnson, T.O., Ermolieff, J. & Jirousek, M.R. Protein tyrosine phosphatase 1B inhibitors for diabetes. *Nature reviews* **1**, 696-709 (2002).

144. Ukkola, O. & Santaniemi, M. Protein tyrosine phosphatase 1B: a new target for the treatment of obesity and associated co-morbidities. *Journal of internal medicine* **251**, 467-475 (2002).
145. Liu, G. & Trevillyan, J.M. Protein tyrosine phosphatase 1B as a target for the treatment of impaired glucose tolerance and type II diabetes. *Curr Opin Investig Drugs* **3**, 1608-1616 (2002).
146. Tobin, J.F. & Tam, S. Recent advances in the development of small molecule inhibitors of PTP1B for the treatment of insulin resistance and type 2 diabetes. *Current opinion in drug discovery & development* **5**, 500-512 (2002).
147. Dube, N. & Tremblay, M.L. Involvement of the small protein tyrosine phosphatases TC-PTP and PTP1B in signal transduction and diseases: from diabetes, obesity to cell cycle, and cancer. *Biochimica et biophysica acta* **1754**, 108-117 (2005).
148. Barford, D., Das, A.K. & Egloff, M.P. The structure and mechanism of protein phosphatases: insights into catalysis and regulation. *Annual review of biophysics and biomolecular structure* **27**, 133-164 (1998).
149. Barford, D., Keller, J.C., Flint, A.J. & Tonks, N.K. Purification and crystallization of the catalytic domain of human protein tyrosine phosphatase 1B expressed in Escherichia coli. *Journal of molecular biology* **239**, 726-730 (1994).
150. Barford, D., Flint, A.J. & Tonks, N.K. Crystal structure of human protein tyrosine phosphatase 1B. *Science (New York, N.Y* **263**, 1397-1404 (1994).
151. Barrett, W.C*., et al.* Regulation of PTP1B via glutathionylation of the active site cysteine 215. *Biochemistry* **38**, 6699-6705 (1999).
152. Salmeen, A*., et al.* Redox regulation of protein tyrosine phosphatase 1B involves a sulphenyl-amide intermediate. *Nature* **423**, 769-773 (2003).
153. van Montfort, R.L., Congreve, M., Tisi, D., Carr, R. & Jhoti, H. Oxidation state of the active-site cysteine in protein tyrosine phosphatase 1B. *Nature* **423**, 773-777 (2003).
154. Barrett, W.C*., et al.* Roles of superoxide radical anion in signal transduction mediated by reversible regulation of protein-tyrosine phosphatase 1B. *The Journal of biological chemistry* **274**, 34543-34546 (1999).
155. Lee, S.R., Kwon, K.S., Kim, S.R. & Rhee, S.G. Reversible inactivation of protein-tyrosine phosphatase 1B in A431 cells stimulated with epidermal growth factor. *The Journal of biological chemistry* **273**, 15366-15372 (1998).
156. Sivaramakrishnan, S., Keerthi, K. & Gates, K.S. A chemical model for redox regulation of protein tyrosine phosphatase 1B (PTP1B) activity. *Journal of the American Chemical Society* **127**, 10830-10831 (2005).
157. Salmeen, A. & Barford, D. Methods for Preparing Crystals of Reversibly Oxidized Proteins: Crystallization of Protein Tyrosine Phosphatase 1B as an Example. *Methods in molecular biology (Clifton, N.J* **476**, 97-112 (2009).
158. Salmeen, A. & Barford, D. Methods for preparing crystals of reversibly oxidized proteins: crystallization of protein tyrosine phosphatase 1B as an example. *Methods in molecular biology (Clifton, N.J* **476**, 101-116 (2008).
159. Sun, H*., et al.* PTEN modulates cell cycle progression and cell survival by regulating phosphatidylinositol 3,4,5,-trisphosphate and Akt/protein kinase B signaling pathway. *Proceedings of the National Academy of Sciences of the United States of America* **96**, 6199-6204 (1999).
160. Cruz, C.M*., et al.* ATP activates a reactive oxygen species-dependent oxidative stress response and secretion of proinflammatory cytokines in macrophages. *The Journal of biological chemistry* **282**, 2871-2879 (2007).

161. Delgado-Esteban, M., Martin-Zanca, D., Andres-Martin, L., Almeida, A. & Bolanos, J.P. Inhibition of PTEN by peroxynitrite activates the phosphoinositide-3-kinase/Akt neuroprotective signaling pathway. *Journal of neurochemistry* **102**, 194-205 (2007).
162. Kopperud, R., Krakstad, C., Selheim, F. & Doskeland, S.O. cAMP effector mechanisms. Novel twists for an 'old' signaling system. *FEBS letters* **546**, 121-126 (2003).
163. Humphries, K.M., Deal, M.S. & Taylor, S.S. Enhanced dephosphorylation of cAMP-dependent protein kinase by oxidation and thiol modification. *The Journal of biological chemistry* **280**, 2750-2758 (2005).
164. Humphries, K.M., Juliano, C. & Taylor, S.S. Regulation of cAMP-dependent protein kinase activity by glutathionylation. *The Journal of biological chemistry* **277**, 43505-43511 (2002).
165. de Pina, M.Z*., et al.* Signaling the signal, cyclic AMP-dependent protein kinase inhibition by insulin-formed H2O2 and reactivation by thioredoxin. *The Journal of biological chemistry* **283**, 12373-12386 (2008).
166. Padmanabhan, S*., et al.* A PP2A regulatory subunit regulates C. elegans insulin/IGF-1 signaling by modulating AKT-1 phosphorylation. *Cell* **136**, 939-951 (2009).
167. Witczak, C.A., Sharoff, C.G. & Goodyear, L.J. AMP-activated protein kinase in skeletal muscle: from structure and localization to its role as a master regulator of cellular metabolism. *Cell Mol Life Sci* **65**, 3737-3755 (2008).
168. Suter, M*., et al.* Dissecting the role of 5'-AMP for allosteric stimulation, activation, and deactivation of AMP-activated protein kinase. *The Journal of biological chemistry* **281**, 32207-32216 (2006).
169. Sanders, M.J*., et al.* Defining the mechanism of activation of AMP-activated protein kinase by the small molecule A-769662, a member of the thienopyridone family. *The Journal of biological chemistry* **282**, 32539-32548 (2007).
170. Davies, S.P., Helps, N.R., Cohen, P.T. & Hardie, D.G. 5'-AMP inhibits dephosphorylation, as well as promoting phosphorylation, of the AMP-activated protein kinase. Studies using bacterially expressed human protein phosphatase-2C alpha and native bovine protein phosphatase-2AC. *FEBS letters* **377**, 421-425 (1995).
171. Rao, R.K. & Clayton, L.W. Regulation of protein phosphatase 2A by hydrogen peroxide and glutathionylation. *Biochemical and biophysical research communications* **293**, 610-616 (2002).
172. Sandstrom, M.E*., et al.* Role of reactive oxygen species in contraction-mediated glucose transport in mouse skeletal muscle. *The Journal of physiology* **575**, 251-262 (2006).
173. Toyoda, T*., et al.* Possible involvement of the alpha1 isoform of 5'AMP-activated protein kinase in oxidative stress-stimulated glucose transport in skeletal muscle. *American journal of physiology* **287**, E166-173 (2004).
174. Jensen, T.E., Schjerling, P., Viollet, B., Wojtaszewski, J.F. & Richter, E.A. AMPK alpha1 activation is required for stimulation of glucose uptake by twitch contraction, but not by H2O2, in mouse skeletal muscle. *PloS one* **3**, e2102 (2008).
175. Kim, J.S., Saengsirisuwan, V., Sloniger, J.A., Teachey, M.K. & Henriksen, E.J. Oxidant stress and skeletal muscle glucose transport: roles of insulin signaling and p38 MAPK. *Free radical biology & medicine* **41**, 818-824 (2006).
176. Dioum, E.M*., et al.* Regulation of hypoxia-inducible factor 2alpha signaling by the stress-responsive deacetylase sirtuin 1. *Science (New York, N.Y* **324**, 1289-1293 (2009).
177. Tissenbaum, H.A. & Guarente, L. Increased dosage of a sir-2 gene extends lifespan in Caenorhabditis elegans. *Nature* **410**, 227-230 (2001).
178. Korashy, H.M. & El-Kadi, A.O. The role of redox-sensitive transcription factors NF-kappaB and AP-1 in the modulation of the Cyp1a1 gene by mercury, lead, and copper. *Free radical biology & medicine* **44**, 795-806 (2008).

179. Reddy, S., Jones, A.D., Cross, C.E., Wong, P.S. & Van Der Vliet, A. Inactivation of creatine kinase by S-glutathionylation of the active-site cysteine residue. *The Biochemical journal* **347 Pt 3**, 821-827 (2000).
180. Mohr, S., Hallak, H., de Boitte, A., Lapetina, E.G. & Brune, B. Nitric oxide-induced S-glutathionylation and inactivation of glyceraldehyde-3-phosphate dehydrogenase. *The Journal of biological chemistry* **274**, 9427-9430 (1999).
181. Kim, G. & Levine, R.L. Molecular determinants of S-glutathionylation of carbonic anhydrase 3. *Antioxidants & redox signaling* **7**, 849-854 (2005).
182. Meglasson, M.D*., et al.* Antihyperglycemic action of guanidinoalkanoic acids: 3-guanidinopropionic acid ameliorates hyperglycemia in diabetic KKAy and C57BL6Job/ob mice and increases glucose disappearance in rhesus monkeys. *J Pharmacol Exp Ther* **266**, 1454-1462 (1993).
183. Larsen, S.D*., et al.* Synthesis and biological activity of analogues of the antidiabetic/antiobesity agent 3-guanidinopropionic acid: discovery of a novel aminoguanidinoacetic acid antidiabetic agent. *J Med Chem* **44**, 1217-1230 (2001).
184. Vaillancourt, V.A*., et al.* Synthesis and biological activity of aminoguanidine and diaminoguanidine analogues of the antidiabetic/antiobesity agent 3-guanidinopropionic acid. *J Med Chem* **44**, 1231-1248 (2001).
185. Pandke, K.E., Mullen, K.L., Snook, L.A., Bonen, A. & Dyck, D.J. Decreasing intramuscular phosphagen content simultaneously increases plasma membrane FAT/CD36 and GLUT4 transporter abundance. *Am J Physiol Regul Integr Comp Physiol* **295**, R806-813 (2008).
186. Fisher, J.S. Potential Role of the AMP-activated Protein Kinase in Regulation of Insulin Action. *Cellscience* **2**, 68-81 (2006).
187. Jensen, T.E., Wojtaszewski, J.F. & Richter, E.A. AMP-activated protein kinase in contraction regulation of skeletal muscle metabolism: necessary and/or sufficient? *Acta Physiol (Oxf)* **196**, 155-174 (2009).
188. Hardie, D.G. AMPK: a key regulator of energy balance in the single cell and the whole organism. *Int J Obes (Lond)* **32 Suppl 4**, S7-12 (2008).
189. Reznick, R.M*., et al.* Aging-associated reductions in AMP-activated protein kinase activity and mitochondrial biogenesis. *Cell Metab* **5**, 151-156 (2007).
190. Williams, D*., et al.* Muscle Specific Differences in the Response of Mitochondrial Proteins to {beta}-GPA Feeding: An Evaluation of Potential Mechanisms. *Am J Physiol Endocrinol Metab* (2009).
191. Bergeron, R*., et al.* Chronic activation of AMP kinase results in NRF-1 activation and mitochondrial biogenesis. *Am J Physiol Endocrinol Metab* **281**, E1340-1346 (2001).
192. Towler, M.C. & Hardie, D.G. AMP-activated protein kinase in metabolic control and insulin signaling. *Circ Res* **100**, 328-341 (2007).
193. Mc Clean, C.M*., et al.* The effect of acute aerobic exercise on pulse wave velocity and oxidative stress following postprandial hypertriglyceridemia in healthy men. *Eur J Appl Physiol* **100**, 225-234 (2007).
194. Wallace, J.P., Johnson, B., Padilla, J. & Mather, K. Postprandial lipaemia, oxidative stress and endothelial function: a review. *Int J Clin Pract* **64**, 389-403 (2010).
195. Wallace, J.P., Johnson, B., Padilla, J. & Mather, K. Postprandial lipaemia, oxidative stress and endothelial function: a review. *Int J Clin Pract* **64**, 389-403.
196. Ceriello, A. Impaired glucose tolerance and cardiovascular disease: the possible role of post-prandial hyperglycemia. *Am Heart J* **147**, 803-807 (2004).
197. Zhu, W., Zhong, C., Yu, Y. & Li, K. Acute effects of hyperglycaemia with and without exercise on endothelial function in healthy young men. *Eur J Appl Physiol* **99**, 585-591 (2007).

198. Neri, S*., et al.* Effects of antioxidants on postprandial oxidative stress and endothelial dysfunction in subjects with impaired glucose tolerance and Type 2 diabetes. *Eur J Nutr* (2010).
199. Tsai, W.C., Li, Y.H., Lin, C.C., Chao, T.H. & Chen, J.H. Effects of oxidative stress on endothelial function after a high-fat meal. *Clin Sci (Lond)* **106**, 315-319 (2004).
200. Bloomer, R.J. & Fisher-Wellman, K.H. Systemic oxidative stress is increased to a greater degree in young, obese women following consumption of a high fat meal. *Oxid Med Cell Longev* **2**, 19-25 (2009).
201. Bae, J.H*., et al.* Postprandial hypertriglyceridemia impairs endothelial function by enhanced oxidant stress. *Atherosclerosis* **155**, 517-523 (2001).
202. Fisher-Wellman, K.H. & Bloomer, R.J. Exacerbated postprandial oxidative stress induced by the acute intake of a lipid meal compared to isoenergetically administered carbohydrate, protein, and mixed meals in young, healthy men. *J Am Coll Nutr* **29**, 373-381.
203. Tsetsonis, N.V. & Hardman, A.E. Effects of low and moderate intensity treadmill walking on postprandial lipaemia in healthy young adults. *Eur J Appl Physiol Occup Physiol* **73**, 419-426 (1996).
204. Tsetsonis, N.V. & Hardman, A.E. Reduction in postprandial lipemia after walking: influence of exercise intensity. *Med Sci Sports Exerc* **28**, 1235-1242 (1996).
205. Katsanos, C.S. & Moffatt, R.J. Acute effects of premeal versus postmeal exercise on postprandial hypertriglyceridemia. *Clin J Sport Med* **14**, 33-39 (2004).
206. Zhang, J.Q., Thomas, T.R. & Ball, S.D. Effect of exercise timing on postprandial lipemia and HDL cholesterol subfractions. *J Appl Physiol* **85**, 1516-1522 (1998).
207. Gill, J.M., Herd, S.L., Vora, V. & Hardman, A.E. Effects of a brisk walk on lipoprotein lipase activity and plasma triglyceride concentrations in the fasted and postprandial states. *Eur J Appl Physiol* **89**, 184-190 (2003).
208. Petitt, D.S. & Cureton, K.J. Effects of prior exercise on postprandial lipemia: a quantitative review. *Metabolism* **52**, 418-424 (2003).
209. Bloomer, R.J., Cole, B. & Fisher-Wellman, K.H. Racial differences in postprandial oxidative stress with and without acute exercise. *Int J Sport Nutr Exerc Metab* **19**, 457-472 (2009).
210. Melton, C.E., Tucker, P.S., Fisher-Wellman, K.H., Schilling, B.K. & Bloomer, R.J. Acute exercise does not attenuate postprandial oxidative stress in prediabetic women. *Phys Sportsmed* **37**, 27-36 (2009).
211. Paillard, M*., et al.* Postconditioning inhibits mPTP opening independent of oxidative phosphorylation and membrane potential. *J Mol Cell Cardiol* **46**, 902-909 (2009).
212. Straight, A.F*., et al.* Dissecting temporal and spatial control of cytokinesis with a myosin II Inhibitor. *Science* **299**, 1743-1747 (2003).
213. Kovacs, M., Toth, J., Hetenyi, C., Malnasi-Csizmadia, A. & Sellers, J.R. Mechanism of blebbistatin inhibition of myosin II. *J Biol Chem* **279**, 35557-35563 (2004).
214. Allingham, J.S., Smith, R. & Rayment, I. The structural basis of blebbistatin inhibition and specificity for myosin II. *Nat Struct Mol Biol* **12**, 378-379 (2005).
215. Wilson, C.A*., et al.* Myosin II contributes to cell-scale actin network treadmilling through network disassembly. *Nature* **465**, 373-377.
216. Labajova, A*., et al.* Evaluation of mitochondrial membrane potential using a computerized device with a tetraphenylphosphonium-selective electrode. *Anal Biochem* **353**, 37-42 (2006).
217. Cossarizza, A., Ceccarelli, D. & Masini, A. Functional heterogeneity of an isolated mitochondrial population revealed by cytofluorometric analysis at the single organelle level. *Exp Cell Res* **222**, 84-94 (1996).
218. Ascensao, A*., et al.* Acute exercise protects against calcium-induced cardiac mitochondrial permeability transition pore opening in doxorubicin-treated rats. *Clin Sci (Lond)* **120**, 37-49.

219. Bernardi, P.*, et al.* The mitochondrial permeability transition from in vitro artifact to disease target. *FEBS J* **273**, 2077-2099 (2006).
220. Zoratti, M. & Szabo, I. The mitochondrial permeability transition. *Biochim Biophys Acta* **1241**, 139-176 (1995).
221. Lemasters, J.J., Theruvath, T.P., Zhong, Z. & Nieminen, A.L. Mitochondrial calcium and the permeability transition in cell death. *Biochim Biophys Acta* **1787**, 1395-1401 (2009).
222. Battaglia, V., Salvi, M. & Toninello, A. Oxidative stress is responsible for mitochondrial permeability transition induction by salicylate in liver mitochondria. *J Biol Chem* **280**, 33864-33872 (2005).
223. Clarke, S.J.*, et al.* Inhibition of mitochondrial permeability transition pore opening by ischemic preconditioning is probably mediated by reduction of oxidative stress rather than mitochondrial protein phosphorylation. *Circ Res* **102**, 1082-1090 (2008).
224. Abdul-Ghani, M.A.*, et al.* Mitochondrial reactive oxygen species generation in obese non-diabetic and type 2 diabetic participants. *Diabetologia* **52**, 574-582 (2009).
225. Yao, J.*, et al.* Mitochondrial bioenergetic deficit precedes Alzheimer's pathology in female mouse model of Alzheimer's disease. *Proc Natl Acad Sci U S A* **106**, 14670-14675 (2009).
226. Schapira, A.H. & Tolosa, E. Molecular and clinical prodrome of Parkinson disease: implications for treatment. *Nat Rev Neurol* **6**, 309-317.
227. Rees, M.D., Kennett, E.C., Whitelock, J.M. & Davies, M.J. Oxidative damage to extracellular matrix and its role in human pathologies. *Free Radic Biol Med* **44**, 1973-2001 (2008).
228. Anderson, E.J. & Neufer, P.D. Type II skeletal myofibers possess unique properties that potentiate mitochondrial H(2)O(2) generation. *Am J Physiol Cell Physiol* **290**, C844-851 (2006).
229. Anderson, E.J., Yamazaki, H. & Neufer, P.D. Induction of endogenous uncoupling protein 3 suppresses mitochondrial oxidant emission during fatty acid-supported respiration. *J Biol Chem* **282**, 31257-31266 (2007).
230. Chen, Z., Zhang, H., Lu, W. & Huang, P. Role of mitochondria-associated hexokinase II in cancer cell death induced by 3-bromopyruvate. *Biochim Biophys Acta* (2009).
231. Parker, N., Affourtit, C., Vidal-Puig, A. & Brand, M.D. Energization-dependent endogenous activation of proton conductance in skeletal muscle mitochondria. *Biochem J* **412**, 131-139 (2008).
232. Csukly, K.*, et al.* Muscle denervation promotes opening of the permeability transition pore and increases the expression of cyclophilin D. *J Physiol* **574**, 319-327 (2006).
233. Lablanche, S.*, et al.* Protection of pancreatic INS-1 beta-cells from glucose- and fructose-induced cell death by inhibiting mitochondrial permeability transition with cyclosporin A or metformin. *Cell Death Dis* **2**, e134.
234. El-Mir, M.Y.*, et al.* Neuroprotective role of antidiabetic drug metformin against apoptotic cell death in primary cortical neurons. *J Mol Neurosci* **34**, 77-87 (2008).
235. Petronilli, V.*, et al.* Switch from inhibition to activation of the mitochondrial permeability transition during hematoporphyrin-mediated photooxidative stress. Unmasking pore-regulating external thiols. *Biochim Biophys Acta* **1787**, 897-904 (2009).
236. Anderson, E.J.*, et al.* Substrate-specific derangements in mitochondrial metabolism and redox balance in the atrium of the type 2 diabetic human heart. *J Am Coll Cardiol* **54**, 1891-1898 (2009).
237. Ciapaite, J.*, et al.* Functioning of oxidative phosphorylation in liver mitochondria of high-fat diet fed rats. *Biochim Biophys Acta* **1772**, 307-316 (2007).
238. Pasdois, P., Parker, J.E., Griffiths, E.J. & Halestrap, A.P. The role of oxidized cytochrome c in regulating mitochondrial reactive oxygen species production and its perturbation in ischaemia. *Biochem J* **436**, 493-505.

239. Chavez, A.O.*, et al.* Effect of short-term free Fatty acids elevation on mitochondrial function in skeletal muscle of healthy individuals. *J Clin Endocrinol Metab* **95**, 422-429.
240. Vettor, R.*, et al.* Changes in FAT/CD36, UCP2, UCP3 and GLUT4 gene expression during lipid infusion in rat skeletal and heart muscle. *Int J Obes Relat Metab Disord* **26**, 838-847 (2002).
241. Zackova, M., Skobisova, E., Urbankova, E. & Jezek, P. Activating omega-6 polyunsaturated fatty acids and inhibitory purine nucleotides are high affinity ligands for novel mitochondrial uncoupling proteins UCP2 and UCP3. *J Biol Chem* **278**, 20761-20769 (2003).
242. Jaburek, M.*, et al.* Transport function and regulation of mitochondrial uncoupling proteins 2 and 3. *J Biol Chem* **274**, 26003-26007 (1999).
243. Fink, B.D.*, et al.* Mitochondrial proton leak in obesity-resistant and obesity-prone mice. *Am J Physiol Regul Integr Comp Physiol* **293**, R1773-1780 (2007).
244. Herlein, J.A., Fink, B.D. & Sivitz, W.I. Superoxide production by mitochondria of insulin-sensitive tissues: mechanistic differences and effect of early diabetes. *Metabolism* **59**, 247-257.
245. Ferreira, F.M., Palmeira, C.M., Seica, R. & Santos, M.S. Alterations of liver mitochondrial bioenergetics in diabetic Goto-Kakizaki rats. *Metabolism* **48**, 1115-1119 (1999).
246. Palmeira, C.M.*, et al.* Higher efficiency of the liver phosphorylative system in diabetic Goto-Kakizaki (GK) rats. *FEBS Lett* **458**, 103-106 (1999).
247. Oliveira, P.J.*, et al.* Enhanced permeability transition explains the reduced calcium uptake in cardiac mitochondria from streptozotocin-induced diabetic rats. *FEBS Lett* **554**, 511-514 (2003).
248. Gao, C.L.*, et al.* Mitochondrial dysfunction is induced by high levels of glucose and free fatty acids in 3T3-L1 adipocytes. *Mol Cell Endocrinol* **320**, 25-33.
249. Mantena, S.K.*, et al.* High fat diet induces dysregulation of hepatic oxygen gradients and mitochondrial function in vivo. *Biochem J* **417**, 183-193 (2009).
250. Halestrap, A.P. What is the mitochondrial permeability transition pore? *J Mol Cell Cardiol* **46**, 821-831 (2009).
251. Lumini-Oliveira, J.*, et al.* Endurance training improves gastrocnemius mitochondrial function despite increased susceptibility to permeability transition. *Mitochondrion* **9**, 454-462 (2009).
252. Lumini-Oliveira, J.*, et al.* Endurance training reverts heart mitochondrial dysfunction, permeability transition and apoptotic signaling in long-term severe hyperglycemia. *Mitochondrion* **11**, 54-63.
253. Halestrap, A.P., Woodfield, K.Y. & Connern, C.P. Oxidative stress, thiol reagents, and membrane potential modulate the mitochondrial permeability transition by affecting nucleotide binding to the adenine nucleotide translocase. *J Biol Chem* **272**, 3346-3354 (1997).
254. Haworth, R.A. & Hunter, D.R. Control of the mitochondrial permeability transition pore by high-affinity ADP binding at the ADP/ATP translocase in permeabilized mitochondria. *J Bioenerg Biomembr* **32**, 91-96 (2000).
255. Linard, D.*, et al.* Redox characterization of human cyclophilin D: identification of a new mammalian mitochondrial redox sensor? *Arch Biochem Biophys* **491**, 39-45 (2009).
256. Hurd, T.R., Prime, T.A., Harbour, M.E., Lilley, K.S. & Murphy, M.P. Detection of reactive oxygen species-sensitive thiol proteins by redox difference gel electrophoresis: implications for mitochondrial redox signaling. *J Biol Chem* **282**, 22040-22051 (2007).
257. Costantini, P.*, et al.* Oxidation of a critical thiol residue of the adenine nucleotide translocator enforces Bcl-2-independent permeability transition pore opening and apoptosis. *Oncogene* **19**, 307-314 (2000).
258. Zong, H.*, et al.* AMP kinase is required for mitochondrial biogenesis in skeletal muscle in response to chronic energy deprivation. *Proc Natl Acad Sci U S A* **99**, 15983-15987 (2002).

259. Woods, A.*, et al.* Characterization of the role of AMP-activated protein kinase in the regulation of glucose-activated gene expression using constitutively active and dominant negative forms of the kinase. *Molecular and cellular biology* **20**, 6704-6711 (2000).
260. Stapleton, D.*, et al.* Mammalian AMP-activated protein kinase subfamily. *The Journal of biological chemistry* **271**, 611-614 (1996).
261. Koh, H.J., Brandauer, J. & Goodyear, L.J. LKB1 and AMPK and the regulation of skeletal muscle metabolism. *Current opinion in clinical nutrition and metabolic care* **11**, 227-232 (2008).
262. Mu, J., Brozinick, J.T., Jr., Valladares, O., Bucan, M. & Birnbaum, M.J. A role for AMP-activated protein kinase in contraction- and hypoxia-regulated glucose transport in skeletal muscle. *Molecular cell* **7**, 1085-1094 (2001).
263. Guerre-Millo, M.*, et al.* PPAR-alpha-null mice are protected from high-fat diet-induced insulin resistance. *Diabetes* **50**, 2809-2814 (2001).
264. Cheung, A.*, et al.* A small-molecule inhibitor of skeletal muscle myosin II. *Nat Cell Biol* **4**, 83-88 (2002).
265. Cortright, R.N.*, et al.* Protein kinase C modulates insulin action in human skeletal muscle. *Am J Physiol Endocrinol Metab* **278**, E553-562 (2000).
266. Dohm, G.L.*, et al.* An in vitro human muscle preparation suitable for metabolic studies. Decreased insulin stimulation of glucose transport in muscle from morbidly obese and diabetic subjects. *J Clin Invest* **82**, 486-494 (1988).
267. Noland, R.C.*, et al.* Peroxisomal-mitochondrial oxidation in a rodent model of obesity-associated insulin resistance. *Am J Physiol Endocrinol Metab* **293**, E986-E1001 (2007).
268. Tian, Y.F.*, et al.* The importance of cyclooxygenase 2-mediated oxidative stress in obesity-induced muscular insulin resistance in high-fat-fed rats. *Life Sci* **89**, 107-114.
269. Fujii, N.*, et al.* AMP-activated protein kinase alpha2 activity is not essential for contraction- and hyperosmolarity-induced glucose transport in skeletal muscle. *The Journal of biological chemistry* **280**, 39033-39041 (2005).
270. Jornayvaz, F.R.*, et al.* Hepatic insulin resistance in mice with hepatic overexpression of diacylglycerol acyltransferase 2. *Proc Natl Acad Sci U S A* **108**, 5748-5752.
271. Hurd, T.R., Filipovska, A., Costa, N.J., Dahm, C.C. & Murphy, M.P. Disulphide formation on mitochondrial protein thiols. *Biochemical Society transactions* **33**, 1390-1393 (2005).
272. Hurd, T.R.*, et al.* Glutathionylation of mitochondrial proteins. *Antioxidants & redox signaling* **7**, 999-1010 (2005).
273. Chen, C.L.*, et al.* Site-specific S-glutathiolation of mitochondrial NADH ubiquinone reductase. *Biochemistry* **46**, 5754-5765 (2007).
274. Beer, S.M.*, et al.* Glutaredoxin 2 catalyzes the reversible oxidation and glutathionylation of mitochondrial membrane thiol proteins: implications for mitochondrial redox regulation and antioxidant DEFENSE. *The Journal of biological chemistry* **279**, 47939-47951 (2004).
275. Taylor, E.R.*, et al.* Reversible glutathionylation of complex I increases mitochondrial superoxide formation. *The Journal of biological chemistry* **278**, 19603-19610 (2003).
276. Dahm, C.C., Moore, K. & Murphy, M.P. Persistent S-nitrosation of complex I and other mitochondrial membrane proteins by S-nitrosothiols but not nitric oxide or peroxynitrite: implications for the interaction of nitric oxide with mitochondria. *The Journal of biological chemistry* **281**, 10056-10065 (2006).
277. Zhang, L.*, et al.* Mass spectrometry profiles superoxide-induced intramolecular disulfide in the FMN-binding subunit of mitochondrial Complex I. *Journal of the American Society for Mass Spectrometry* **19**, 1875-1886 (2008).

278. Hurd, T.R.*, et al.* Complex I within oxidatively stressed bovine heart mitochondria is glutathionylated on Cys-531 and Cys-704 of the 75-kDa subunit: potential role of CYS residues in decreasing oxidative damage. *The Journal of biological chemistry* **283**, 24801-24815 (2008).
279. Chen, Y.R., Chen, C.L., Zhang, L., Green-Church, K.B. & Zweier, J.L. Superoxide generation from mitochondrial NADH dehydrogenase induces self-inactivation with specific protein radical formation. *The Journal of biological chemistry* **280**, 37339-37348 (2005).
280. Lowell, B.B. & Shulman, G.I. Mitochondrial dysfunction and type 2 diabetes. *Science* **307**, 384-387 (2005).
281. Finck, B.N.*, et al.* A potential link between muscle peroxisome proliferator- activated receptor-alpha signaling and obesity-related diabetes. *Cell Metab* **1**, 133-144 (2005).

APPENDIX: INSTITUTIONAL ANIMAL CARE AND USE COMMITTEE ANIMAL USE PROTOCOL APPROVAL LETTERS

Animal Care and Use Committee
212 Ed Warren Life Sciences Building
East Carolina University
Greenville, NC 27834

252-744-2436 office
252-744-2355 fax

December 4, 2009

Darrell Neufer, Ph.D.
Department of Physiology
Brody 6N-98
ECU Brody School of Medicine

Dear Dr. Neufer:

Your Animal Use Protocol entitled, "Mitochondrial Bioenergetics and Metabolic Disease - Mice," (AUP #Q237a) was reviewed by this institution's Animal Care and Use Committee on 12/3/09. The following action was taken by the Committee:

"Approved as submitted"

This AUP approves total animal numbers, strains of animals, and procedures that can be done in various combinations. **As each specific experiment is designed, please submit an amendment to the IACUC specifying number of animals per experimental group, strain(s), and procedures to be done.**

A copy is enclosed for your laboratory files. Please be reminded that all animal procedures must be conducted as described in the approved Animal Use Protocol. Modifications of these procedures cannot be performed without prior approval of the ACUC. The Animal Welfare Act and Public Health Service Guidelines require the ACUC to suspend activities not in accordance with approved procedures and report such activities to the responsible University Official (Vice Chancellor for Health Sciences or Vice Chancellor for Academic Affairs) and appropriate federal Agencies.

Sincerely yours,

Robert G. Carroll, Ph.D.
Chairman, Animal Care and Use Committee

RGC/jd

enclosure

East Carolina University

Animal Care and Use Commitee
212 Ed Warren Life Sciences Building
East Carolina University
Greenville, NC 27834

252-744-2436 office
252-744-2355 fax

December 16, 2010

Darrell Neufer, Ph.D.
Department of Physiology
Brody 6N-98
ECU Brody School of Medicine

Dear Dr. Neufer:

Your Animal Use Protocol entitled, "Mitochondrial Bioenergetics and Metabolic Disease - Rats," (AUP #Q238a) was reviewed by this institution's Animal Care and Use Committee on December 14, 2010. The following action was taken by the Committee:

Approved with the following comment:

1. Amendments to AUPs are no longer limited to 3. Minor or administrative amendments as defined in the ECU IACUC amendment policy (see attached) will not need to go to full committee review. However, amendments requesting deviations in numbers or procedures, and surgical procedures in the already approved AUP will require full committee review and approval for all future amendments.

Please contact me if I can be of further assistance.

Sincerely yours,

Robert G. Carroll, Ph.D.
Chairman, Animal Care and Use Committee

RGC/jd

enclosure

East Carolina University

1907-2007 CENTENNIAL

Animal Care and Use Committee
212 Ed Warren Life Sciences Building
East Carolina University
Greenville, NC 27834

252-744-2436 office
252-744-2355 fax

December 4, 2009

Darrell Neufer, Ph.D.
Department of Physiology
Brody 6N-98
ECU Brody School of Medicine

Dear Dr. Neufer:

Your Animal Use Protocol entitled, "Breeding of Mice for Mitochondrial Bioenergetics and Metabolic Disease Studies," (AUP #Q285) was reviewed by this institution's Animal Care and Use Committee on 12/3/09. The following action was taken by the Committee:

"Approved as submitted"

Note: Please send a registration to the Biological Safety Committee for the breeding of transgenic/outcross animals.

A copy is enclosed for your laboratory files. Please be reminded that all animal procedures must be conducted as described in the approved Animal Use Protocol. Modifications of these procedures cannot be performed without prior approval of the ACUC. The Animal Welfare Act and Public Health Service Guidelines require the ACUC to suspend activities not in accordance with approved procedures and report such activities to the responsible University Official (Vice Chancellor for Health Sciences or Vice Chancellor for Academic Affairs) and appropriate federal Agencies.

Sincerely yours,

Robert G. Carroll, Ph.D.
Chairman, Animal Care and Use Committee

RGC/jd

enclosure